SOVIET PHYSICS

USPEKHI

A Translation of Uspekhi Fizicheskikh Nauk

É. V. Shpol'skiĭ (Editor in Chief), S. G. Suvorov (Associate Editor),
D. I. Blokhintsev, V. I. Veksler, S. T. Konobeevskiĭ (Editorial Board).

SOVIET PHYSICS USPEKHI (Russian Vol. 82, Nos. 1 and 2) JULY-AUGUST, 1964

539.12.01

STRONG INTERACTIONS AT VERY HIGH ENERGY

E. L. FEĬNBERG and D. S. CHERNAVSKIĬ

Usp. Fiz. Nauk **82**, 3-81 (January, 1964)

I. Introduction . . . 1
II. The Method of Moving Poles . . . 3
1. Introductory Remarks . . . 3
2. Derivation of the Fundamental Asymptotic Formula . . . 4
3. Properties of the Elastic Scattering Amplitude at High Energies . . . 7
4. Extension to Other Processes . . . 9
5. Elastic π^-p Scattering and Contradiction Between Theory and Experiment . . . 11
III. Theory of Peripheral Interactions . . . 12
1. Initial Concepts and Formula for Total Cross Section . . . 12
2. Classification of Methods . . . 14
3. The Two-center Model . . . 16
4. The Multiperipheral Model . . . 20
5. Supplementary Remarks . . . 24
IV. Experimental Data for $E_L \gtrsim 10^{11}$ eV. Comparison with Theory . . . 24
1. Summary of Earlier Results . . . 24
2. Methods of Experiment Analysis . . . 25
3. Fundamental Experimental Results of Recent Years and Their Significance for the Theory . . . 29
4. Conclusion . . . 37
V. Connection Between the Method of Moving Poles with the Diagram Approach and the One-meson Approximation . . . 38
1. Formulation of the Problem . . . 38
2. Diagram Interpretation of the MMP . . . 38
3. Mixed Model . . . 39
4. Inelastic Processes in the OMA and the MMP . . . 41
Appendix . . . 44
Cited References . . . 46

1. INTRODUCTION

IN the last few years major changes have occurred in the study of strong interactions at very high energies. We refer here to experiments at $(1-3) \times 10^{10}$ eV in special accelerators and above 10^{11} eV in cosmic rays. At the same time, new approaches have been devised, and new theories developed, leading to definite predictions with respect to details of the process; these predictions are already amenable to experimental verification. The present article is devoted to a brief review of the experimental facts, primarily obtained with cosmic rays at energies $E > 10^{11}$ eV (but also with accelerators, where results of basic importance were attained at the beginning of 1963), to the principal aspects of the theories and to their interrelation and to the agreement with the experimental data.

There is no doubt that the earlier reviews [1-3] have become obsolete. As to the theories, their development has been marked, on the one hand, by the appearance of the method of moving poles (or the method of complex orbital momenta, the Regge pole method),

henceforth designated the MMP, the two-year history of which is brilliant and dramatic. On the other hand, the so-called one-meson approximation (OMA), which is physically based on the old almost-naive representations of the Weizsäcker–Williams method and has grown from the pole method, has received a much more complete, rigorous, and developed form.

Of course, the very use of the word "theory" in the plural is not very reassuring. If there were one good theory, it would be sufficient. The two mentioned methods do not start from some fundamental base, but contain hypotheses or postulates. Each method covers only part of the processes: the moving pole method deals only with elastic (at best quasielastic) processes and the total cross section connected with them by the optical theorem; the one-meson approximation deals with inelastic peripheral collisions and the elastic ones connected with them.

The simplicity and clarity of the MMP and the whole tendency connected with it—"Reggistics"—have attracted many adherents. The mathematical orderliness of the method expiates some of its abstractness and the fact that the physical meaning of some of its postulates is not perfectly clear.

The enthusiasm has increased even more when proton-proton (pp) scattering experiments in accelerators, in the 10—20 BeV region, have confirmed one of the main conclusions of the MMP. The opinion has been advanced that the MMP, even in the form where only one extreme right-hand pole is taken into account is an all-inclusive theory and describes all the processes at high energies.

It soon became clear, however, that this is not the case. The principal role has been played here by data concerning elastic π^-p interaction in the same energy region, published approximately one year after the pp-scattering experiments and in decisive disagreement with the MMP predictions.

It became clear that the region of applicability of the MMP, at least in its presently known form, was more limited than its most ardent adherents believed. Many have therefore interpreted this failure as a breakdown of the entire method.

It seems to us that by now its strong and weak aspects and its connection with other methods have become clarified to some degree, and the method is assuming a firm and important position, albeit more modest than first prophesied, in the physics of high-energy processes.

On the other hand, the one-meson-approximation method, which is developed in parallel with and independently of the Regge method, was more traditional, perhaps less brilliant, and did not claim an all-embracing role. At the same time, during the course of its gradual development, it explained many experimental facts. Its attractive feature is that it is concrete.

It is therefore particularly important to clarify the extent to which the deductions of both theories agree with the actual facts.

At the present time we have reached, in some sense, a new stage in the investigation of strong interactions at high energies, where the mutual connection between elastic and inelastic processes can already be studied. In light of this, it is necessary to re-evaluate the position of the hydrodynamic theory, which for a long time was the only serious theoretical scheme for processes at superhigh energies. The very existence or nonexistence of hydrodynamic processes is of great significance to the theory.

Particular attention must be paid to the information that can be extracted from the experimental data obtained on cosmic rays. Of course, the picture which they present is far from complete. As is always the situation with cosmic rays, experiments are difficult, hard to control, and frequently ambiguous. However, as is always the case at lower energies, under careful analysis it yields new fundamental information. Even now, many distinct characteristics of the interaction act, which have a decisive importance in the discussion of theoretical problems, have been obtained with its aid in the 10^{11}—10^{13} eV energy region. Many reliably determined quantitative characteristics pertain to energies up to 10^{15}—10^{16} eV.

We shall consider below essentially nucleon-nucleon and nucleon-meson interactions, with the nucleon laboratory energy E_L exceeding 10^{11} eV. This value is chosen for three reasons.

First, it is probable that this energy will remain the upper limit attainable by accelerators for the next five or ten years.

Second, the essentially new features of the phenomena dealt with (production of independently decaying particle clusters, etc.) appear when the number of produced particles is large, $n \gg 1$. However, experiment shows that in the mean

$$\bar{n} \sim \left(\frac{E_L}{\mu}\right)^{\frac{1}{4}},$$

where μ is the pion mass.* Thus, if $n \sim 5$ then $E_L \sim \mu n^4 \sim 10^{11}$ eV.

Third, it is already clear that an important role is played by the following condition, which is encountered both in the moving-pole method and in the one-meson approximation,

$$\ln \frac{s}{s_0} \gg 1,$$

where

$$\frac{s}{s_0} = \frac{E_L}{M}$$

(M — nucleon mass), with the $\gg$ symbol significant. When $E_L \sim 10^{11}$ eV we have $\ln(s/s_0) \approx 4$. Thus, the region $E_L > 10^{11}$ is indeed physically singled out.

*Here and throughout we use $\hbar = c = 1$.

A few words about the character of the treatment of the theoretical problems. There is apparently no published exposition of the fundamentals of the moving-pole method accessible to the non-specialist. We have attempted to treat them here quite fully, avoiding complicated elements, as a result of which the corresponding chapter (II) is large and contains more material than necessary for a mere comparison of the theoretical deductions with experiment. The mathematics is relegated where possible to the appendix.

The same can be said to some degree concerning the one-meson approximation (Chapter III), which is extensively used by many workers to analyze a great variety of experiments, but is employed in different variants without sufficient differentiation in the terminology and in the assumptions made. It was necessary to broaden the exposition here, too, in order to clarify these questions.

In Chapter IV we present a few experimental results of research in the region $E_L > 10^{11}$ eV (cosmic rays), with considerable space allotted to special methods of analysis of the data used in these questions. The experimental data obtained in the verification of the predictions of the MMP at accelerator energies are given in Chapter II during the course of the exposition of the theory, and also in Chapter V, in which the connection between the two theoretical methods is considered. It must be stipulated that here, in spite of widely used and recognized considerations, we develop also our own general point of view, based on many not yet extensively discussed recent investigations. The deductions resulting from these investigations and the mentioned point of view reduce to a statement that the asymptotic properties of elastic scattering, which follow from the MMP in its traditional form (inclusion of only the one pole on the extreme right) reflect the result of one-meson inelastic interactions of the same particles. Although we cannot assume that this statement can be proved rigorously, it seems to us justified to a certain degree both experimentally and theoretically. It enables us to outline a single scheme, in which the MMP and the OMA are not in opposition but complement each other.

II. THE METHOD OF MOVING POLES

1. Introductory Remarks

The fact that quantum field theory, which has been so successfully applied to electrodynamics, proved to be ineffective when attempts were made to use it for strong interactions, has spurred the efforts to construct a theory on different formal principles. At first, the diagram method became popular. In this method, the calculation of the amplitude of the transition probability is based on the assumption of some Feynman diagram (or a set of such diagrams), in which, however, the vertex parts and the propagation functions are assumed to be "overgrown," and to include all orders of perturbation theory, They must obey a whole series of general relations established in field theory (the Lehmann spectral representations, etc.) and owing to the lack of a consistent theory they can sometimes take into account information extracted from a comparison of calculation results with experiment. An example of the diagram method is the one-meson approximation (Chapter III). Thus, the only departure from ordinary field theory is in practice the discarding of perturbation theory.

Gradually, however, a more extreme trend began to develop, based on the use of only the most general theoretical premises, which are regarded as obligatory for any theory. Indeed, we must face the possibility that in the new range of phenomena of interest to us it may be inconvenient to use the customary description with the aid of ψ functions, ψ operators, and the Hamiltonian, which are applied to each stage of the process. As far back as in 1943, Heisenberg proposed a program for describing collisions between elementary particles exclusively in terms of matrix elements (probability amplitudes) of transitions from the initial (really observed) state of a system of non-interacting particles to the final (also really observed) state of likewise free particles. This concept starts from the possibility that it is actually impossible in principle to trace the process of interaction between particles by using in each stage the detailed representations of quantum field theory. The aggregate of the transition amplitudes forms the S matrix, which encompasses all the possible information on the processes. Of course, the future theory should contain a certain algorithm (like an equation of motion), which would permit calculation of the S matrix. For the time being we must attempt to make as full use as possible of the fact that the S matrix must satisfy some general requirements. These are: (1) causality, defined as the absence of connections between observed events if the events are separated by space-like intervals (when the signal would have to propagate with a velocity exceeding that of light); (2) the closely associated relativistic covariance of all relations, which is closely associated with the first requirement; (3) unitarity, that is, the normalization requirement; the total probability of a transition from each initial state (summed over all the final states) should remain equal to unity; (4) the correspondence principle, that is, the requirement that on going to a case which can be described from the point of view of quantum field theory (for example, to quantum electrodynamics) the S-matrix theory must go over into the corresponding ordinary theory (for more details see [4]).

Of course, the results obtained in this way (if obtainable at all) should remain in force even if it turns out that the general principles and methods of the ordinary theory remain valid also in the problems under consideration.

The foregoing postulates, of course, are not enough to produce a theory. Since the equation for the S matrix is not known, all attempts (including the moving-pole method) are based on finding additional conditions imposed on the S matrix, conditions which would make it possible to specify it for at least a few particular cases. Usually an attempt is made to obtain them from general considerations, by studying the properties of the S matrix in electrodynamics or by perturbation theory, etc., and then postulating the correctness of some of these properties in the new situation. This, in particular, is how the double dispersion relations for the scattering amplitude were formulated, the crossing symmetry condition imposed, etc. The method of moving poles is also based on these principles.

Both the double dispersion relations and the MMP consider only the amplitude of mutual scattering of two particles. This amplitude is a function of the energy and the scattering angle or the momentum transfer. It describes the transition from particles with 4-momenta p_1 and p_2 to particles with 4-momenta p_3 and p_4. Convenient relativistic invariants reflecting the energy and the scattering angle θ_s are

$$s = -(p_1 + p_2)^2 \text{ and } t = -(p_1 - p_3)^2 *.$$

In the center-of-mass system, where, if we speak of collisions between identical particles, the energy of each particle is equal to E, the momenta before collision are $\mathbf{p}$ and $-\mathbf{p}$, and those after collision are $\mathbf{p}'$ and $-\mathbf{p}'$, these variables have the form

$$s = (p_{10} + p_{20})^2 - (\mathbf{p}_1 + \mathbf{p}_2)^2 = 4E^2, \tag{2.1}$$

$$t = (p_{10} - p_{30})^2 - (\mathbf{p}_1 - \mathbf{p}_3)^2 = -2\mathbf{p}^2(1 - \cos\theta_s). \tag{2.2}$$

We shall speak in what follows of an amplitude $A(s,t)$, which is connected with the cross section $d\sigma_{el}(\theta_s)$ of elastic scattering through an angle θ_s by the following relation (we introduce the "invariant amplitude" A in place of the nonrelativistic amplitude F, $d\sigma_{el} = |F|^2 d\Omega$)

$$d\sigma_{el} = \frac{16\pi}{s^2} |A(s,t)|^2 dt \quad \left(A = \frac{s}{4|\mathbf{p}|} F\right). \tag{2.3}$$

The investigation of the elastic-scattering amplitude is of value, in particular, because according to the optical theorem, which holds true under the most general assumptions, knowledge of A for the angle $\theta_s = 0$ ensures knowledge of the total cross section $\sigma(s)$:

$$\operatorname{Im} A(s, 0) = \frac{s}{16\pi} \sigma(s). \tag{2.4}$$

2. Derivation of the Fundamental Asymptotic Formula

The diagram of Fig. 1, which describes the mutual scattering of particles 1 and 2, shows the time flowing downward. The same diagram, however, can be read differently by imagining that the time flows from left to right. In such a case we encounter lines of particles with 4-momenta p_3 and p_2, directed opposite to the time axis. As is well known, these describe antiparticles with 4-momenta $-p_3$ and $-p_2$. Consequently, from the point of view of the general rule, when the diagram is read in this manner we are dealing with elastic scattering of a particle with 4-momentum $p_1' = p_1$ by an antiparticle $p_2' = -p_3$, yielding an antiparticle $p_3' = -p_2$ and a particle $p_4' = p_4$. For this second process, the parameters s and t (denoted s′ and t′) are

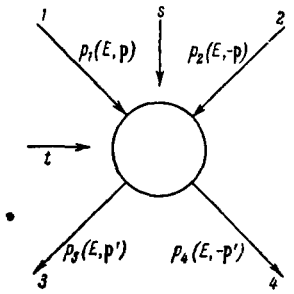

FIG. 1. Notation for the momenta.

$$s' = -(p_1' + p_2')^2 = -(p_1 - p_3)^2 = t = -2\mathbf{p}^2(1 - \cos\theta_s), \tag{2.5}$$

$$t' = -(p_1' - p_3')^2 = -(p_1 + p_2)^2 = s = 4E^2. \tag{2.6}$$

Thus, in the crossed channel of the reaction, the role of the "energy" parameter is played by s′, which is equal to the square of the 4-momentum transfer in the direct channel t, while the role of the square of the momentum transfer is played by the quantity t′, which is equal to the square of the energy s in the direct channel. Usually we do not introduce the new (primed) quantities s′ and t′, retaining the foregoing quantities s and t, but saying that the first channel is the "s-channel," since the role of the (square of the) energy is played here by s, while the second channel is the "t-channel," since the square of the energy is given here by t. All this in indicated by the supplementary arrows in Fig. 1.

In (2.2) and (2.6) we have the cosine of the scattering angle in the direct channel (in which s is the square of the energy). We can introduce the cosine of the scattering angle in the crossing channel, $\cos\theta_t = z$; in the future this quantity will play an important role. In analogy with (2.1) and (2.2) we have

$$s = -2\mathbf{p}^2(1 - \cos\theta_t), \tag{2.5a}$$

$$t = 4E^2, \tag{2.6a}$$

where E and p are the energy and momentum in the c.m.s. of the particles that collide in the crossed channel. $\mathbf{p}^2$ is connected by the conservation laws with the masses of the interacting particles and with the energy $\sqrt{t}$. In the case when the masses are identical and equal to m, we have in the t-channel

$$\mathbf{p}^2 = \frac{1}{4}(t - 4m^2), \tag{2.5b}$$

*The square of the 4-vector is understood in the sense $p^2 = p^2 - p_0^2$, where p is a space vector.

$$\cos\theta_t \equiv z = 1 - \frac{2s}{t-4m^2}\ ^*. \qquad (2.6b)$$

Consequently, the amplitude A(s,t) represented by the diagram of Fig. 1 can be regarded either as the elastic-scattering amplitude in the s-channel with s as the square of the total energy and t as the 4-momentum transfer, or as the amplitude elastic-scattering in the t-channel for a particle and antiparticle with t as the square of the total energy and s the square of the 4-momentum transfer. An important complication arises here. If we know A(s,t) for a real process in the s-channel, then $s > 0$ and $t < 0$ [see (2.1) and (2.2)]. But in the t-channel we should have for a real process $t > 0$ (for here it is the square of the total energy) and $s < 0$ (for here it is the square of the 3-momentum transfer taken with the negative sign). When we deal with some single amplitude A(s,t) for both channels, we essentially unify mechanically two different functions, defined in different (non-overlapping) intervals of variables: one for $s > 0$ and $t < 0$, and the other for $s < 0$ and $t > 0$. In particular, of course, knowledge of A(s,t) for the real process in one channel does not add anything, for the time being, in the sense of knowledge of the amplitude of scattering for the real process in the other channel. Using the coordinates s and t (Fig. 2) we can state that if m is the mass of the particles and antiparticles, then the regions of values of the variables s and t corresponding to different channels are different in this case (they are shown shaded in Fig. 2). A new situation arises only if we state that this is actually a single analytic function. In this case, knowing it as a function of its variables in one channel, we can go over (continue it analytically) to the other channel. This postulate is used in the MMP and in the double dispersion relations.

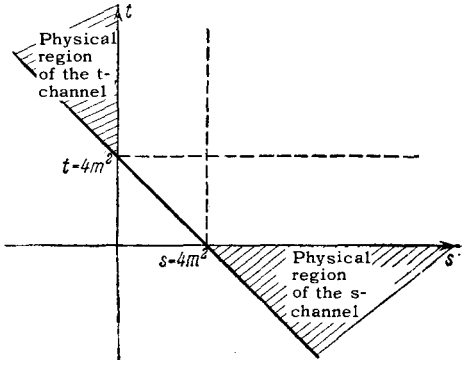

FIG. 2. Physical regions of the values of the parameters s and t.

We note that the problem is usually symmetrized (for convenience in notation). Instead of the usual elastic scattering we consider elastic scattering with conversion into antiparticles (Fig. 3). Then the parameters s and t, and also a third parameter u which is analogous to them and which is determined uniquely in terms of s and t, are equal to

$$s = -(p_1+p_2)^2, \quad t = -(p_1+p_3)^2, \quad u = -(p_1+p_4)^2, \qquad (2.7)$$

$$p_1+p_2+p_3+p_4 = 0, \quad p_1^2 = p_2^2 = p_3^2 = p_4^2 = -m^2,$$

$$s+t+u = 4m^2. \qquad (2.8)$$

Accordingly, it is convenient to choose oblique coordinates in the (s,t) plane. We then have the scheme shown in Fig. 4. Thus, the physical (real) regions of different channels (to which we add the u-channel—collision of particles 1 and 4) do not overlap.

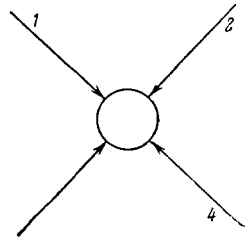

FIG. 3. Symmetrized collision scheme.

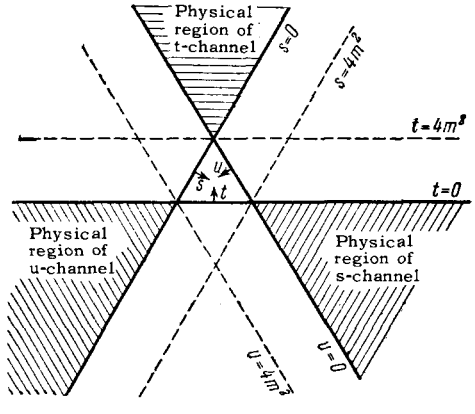

FIG. 4. Physical regions of the values of the variables s, t, and u.

In this formulation of the problem it becomes understandable why the problem of the analytical properties of the function A(s,t) is of prime significance. By solving this problem we can relate the probabilities of entirely different processes and make definite (albeit limited in content) predictions for the experiments.

The analytical properties of A(s,t) are already determined to some degree by the requirements of causality and unitarity, on which is based the derivation of the so-called dispersion relations. We note

*In the more general case the expression for z becomes more complicated. Thus, if as a result of collision between particles of mass m one of them acquires a mass $\mathfrak{M}$, then by using the conservation laws we obtain after some computation

$$z = \frac{-t(s_2-m^2-t)+2t(s-4m^2)}{(t^2-4m^2t)^{1/2}[(s_2-m^2-t)^2-4m^2t]^{1/2}}, \quad s_2 = \mathfrak{M}^2. \qquad (2.6c)$$

If we deal with mutual elastic scattering of two particles of different masses μ and m, we have

$$z = \frac{t-2(m^2+\mu^2)-2s}{\sqrt{t-4m^2}\sqrt{t-4\mu^2}}. \qquad (2.6d)$$

that the ordinary dispersion relations have yielded the important deduction that if the cross section of the interaction of particle A with particle B tends to a constant value with increasing energy, then the cross section of the interaction of the antiparticle $\bar{A}$ with the same particle B should tend to the same constant value (this is called the Pomeranchuk theorem [5]). Experiments on pp and πp interactions apparently confirm this relation. Further, on the basis of the double dispersion relations—and consequently, after addition of some not-obvious postulates—it was deduced that the total cross section cannot increase with energy $E = \sqrt{s/4}$ more rapidly than [6]

$$(\ln E)^2 \sim \left(\ln \frac{s}{4}\right)^2.$$

The experimental data certainly satisfy this condition.

Before we discuss the analytic properties of the function $A(s,t)$, let us represent it in different form.

In place of considering the function A directly, we can, taking this function in the t-channel when $s = s(\theta_t)$, expand this function in Legendre polynomials $P_l(\cos\theta_t)$

$$A(s,t) = \sum_l f_l(t) P_l(\cos\theta_t)(2l+1),$$

and analyze the expansion coefficients $f_l(t)$ (which have the sense of scattering amplitudes of particles with a definite orbital angular momentum l) as functions of t and l.

The central point in this case is the formal procedure, namely the transformation of a sum over discrete values of l (which has a clear-cut physical meaning) into an integral over a certain contour in the complex l plane (which has no physical meaning).* This procedure has long been known in the theory of propagation of radio waves around the spherical earth (the Watson-Sommerfeld transformation [7]), where the wave equation has the same form as the nonrelativistic Schrödinger equation, and the spherically symmetrical potential corresponds to a radial decrease in the difference $\epsilon(r) - 1$, where $\epsilon(r)$ is the dielectric constant of the medium.

Everything which follows depends essentially on the analytical properties of the function $f(l,t)$ (where l is a continuous complex variable), that is, on the singularities of these functions in the l-plane. The character and number of these singularities determine the physical content of the method of complex orbital angular momenta.

We now arrive at the central point. Since there is no consistent relativistic theory of strongly interacting fields, we are forced to make use of some additional considerations. The way was pointed by Regge's paper [8]. Regge considered a problem which at first glance is purely academic. He investigated the analytic properties of the function $f(l,t)$ in the nonrelativistic theory for a particle in a potential field (the Schrödinger equation), but for a wide class of potentials of the Yukawa type with an arbitrary interaction force. Regge has shown that in this case the function $f(l,t)$ has in the l-plane (for $\mathrm{Re}\, l > -\frac{1}{2}$) only simple poles which are located in the first quadrant.

We note that the same holds in the problem of propagation of radio waves in a homogeneous atmosphere around a homogeneous spherical earth. In the Regge problem this corresponds to a potential in the form of a rectangular spherically-symmetrical ledge. Actually (in a somewhat different form), this property holds also when the earth is surrounded by an inhomogeneous (spherically symmetrical) atmosphere, as demonstrated by V. A. Fock [9] under rather general assumptions with respect to the variation of $\epsilon(r)$.

The rigorous result obtained by Regge in the nonrelativistic theory was further developed by Chew, Gribov, and others in the relativistic theory, with which we are dealing here. Two ways are used.

On the one hand, it is possible to stipulate simply that in the relativistic theory we have exactly the same singularities—simple poles in the first quadrant—as found by Regge. This bold postulate is indeed the basis of the MMP. Mathematically its content can be formulated as a principle of maximum analyticity in the

*Let us explain how this is done. Since the sum over l is taken over the points $l = 0, 1, 2, \ldots$, each term of the sum can be replaced by the integral over a small circle Γ_l around the corresponding points in the complex plane l (Fig. 5):

$$A(s,t) = \sum_{l=0}^{\infty} (2l+1) f_l(t) P_l(\cos\theta_t)$$

$$= \sum_{l=0}^{\infty} \frac{1}{2\pi i} \oint_{\Gamma_l} \frac{\pi(-1)^l f_l(t)}{\sin \pi l} (2l+1) P_l(\cos\theta_t)\, dl. \qquad (2.8')$$

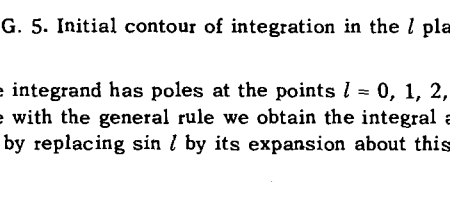

FIG. 5. Initial contour of integration in the l plane.

Indeed, the integrand has poles at the points $l = 0, 1, 2, \ldots$, and in accordance with the general rule we obtain the integral along the contour Γ_i by replacing $\sin l$ by its expansion about this pole $l^{(i)}$

$$\sin \pi l \approx \sin \pi l^{(i)} + \pi \cos \pi l^{(i)} (l - l^{(i)}) = \pi (-1)^{l^{(i)}} (l - l^{(i)}),$$

after which the residue of the integral yields the required quantity.

Now we can replace the sum of the contours by a single contour Γ, if we first put $(-1)^l = e^{i\pi l}$:

$$A(s,t) = \frac{1}{2i} \int_{\Gamma} \frac{e^{i\pi l} f_l(t)(2l+1) P_l(\cos\theta_t)}{\sin \pi l}\, dl. \qquad (2.8'')$$

A certain complication is caused by the need for considering even and odd l separately (for details see the appendix)[10].

sense that the only singularities admitted are those which must be retained from considerations of the correspondence between the relativistic and nonrelativistic theories. The physical gist of this method is not obvious. We shall return to this question in Chapter V.

On the other hand, attempts were made to prove this property on the basis of the Mandelstam double dispersion relations which, as already mentioned, in themselves contain a strong postulative element. These attempts were not fully successful. It was only possible to prove [10] that the function $f(l,t)$ should have poles in the first quadrant, but it was not proved that there are no other singularities.

The desired property could be proved in consistent fashion only for a limited class of diagrams [11,12] or under definite assumptions concerning the relativistic potential [13].

Thus, we assume this premise. Then, in accord with the main property of analytic functions, $f(l,t)$ can be represented as an expansion in terms of the poles

$$f(l,t)=\sum_i \frac{r_i(t)}{l-l_i(t)}+f_1, \qquad (2.9)$$

where $l_i(t)$ is the pole at the given t, $r_i(t)$ the corresponding residue, and f_1 a function which has no singularities in the right-hand half-plane of l (more accurately, for Re $l > -1$).

Using this expression, we can transform the contour in the l-plane in such a way that $A(s,t)$ reduces to an integral J along a vertical straight line and the sum of residues at the poles $l_i(t)$ situated, as already mentioned, in the first quadrant to the right of the aforementioned line (Fig. 6).*

When t changes, the position of the poles can change, $l_i = l_i(t)$, and the poles will move along certain trajectories (hence the name of the method). The residues will contain Legendre polynomials of complex index $P_{l_i(t)}(\cos\theta_t)$, the analytic properties of which have been thoroughly investigated [14]. In the final expression it is convenient to go over from $\cos\theta_t$ again to s [using formula (2.6b)]. We obtain an analytic expression for $A(s,t)$ in which we can substitute for s and t the values $t > 0$ and $s < 0$, and, in particular, we can take values which lie in the physical region of the other channel, where s is the square of the energy (and is positive) and t is the square of the momentum transfer with the sign reversed (and negative). In this expression, $A(s,t)$ is represented by a sum of residues and an integral along the vertical line which lies to the left of all the poles which are included in the sum.

This expression is particularly simple and convenient when s is large, that is, for high energies, when

*To this end we deform the contour Γ into the contour C, and add integrals over the contours C_0, C_1, C_2, ... surrounding the poles l_0, l_1, l_2, ... of the function $f(l,t)$.

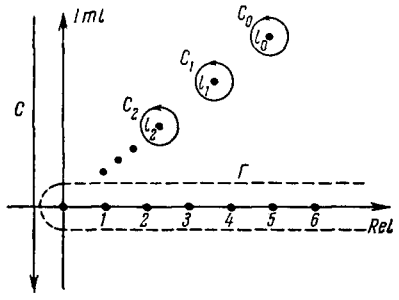

FIG. 6. Transformed integration contour in the l plane.

we can substitute for $P_{l_i}(\cos\theta_t)$ an asymptotic expression. Indeed*

$$A(s,t)=\frac{1}{16\pi}\sum_i B_i(t)\,s^{l_i(t)}+J(s,t). \qquad (2.10)$$

Here B_i contains the residue of the function $f(l,t)$ at the point $l_i(t)$ and some additional factors.

3. Properties of the Elastic Scattering Amplitude at High Energies

Let us consider extremely large s, $s \to \infty$. It is obvious that it is possible to retain in the sum over the poles the higher-order terms with the largest real part of l_i, which play the principal role as $s \to \infty$. This raises the question of how many such terms make an appreciable contribution. In the MMP, as formulated in [10,15-17], one makes at this point still another important assumption, that among the poles $l_i(t)$ there is one and only one pole $l_0(t)$ which has the largest real part in the range of values of t of interest.† This

*The expressions

$$P_{l_i}(\cos\theta_t)=P_{l_i}\left(1+\frac{2s}{t-4m^2}\right)$$

which are contained in the residues must then be taken for arbitrarily large positive values of the argument. The asymptotic behavior of P_{l_i} is as follows[14]:**

$$P_{l_i}(\mathrm{ch}\,\eta)=\frac{\Gamma\left(l+\frac{1}{2}\right)e^{l\eta}}{\sqrt{\pi}\,\Gamma(l+1)},$$

where

$$\cos\theta_t=\mathrm{ch}\,\eta\approx\frac{1}{2}e^{\eta}.$$

consequently

$$\eta=\ln\left(2\left(1-\frac{2s}{t-4m^2}\right)\right)\approx\ln\frac{s}{t-4m^2}$$

and

$$P_{l_i}(\cos\theta_t)\sim e^{l_i\ln\frac{s}{t-4m^2}}\sim\left(\frac{s}{t-4m^2}\right)^{l_i}.$$

**ch = cosh.

†The limits of this region are not discussed especially in [10,15]. As a rule, it is assumed that the interval of interest is $-M^2 \lesssim t \lesssim 16\mu^2$. The left half of this interval encloses part of the physical region of the s-channel. The right half, namely the region $t \gtrsim 4\mu^2$, determines the principal analytical properties of the function $l_0(t)$.

assumption has no connection with the preceding assumptions. Its physical meaning is not perfectly clear (some considerations in this respect are advanced in Chapter V). However, it greatly simplifies the calculations and yields results which are usually connected with the MMP.

Making this assumption, we can as $s \to \infty$ retain in the sum (2.10) one higher-order term, since the remaining terms will make an asymptotically decreasing contribution. For the same reason we can discard the integral J(s,t) along the straight line C.* Consequently, as $s \to \infty$,

$$A(s,t) \to \frac{iB_0(t)}{16\pi} s^{l_0(t)} = \frac{s}{16\pi} iB_0(t) e^{(l_0(t)-1)\ln s}, \quad (2.10a)$$

with $B_0(0)$ regarded as pure real [see (2.14a) below]. Now, using the optical theorem (2.4), we can obtain the total interaction cross section $\sigma \to B(0)s^{l_0(0)-1}$. We see that the result depends on the limiting position of the most essential—the extreme right—pole at $t = 0$. In this theory it cannot be calculated (to this end it would be necessary to have the equation which $l_0(t)$ obeys; knowledge of this equation—the "dynamic principle"—would be equivalent to some degree to knowledge of the S-matrix algorithm referred to above). We can, however, proceed in two ways. We can either accept as experimental the fact that the total cross section at superhigh energies tends to a constant. Then we should have $l_0(0) = 1$. We can alternately assume the double dispersion relations and the conclusion based on them that if σ increases at all it does so not in accordance with a power law [see above, $\sigma \leq (\ln s)^2$], and therefore impose the "principle of maximum force" (Chew [18]), that is, to stipulate the maximum cross section which is still compatible with the double dispersion relations. We again obtain $l_0(0) = 1$.

Thus

$$\lim_{E\to\infty} \sigma(s) = \sigma_0 = B_0(0). \quad (2.11)$$

We present, in addition, an expression for A(s,t) in terms of the residue $r_0(t)$ of the function $f(l,t)$ in the extreme right-hand pole

$$A(s,t) = r_0(t) \frac{1+e^{i\pi l_0(t)}}{\sin \pi l_0(t)} (2l_0(t)+1) \left(\frac{s}{2m^2}\right)^{l_0(t)}. \quad (2.11a)$$

Of great importance for what follows is the question of the dependence of l_0 on t, the question of the character of the principal pole trajectory. If $l_0 = 1$ and does not depend on t (the pole is then called "standing") the amplitude can be represented in the form

$$A(s,t) = \operatorname{Im} A(s,t) = s\varphi(t) \quad (\operatorname{Re} A(s,t) = 0). \quad (2.12)$$

This multiplicative form corresponds completely to the classical diffraction pattern: the angular distribution of the scattered particles depends on the angles and the energy only in the combination

$$t = -2p^2(1-\cos\theta_s).$$

However, as shown by Gribov [10], this is impossible by virtue of the unitarity condition and the double dispersion relations, and the pole cannot be standing (see the appendix). Therefore l_0 should depend on t and, it turns out that its derivative

$$\left(\frac{\partial l_0(t)}{\partial t}\right)_{t=0} = l'(0)$$

should be positive and cannot vanish (otherwise the residue r_0 and the total cross section also vanish). The latter property is very important for it leads to the important and not trivial consequences of the MMP. For sufficiently small t, confining ourselves to the first terms of the expansion.

$$l_0(t) \approx l_0(0) + l_0'(0)t = 1 + \gamma t, \quad \gamma = l'(0),$$

we have

$$\operatorname{Im} A(s,t) \approx \frac{s}{16\pi} B_0(t) e^{-\gamma|t|\ln\frac{s}{s_0}}, \quad s_0 = 2m^2. \quad (2.13)$$

Further, according to (2.11a)

$$\operatorname{Re} A(s,t) \approx \gamma t \operatorname{Im} A(s,t). \quad (2.14)$$

From these formulas, first derived by V. N. Gribov [10]*, follow the important properties of elastic scattering at extremely large energies.

First, the characteristic values of the momentum transferred in elastic scattering are, according to (2.13),

$$\sqrt{|t|_{\text{eff}}} \sim \frac{1}{\sqrt{\gamma \ln \frac{s}{s_0}}}, \quad (2.15)$$

that is, $\sqrt{|t|_{\text{eff}}}$ and the transverse component of the momentum transfer decrease with energy, albeit weakly. It can be stated that the reciprocal quantity, which has the meaning of the effective interaction radius, increases like

$$\frac{1}{\sqrt{|t_{\text{eff}}|}} = r_{\text{eff}} \sim \sqrt{\gamma \ln \frac{s}{s_0}}. \quad (2.15a)$$

Accordingly

$$|\operatorname{Re} A(s,t)| \sim \frac{1}{\ln \frac{s}{s_0}} |\operatorname{Im} A(s,t)| \ll |\operatorname{Im} A(s,t)|, \quad (2.14a)$$

that is, the amplitude becomes pure imaginary as $s \to \infty$ and in this sense elastic scattering becomes pure diffraction and is brought about by inelastic processes. However, if we now substitute A(s,t)

*We note that in the theory of radio wave propagation in a homogeneous atmosphere around a homogeneous earth this integral vanishes because the integrand is odd [9].

*Outwardly they coincide exactly with the formulas obtained by Regge in the nonrelativistic theory, and some authors[15,19] have simply transferred them to our relativistic problem without any special discussion.

$\approx$ Im A(s,t) from (2.13) in (2.3) and calculate the total elastic scattering cross section, then, as can be readily seen, we obtain (neglecting the dependence of B on t, that is, assuming $B(t) \approx B(0) = \sigma_0$)

$$\sigma_{el} \sim \frac{1}{\ln \frac{s}{s_0}} \sigma_0^2.$$

Consequently, σ_{el} decreases with energy. Thus, in the limit elastic scattering disappears completely. This means that the particles "swell up" so to speak [see (2.15a)], but at the same time they become "grayer" and more transparent, in such a way furthermore that the total absorption remains unchanged, $\sigma = \sigma_0$, and the diffraction scattering by such a rarefied cloud vanishes.

Formula (2.13) in conjunction with (2.3) is frequently written in the form

$$\frac{d\sigma_{el}/dt}{(d\sigma_{el}/dt)_{t=0}} \approx e^{At}, \quad A = 2\gamma \ln \frac{s}{s_0} \qquad (2.16)$$

It is clear that in accordance with the "principle of maximum force" (for a more detailed derivation see the appendix) the results must not depend on the type of the strongly interacting particles, that is, $l_0(t)$ should be the same, for example, for $\pi\pi$, πN, and NN (N is the symbol for the nucleon). For all these processes the scattering cone should shrink in the t scale with increasing s. This differs from the ordinary picture of diffraction scattering by a black sphere, which, as already mentioned, would correspond to the multiplicative form (2.12). In this sense it is sometimes stated that in the MMP the scattering does not have a diffraction character. Thus, the term "diffraction scattering" is used with different meanings.

These conclusions were experimentally confirmed in investigations of proton-proton scattering energies in the accelerator range (from 3 to 26 BeV). First, these experiments show clearly shrinkage of the diffraction cone with increasing energy [20,21]. This fact is seen from Fig. 7 [21] (see also the reviews [22] and [23]). Second, on the basis of the experimental data it became possible to determine the parameter $\gamma = l'(0)$, which was found to be $\gamma \approx 1/M^2$ [24,25] (according to the latest determinations $\gamma \approx 1/1.5\,M^2$ for $10 < E_L < 20\,M$ [21]).

Third, the form of the function $P_0(t)$ could be determined approximately. For $|t| < 0.5\,M^2$ it can be approximated by the expression $B_0(t) \approx \exp(1.6t)$ (see [23]).

On the whole, the amplitude of the pp scattering can be represented for $0 < -t < M^2/2$ in the form

$$A(s,t) \approx \mathrm{Im}\,A(s,t) = \frac{s\sigma_0}{16\pi} e^{\left(1.6 + \frac{1}{M^2} \ln \frac{s}{2M^2}\right)t}. \qquad (2.17)$$

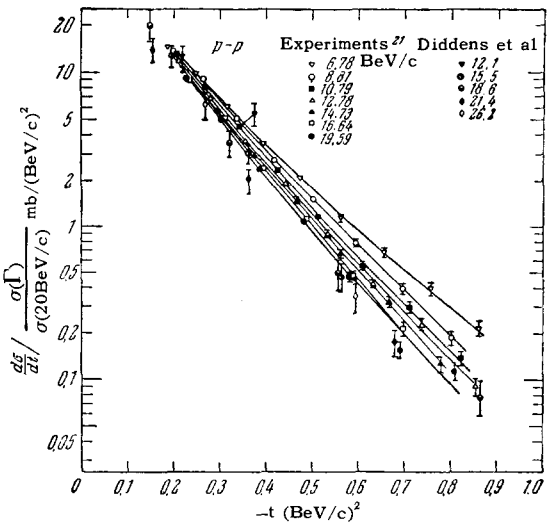

FIG. 7. Experimental data on elastic pp scattering (according to [21]). Different energies correspond to different dependences of the differential cross section on t.

4. Extension to Other Processes

This success of the theory has stimulated interest in broadening the field of application of the MMP and relating it with the problem of the systematics of strongly interacting particles. We first call attention to the fact that asymptotically, as $E \to \infty$, the scattering amplitude reduces to a single term corresponding to a single pole trajectory $l_0(t)$, which produces in the crossed channel scattering with energy $\sqrt{t/4}$, which in the limit is equal to zero, and with angular momentum $l = l(0) = 1$. It can be interpreted (in the s-channel) as scattering with the transfer of a "particle" which has at $t = 0$ an angular momentum $l = 1$ (the zigzag line on Fig. 8). Since the scattering is elastic, this "particle" does not transfer either charge or baryon number or strangeness. In other words, it has the same quantum numbers as vacuum. It is sometimes called a vacuum reggeon. Accordingly, this pole and the entire trajectory are called the vacuum or Pomeranchuk pole (to highlight its connection with the Pomeranchuk theorem on the asymptotic equality of the particle and antiparticle cross sections). Such a particle can be observed as a free particle, with mass $\sqrt{t} > 0$, as a resonance in a system of two pions for even l. There are experimental indications [26] that it actually exists and manifests itself as a resonance of π particles with $t \sim 25\mu^2$ and $l = 2$, the remaining quantum numbers coinciding with those of vacuum.

In such a case the other non-vacuum trajectories correspond to exchange of quanta with different quan-

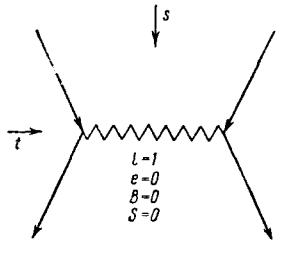

FIG. 8. Interaction via exchange of a vacuum pole.

tum numbers and can correspond to really observed particles. Further, in πN scattering we can expect the next pole, the one closest to the principal pole in the t-channel, to correspond to a ρ particle—the resonance state of two pions (Fig. 9)—which is an unstable formation with isospin T = 1 (here, furthermore, T_z = 0) and with spin and parity 1^+, with decay into two pions with mass $\sqrt{t}$ = 750 MeV ≈ 5.5μ.

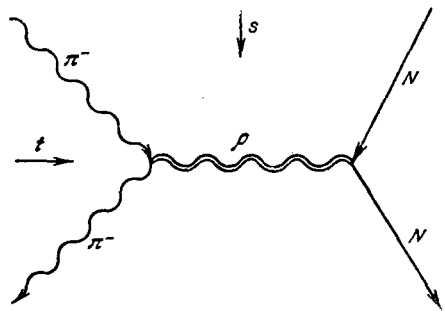

FIG. 9. Interaction via exchange of a ρ meson.

Chew[27] postulated in this connection that any elementary particle (including a "stable" one, say a pion) has its own pole trajectory $l_i(t)$. At the point where t is equal to the square of the particle mass, $t = m_i^2$, l_i should equal the momentum of the particle, that is, its spin J_i:

$$l_i(m_i^2) = J_i.$$

Chew proposed further that in the region $|t| \lesssim M^2$ (M —nucleon mass) all the trajectories can be approximated by straight lines of constant slope

$$l_i(t) = b_i + \gamma t,$$

where γ is a constant on the order of $1/M^2$ and is the same for all trajectories. In this case we can readily determine b_i from the condition $l_i(m_i^2) = J_i$:

$$b_i = J_i - \gamma m_i^2 \approx J_i - \frac{m_i^2}{M^2}.$$

This hypothesis makes it possible to look at the systematics of strongly interacting particles from a new point of view. Although the existing experimental data on masses, spins, and other quantum numbers of particles do not contradict this hypothesis (Fig. 10), it has not yet been adequately confirmed.

If we accept this hypothesis, then the amplitude of elastic scattering via exchange of one quantum or another (vacuum pole, ρ particle, pion, etc.) can be calculated with the aid of diagrams similar to Feynman diagrams (Figs. 8, 9) but with allowance for the following additional rules, which are obvious from (2.11a), where $(s/2m^2)^{l_0(t)}$ is essentially $P_{l_0(t)}(\cos\theta_t)$[25,28].

1. An additional factor $P_{l_i(t)}(z)$ is introduced, where z is the cosine of the angle in the crossed channel and $l_i(t)$ is the trajectory of the pole describing the given elementary particle.

2. The propagation function $D(k^2)$ is replaced by

$$-\frac{\pi\gamma}{2}\left[\sin\frac{\pi l_i(-k^2)}{2}\right]^{-1}.$$

As $k^2 \to -m_i^2$ this quantity goes over for even J_i into

$$D_0(k^2) = (k^2 + m_i^2)^{-1},$$

that is, it coincides with the propagator. However, when $k^2 + m_i^2 \gg M^2$ it can differ noticeably from the propagator. We shall make use below of the possibility of employing these rules.

So far we have referred to scattering of particles of one sort. Naturally, the question arises, what predictions are given by the method with respect to the character of other elastic processes (πp scattering, etc.) and their connection with one another. Here, too, the MMP has yielded significant results.

On the basis of the two-particle unitarity condition in the crossed channel (for more details see the ap-

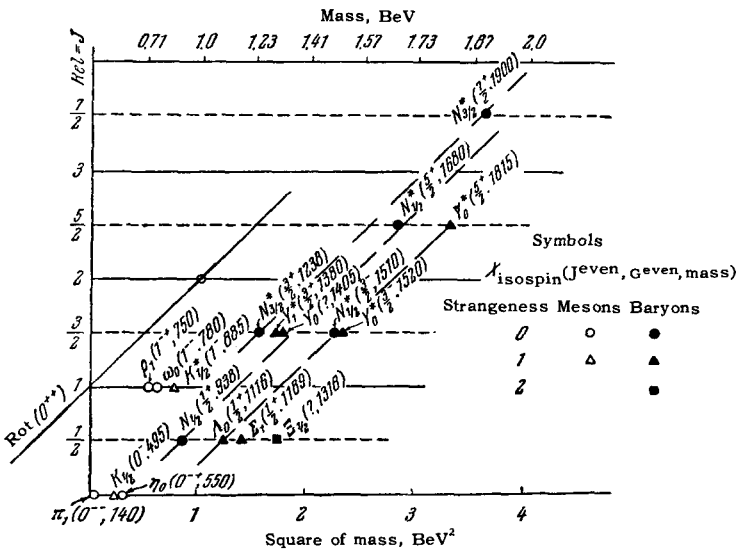

FIG. 10. Systematics of strongly interacting particles and resonances, after Chew [27]. Different lines correspond to different Regge pole trajectories with different quantum numbers (iso-spin T, parity, G-parity). The masses of the individual particles are indicated (in parentheses) in MeV. Real particles and resonances with definite spin correspond to the points of intersection of the given trajectory with the lines l = const = J_i, for integer or half-integer J_i. The particle spins J_i belonging to a given trajectory should differ by ΔJ = 2.

pendix) it was established[10,16,17,28] that: first, all the strong-interaction processes at high energies are determined by the same universal vacuum pole trajectory $l_0(t)$; this means that the shrinkage of the diffraction cone in elastic scattering processes of arbitrary strongly interacting particles should be the same; second, the total cross sections [that is, the values of $B_0(0)$] can be different, but are related by

$$\sigma_{ii}\sigma_{jj}=\sigma_{ij}^2, \tag{2.18}$$

where i and j are the indices of the different particles.

Let us discuss now two specific processes, in which these deductions can be used: the interaction between nucleons and nuclei and scattering of pions by nucleons.

It is important to proceed to the particle-nucleus case primarily because the greater part of the experiments at ultrahigh energies—in cosmic rays—pertain just to this process.

Let us attempt to apply to this process relation (2.18). In this case it assumes the form

$$\sigma_{NN}\sigma_{AA}=\sigma_{NA}^2, \tag{2.18a}$$

where σ_{NN}, σ_{NA}, and σ_{AA} are the cross sections for the interaction between a nucleon and a nucleon, a nucleon and a nucleus of atomic weight A, and a nucleus with a nucleus. It is easy to see that the usually employed "geometrical" dependence of σ_{NA} on A, namely $\sigma_{NA} \sim \sigma_{NN}A^{2/3}$ and $\sigma_{AA} \sim 4\sigma_{NN}A^{2/3}$ does not agree with this condition. Relation (2.18a) is satisfied if $\sigma_{NA} \sim A$ and $\sigma_{AA} \sim A^2$. This somewhat unusual dependence of the cross sections on A can be illustratively interpreted within the framework of the MMP. Indeed, one of the deductions of the MMP, namely the "swelling" and simultaneous "increase of transparency" of particles with increasing energy, predicts the possible character of the particle-nucleus process. When the effective impact paramter

$$k_\perp^{-1} \approx \mu^{-1}\sqrt{\ln\frac{s}{s_0}}$$

($k_\perp$ —transverse component of the momentum transfer) greatly exceeds the nuclear radius, which is equal to $\mu^{-1}A^{1/3}$ (A is the number of nucleons in the nucleus), then the incoming particles can be visualized as a rarefied cloud and all the nucleons of the nucleus should scatter it practically independently. The cross section for the nucleon-nucleus interaction should therefore be of the order of $A\sigma_0$[29]. Yet at moderate energies, according to experiment, so long as $E_L \lesssim 10^{12}$ eV, we have apparently

$$\sigma_A \sim \sigma_0 A^{2/3}.$$

However, even when $E_L \sim 10^{15}$ eV we have $\sqrt{\ln(s/s_0)} \approx 3.5$, so that in the region of conceivable energies such an asymptotic region may perhaps not be attained ($A^{1/3} \approx 6$ for Pb). According to an estimate[30], which to be sure contains arbitrary simplifications and does not claim to be rigorously provable, when $E_L = 10^{15}$ eV the nucleon-nucleus cross section may differ from the geometrical cross section $\sigma_0 A^{2/3}$ for carbon and for lead by approximately 25%. This is precisely the accuracy scale of the experimental data, which thus do not contradict the foregoing conclusion[22].

5. Elastic π^-p Scattering and Contradiction Between Theory and Experiment

We now consider the question of π^-p scattering. According to the MMP, it should behave like pp scattering, that is, the diffraction peak should shrink with increasing energy. However, experiment[21,31] does not confirm this prediction. Experiments offer evidence that the π^-p scattering picture at energies from 7 to 17 BeV is much closer to the classical diffraction picture: the distribution in t is the same at all energies (Fig. 11).

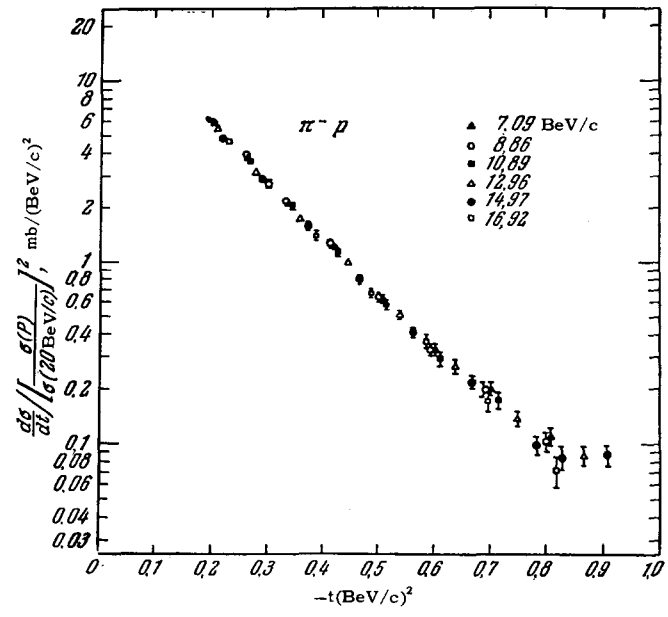

FIG. 11. Elastic π^- p scattering. Different energies correspond to identical dependences of the differential cross section on t.

This departure from theory is of decisive significance to the fate of the entire method. It was therefore natural to attempt immediately to discover within the method itself some unaccounted for elements which would explain the difference between the behaviors of scattering in pp interaction on the one hand, and in π^-p interactions on the other. One of the possibilities is to take into account the trajectories of the other poles that are closest to the vacuum pole trajectory. These are the poles corresponding to the exchange of ρ and ω mesons[32] (see Fig. 10). However, since it is customary, in agreement with Chew, to assume that the trajectories have identical slopes, this simple variant cannot be used to interpret the results. Moreover, a detailed investigation[33] did not lead to the desired result even when account was taken of possible changes

in the slopes. The authors of that paper reach the conclusion (as did the authors of [21]) that it is impossible to explain simultaneously pp and π^-p scattering within the framework of the MMP. Another possibility lies in discarding the assumption of uniqueness of the extreme right pole. We can assume, for example, that at t = 0 two pole trajectories $l_0(t)$ and $l_1(t)$ intersect, and that $l_0(0) = l_1(0)$, but, say,

$$\left(\frac{\partial l_0(t)}{\partial t}\right)_{t=0} \gg \left(\frac{\partial l_1(t)}{\partial t}\right)_{t=0}.$$

This apparently makes it possible to describe both pp and π^-p scattering by choosing suitable parameters (we shall return to this question in Chapter V).

Finally, it is possible, in contradiction to the initial assumption[10,15-17] to assume that other singularities of the amplitude $f(l,t)$ exist in the l plane along with the poles. Recently particular attention has been paid the possibility of appearance of branch points in the l plane. An indication of such a possibility was obtained from an analysis of the contribution of several Feynman diagrams. However, the branch points cannot make a contribution to the cross section that vanishes with increasing energy. In addition, this gives rise to new arbitrary parameters, and the method becomes highly complicated and cumbersome, losing a considerable part of its attractiveness.

Great interest is drawn to the question of the "standing pole" in the l plane (that is, a pole whose position does not depend on l); this is just the pole that can ensure the classical diffraction picture for scattering. However, such poles can be introduced only by discarding the Mandelstam representation. The latter, as indicated above, is itself based on several hypotheses which are far from unconditional. In spite of the fact, it has governed the minds of theoreticians for several years. The failures of the MMP suggest a more critical approach to the Mandelstam representation.

We see that we can distinguish in the described method two aspects. On one hand, we are dealing with representation of the scattering amplitude in the plane of complex orbital angular momenta (the Regge method). In conjunction with the principle of analyticity and the requirements of unitarity and causality, this representation can serve as a useful weapon in the study of interactions at high energies.

On the other hand, a specific variant, (perhaps the simplest one) of the method of complex orbital angular momenta was proposed—the method of moving poles, developed in [10,15-17] and containing additional hypotheses concerning the character of the amplitude singularities. It encounters contradictions when its deductions are compared with experiment. The region of its applicability is apparently limited and can be clarified upon comparison with experiment and with other methods of describing interactions at high energies. At the same time, the physical meaning of the main assumptions made in the MMP and of the results obtained becomes clearer (see Chapter V). A definite stage in the development of this method has thus been completed.

III. THEORY OF PERIPHERAL INTERACTIONS

1. Initial Concepts and Formula for Total Cross Section

Unlike the MMP, which is confined to a study of elastic processes, the theory of peripheral collisions claims also analysis of numerous inelastic processes.

The model representation, according to which the interaction between the nucleons themselves and between nucleons and other particles is realized most frequently via exchange of a single pion, has been for a long time the basis for attempting to treat collisions between particles of very high energy. It started, first, from geometrical considerations: the average impact parameter d ensuring an experimentally observable "geometrical" cross section $\sigma \sim \pi/\mu^2$ must be not small, $d \gtrsim 1/\mu$; second, from notions borrowed from nuclear interactions at low energies, namely that there is an appreciable probability of encountering not more than one virtual pion at such distances from the nucleon. Accordingly, the pattern for nucleon collisions was constructed by the impact parameter method: the meson field of the colliding nucleons (which shrinks relativistically along the motion) was expanded in plane meson waves, a meson flux, and it was assumed [34-37] that such a meson from the cloud of one nucleon interacts with another nucleon as a whole (or with a meson emitted by this other nucleon) in the same manner as the free meson would interact. Without detailing the calculations, the corresponding model was developed by several experimenters [38-40] in the form of a phenomenological picture of the exchange of "energy batches."

This rather primitive treatment gave rise to the concept of "peripheral collisions," which initially was not very distinctly outlined. Essentially, the principal attribute of peripherality was seen in the independence of the decay of two (or more) excited centers produced via meson exchange, something that in the c.m.s. looks like the formation of independent oppositely directed jets. The momentum and energy distributions of the exchanging mesons (determined by the form of the meson cloud of the nucleon or, in other words, by the meson distribution function) determines to some degree the ratio of the two jets [41].

Such an approach could not, of course, be regarded as convincing. It is easy to see, however, that the model representations which it contains serve as a basis of the three more rigorous methods of the theory of peripheral collisions: the Chew and Low method [42], the pole approximation usually called in the literature one-particle exchange [43-47], and the one-meson approximation [48].

It can be stated that the entire theory of peripheral

collisions is based on the assumption that the contribution is made to the amplitude of the inelastic process by the Feynman diagram of Fig. 12, which contains one intermediate meson. The vertex in which this meson interacts with the primary particle can be as complicated as desired* (Fig. 12a), but can also be very simple (Fig. 12b).

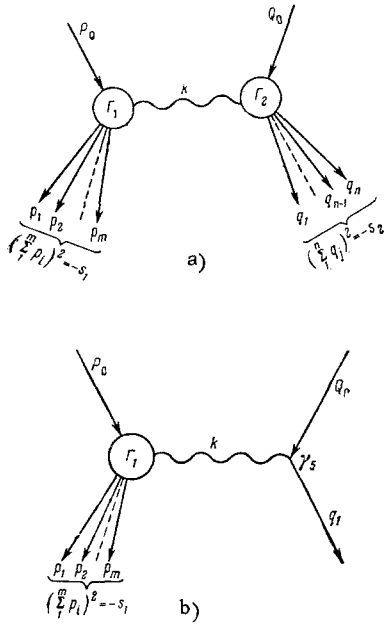

FIG. 12. Feynman diagrams of inelastic one-meson interaction.

The matrix element M_{if} of such a process can be written in accordance with the general rules.

If as collisions between particles of masses m_1 and m_2 and 4-momenta P_0 and Q_0 result in particles with 4-momenta $p_1, p_2, \ldots, p_m$ in one vertex and $q_1, q_2, \ldots, q_n$ in the other vertex, and the transferred meson has a 4-momentum k, then

$$M_{if} = \Gamma_1(k, P_0, p_1, p_2, \ldots, p_m) D(k^2) \Gamma_2(k, Q_0, q_1, \ldots, q_n), \quad (3.1)$$

where $P_0^2 = -m_1^2$, $Q_0^2 = -m_2^2$; Γ_i —vertex parts, which are functions of relativistic invariants constructed from their arguments; $D(k^2)$ —propagation function of the pion, which is close to $(k^2 + \mu^2)^{-1}$ for small k^2.

Strictly speaking, expression (3.1) should be symmetrized with respect to the variables p_i and q_j. In other words, some particles with momenta q_j could generally speaking be produced in the knot 1 but not in knot 2, while particles with momenta p_i —in knot 2. An account of this circumstance would lead to very great complications, since interference terms appear when a symmetrized matrix element is squared.

These effects, however, can be neglected, if the momenta of one group of particles greatly differ from the momenta of the other group, for example, if in the c.m.s. of the entire process the particles are divided into two strongly collimated jets which move in opposite directions. This actually takes place in experiments at very high energies*. In any case, the assumption that there is no interference (owing to the strong collimation of the particles) is always made. This makes it possible to simplify greatly the subsequent calculations. From (3.1) follows an expression for the differential cross section of the process

$$d\sigma = 2\pi \frac{|\Gamma_1|^2 |\Gamma_2|^2}{(k^2+\mu^2)^2} d\varrho_f \delta(P_0 + Q_0 - \Sigma p_i - \Sigma q_j), \quad (3.2)$$

where $d\rho_f$ is the number of final states,

$$d\varrho_f = \prod_i d^3 p_i \prod_j d^3 q_j.$$

The quantity $d\sigma$ can be also represented in the form

$$d\sigma = \frac{d^4k}{(k^2+\mu^2)^2} |\Gamma_1|^2 \prod_i d^3 p_i \delta\left(P_0 + k - \sum p_i\right) \times \prod_j d^3 q_j |\Gamma_2|^2 \delta\left(Q_0 - k - \sum q_j\right). \quad (3.3)$$

Further, the quadruple integration with respect to k, with the integral taken over the azimuthal angle, can reduce to an integration with respect to k^2, s_1 and s_2:

$$d^4k \to \frac{2\pi}{s} dk^2 ds_1 ds_2, \quad k^2 = \mathbf{k}^2 - k_0^2, \quad k_0 \equiv \omega, \quad (3.4)$$

where

$$s_1 = -\left(\sum_{i=1}^{m} p_i\right)^2, \quad s_2 = -\left(\sum_{j=1}^{n} q_j\right)^2, \quad s = -(P_0 + Q_0)^2. \quad (3.5)$$

Thus, with our definition (3.4) of the square of the 4-vector, s_1, s_2, and s are the squares of the energies of the first and second particle groups and of the entire system as a whole, respectively, in their corresponding c.m.s. It is convenient to imagine (so long as we are dealing with kinematic relations this is known to be permissible, but it is possible that this also reflects the physical aspect of the phenomenon, see below) that the particles p_i form in the aggregate a single "cluster" of matter, which then decays into individual particles, and the particles q_j form another cluster. In such a case

$$s_1 = \mathfrak{M}_1^2, \quad s_2 = \mathfrak{M}_2^2, \quad (3.5a)$$

where $\mathfrak{M}_1$ and $\mathfrak{M}_2$ are the masses of the clusters. The region of integration over the variables s_1, s_2, and k^2 is determined by the conservation laws. It can have a rather complicated structure. The principal role in what follows will be played by that part of this region, in which k^2 is small and s_1 and s_2 are large, but both

*Of course, one-meson exchange can lead also to elastic scattering. But it can be assumed that at high energies, when the average number of the particles produced as a result of one-meson exchange is very large, the probability that not a single new particle is produced is exponentially small. Consequently, as will be shown below, the main contribution to elastic scattering can be expected to be made by the two-pion exchange.

*In some papers [49] there are theoretical estimates of the interference terms.

are considerably smaller than s, $M^2 \ll s_1$, and $s_2 \ll s$.* Under these conditions we obtain from the conservation laws at knots 1 and 2 the following formulas for the square of the 4-momentum transfer, for the square of the 3-dimensional momentum, and for the square of its transverse component:

$$k^2 \equiv \mathbf{k}^2 - \omega^2 \approx \frac{(s_1 - m_1^2)(s_2 - m_2^2)}{s} + \frac{(s_1 + s_2)\, s_1 s_2}{s^2} + \frac{s}{2}(1 - \cos\theta_{\mathfrak{M}}), \tag{3.5b}$$

$$\mathbf{k}^2 \approx \frac{(s_1 + s_2)^2}{4s} + \frac{s}{2}(1 - \cos\theta_{\mathfrak{M}}), \tag{3.5c}$$

$$k_\perp^2 \approx \frac{s}{2}(1 - \cos\theta_{\mathfrak{M}}) \approx E^2\theta_{\mathfrak{M}}^2, \tag{3.5d}$$

where ω is the energy transfer; $\theta_{\mathfrak{M}}$ —angle of emission of one of the clusters.

The minimum value of k^2 for fixed s_1 and s_2 is expressed on the basis of these formulas relatively simply: when $\theta_{\mathfrak{M}} \to 0$ it follows from (3.5b) that

$$k^2_{\min} \approx \frac{(s_1 - m_1^2)(s_2 - m_2^2)}{s} + \frac{(s_1 + s_2)\, s_1 s_2}{s^2}. \tag{3.5e}$$

We also emphasize that $k^2 > 0$ in the entire region of integration. Consequently, the 4-momentum of the virtual particle is space-like (for a real pion, to the contrary, $k^2 = -\mu^2 < 0$, where μ is the pion mass).

Let us examine in greater detail part of the diagram of Fig. 12, corresponding to knot 1. It is easy to see that the quantity

$$d\sigma_1(s_1, k^2, p_1, \ldots, p_m) = 2\pi |\Gamma_1|^2 \prod_{i=1}^{m} d^3 p_i \delta\Big(P_0 + k - \sum p_i\Big) \tag{3.3a}$$

can be interpreted as the differential cross section for the production of m particles with momenta $p_1, p_2 \ldots, p_m$ and a total mass $\sqrt{s_1}$ in the interaction between a real particle with momentum P_0 and a virtual pion with momentum k, $s_1 = -(P_0 + k)^2$. If this cross section is summed over all the possible numbers of created particles, over their relative momenta, spins, and other quantum numbers, then the quantity

$$\sum \int d\sigma_1(s_1, k^2, p_1, \ldots, p_m) = \sigma_1(s_1, k^2)$$

can be interpreted as the total cross section for the collision between a virtual pion and a particle, the nature of which (nucleon, pion, etc.) is characterized by the index 1. The quantity $|\Gamma|^2$ can be represented analogously. We note that, owing to the requirements of relativistic invariance, the total cross section $\sigma_i(s_i, k^2)$ of the virtual pion can depend only on the square of the 4-momentum k^2; consequently, the fact that k enters in s_1 and s_2 with opposite signs is of no significance in this case.

The total cross section σ_{12} is obtained from (3.3) after integration with respect to s_1, s_2, and k^2 (assuming the aforementioned summation over the numbers of created particles and their internal variables). It can now be represented in the form

$$\sigma_{12}(s) = \frac{3}{8\pi^2 s^2} \int\int\int \frac{dk^2 s_1\, ds_1 s_2\, ds_2}{(k^2 + \mu^2)^2} \sigma_1(s_1, k^2)\, \sigma_2(s_2, k^2) \times R(s_1, s_2, k^2, m_1, m_2). \tag{3.6}$$

If $s_1, s_2, s \gg m_1^2, m_2^2$, where m_1 and m_2 are the masses of the colliding particles, then $R \approx 1$. In the opposite case the integrand contains the additional factor

$$R = \frac{1}{s_1 s_2}\{[(s_1 - m_1^2 + k^2)^2 + 4m_1^2 k^2]\,[(s_2 - m_2^2 + k^2)^2 + 4m_2^2 k^2]\}^{1/2}. \tag{3.6a}$$

2. Classification of Methods

We now can proceed to describe the different approximations in the theory of peripheral collisions.

1. Of great importance is the particular and simplest process considered by Chew and Low[42], corresponding to the production of only one additional particle upon collision between a nucleon and a pion (Fig. 13), $m_1 = M$, $m_2 = \mu$. It is assumed here that the vertex Γ_i can be written in the form $g(\bar{\psi}\gamma_5\psi)\varphi$. Then we can obtain from (3.3) [taking (3.4) into account]

$$d\sigma_{\pi N} = \frac{f^2}{4\pi} \frac{\sqrt{s_2(s_2 - 4\mu^2)}}{\mu q_L} \frac{k^2\, dk^2\, ds_2}{(k^2 + \mu^2)^2} \sigma_{\pi\pi}(s_2, k^2), \quad f = \frac{\mu}{2M} g, \tag{3.7}$$

where $s_2 = -(Q_0 + k)^2$ —square of the energy of the two colliding (real and virtual) pions in their common c.m.s., $\sigma_{\pi\pi}(s_2, k^2)$ —total cross section for the collision of these pions, and q_L —momentum of the primary meson in the laboratory system. As $k^2 \to -\mu^2$, $\sigma_{\pi\pi}$ goes over into the cross section for the collision of two real mesons. This formula enables us to use the experimental data on the generation of the pion in the πN collision, by extrapolating the quantity

$$\frac{d\sigma_{\pi N}(k^2 + \mu^2)^2}{k^2\, dk^2\, ds_2}$$

to the region $k^2 < 0$, to determine the cross section

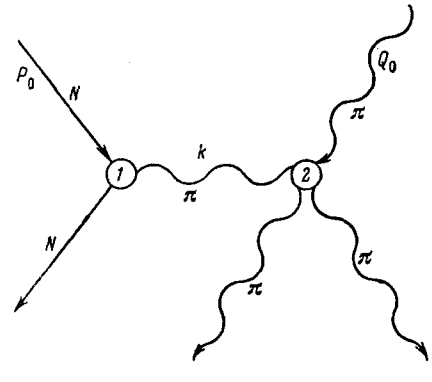

FIG. 13. Diagram of the process considered by Chew and Low.

*The latter condition signifies that the rest energy of the clusters is much smaller than the total energy. This always holds in practice, since the greater part of the total energy goes over into the kinetic energy of the clusters, $\mathfrak{M}_1, \mathfrak{M}_2 \ll \sqrt{s}$, so that the resultant particle jets are collimated.

$\sigma_{\pi\pi}(s_2, -\mu^2)$, which cannot be measured directly for unstable particles such as pions. This method was used quite successfully. In spite of some uncertainty in the extrapolation process, it was used to determine the resonance in the $\pi\pi$ interaction at $s_2 \approx 0.5$ BeV ($\sqrt{s_2} \approx 750$ MeV)[51], subsequently confirmed by a study of the angular correlations and called ρ-resonance.

The method of Chew and Low has been the subject of an extensive literature (see, for example [45]). Furthermore, processes in which so small a number of particles is generated are of rather subordinate significance in the region of very high energies of interest to us. We shall therefore not analyze it in detail. We note only that in order for the extrapolation procedure to be successful, the quantity $\sigma_{\pi\pi}(s, k^2)$ as a function of k^2 must be sufficiently smooth. The agreement obtained as a result of a comparison with experiment shows that at least for small values of s the quantity $\sigma_{\pi\pi}(s, k^2)$ depends weakly on k^2. The difference between k^2 and $-\mu^2$ characterizes the difference between the properties of the virtual meson and those of the real one. Therefore the quantity $k^2 + \mu^2$, which is not equal to zero for a virtual particle, or simply the quantity k^2, is sometimes called the virtuality or degree of virtuality.

Expression (3.6) enables us in principle to calculate also the different characteristics of the process, both integral (for example, the total cross section) and differential (for example, the momentum distribution of the secondary particles), if we know how $\sigma_i(s, k^2)$ depends on k^2 (when we are talking of the integral cross section) or on $\sigma_i(s, k^2, p_1, p_2, \ldots, p_m)$ (when we deal with distributions). This way (which is the opposite of that used in the Chew and Low approximation, where $\sigma_{\pi N}$ was determined from $\sigma_{\pi\pi}$), is used in a different method, called the pole approximation[43-47]. This is based on the assumption that the $\sigma_i(s_i, k^2)$ do not depend at all on k^2, but coincide with the cross sections for the interaction of real particles, that is,

$$\sigma_i(s_i, k^2) \approx \sigma_i(s_i, -\mu^2).$$

It can be stated that it is assumed here that the principal dependence on k^2 in (3.3) is given by the factor $(k^2 + \mu^2)^{-2}$. This assumption is fundamental for the pole method. It could be expected beforehand for it to be valid only in a limited region of the variables s and k^2, primarily so long as k^2 is small. What this region is can be stated more precisely only after comparison with experiment. It was first necessary to verify, on the basis of qualitative considerations, that the principal or at least a major role is played in inelastic interactions with exchange of one pion (or, if we deal with the variation of strangeness in the knot, exchange of one K meson). This could be realized first at low energies and corresponding low multiplicities for nucleon-nucleon collisions. At low energies an appreciable contribution is made by the process in which the interaction between the pion and nucleon in the knots of the diagram (Figs. 12a and b) is resonant, and isobars with $T = 3/2$ and $J = 3/2$ are produced (two isobars are produced at 9 BeV (see I. E. Tamm[52]) and one isobar at 2 BeV[47]). On the basis of this process it becomes easy to explain why the proton conserves its charge and energy in a considerable fraction of proton-neutron collisions (this fact was observed experimentally at 9 BeV independently and somewhat ahead of the theoretical calculations).

These qualitative verifications, as well as more detailed quantitative ones[47,54-56] give valid grounds for assuming that the one-pion exchange causes at any rate an appreciable part of all the strong interactions in the region of accelerator energies.* The use of this method turned out to be quite successful also in the calculation of interactions between γ quanta and nucleons (generation of pions by photoeffect on a virtual meson[45]) and in many other cases. At first many authors attempted[44,46] to adhere to a region of small k^2, for example $k^2 \lesssim \mu^2$, but the pole approximation gave unexpectedly good results in the description of numerous details (energy, charge, and angular distributions of the products) observed in experiments with nucleon-nucleon collisions with $E_L \approx 9$ BeV[55] and at 2 BeV[54,59], for larger values of k^2 up to $k^2 \sim 15\mu^2$.

The agreement between the different characteristics of the nucleon-nucleon interactions, calculated and measured in experiment, makes it possible to state that the one-meson interactions play a principal role in this case. The contribution made to the cross section by central collisions in NN interactions is much smaller than the contribution of the peripheral interactions.

With such an approach to π^-p interactions at 7 BeV, it was shown[56] that the peripheral interactions are significant in this process, too, but on the whole the agreement between the measured characteristics and those calculated in the one-meson approximation is much worse. It was noted in [60] that the cross sections for central and peripheral collisions, σ^C and σ^P, are of the same order in π^-p interactions, whereas in NN collisions σ^C plays a minor role. To estimate the contributions of σ^C and σ^P it is convenient, for example, to use the energy distribution of the recoil nucleons. Peripheral interactions make a contribution principally in the region of small ϵ_k (ϵ_k is the kinetic energy of the recoil nucleons in the laboratory system). Therefore the theoretical curves obtained in accordance with the one-meson approxima-

*General symmetry criteria were formulated to verify the one-meson interaction scheme in individual experiments by means of the angular and momentum distribution [57] (or the charge distribution [58]). They have not been used to a sufficient degree.

tion must be normalized to fit the experimental data for small $\epsilon_k \leq 0.5$ M. The fraction of the observed cases which do not fit on the one-meson approximation curves in the region of large ϵ_k can then be ascribed to central collisions. This procedure was used for a rough estimate of the ratio in pp and π^-p interactions [61] and yielded

$$\left(\frac{\sigma^C}{\sigma^P}\right)_{pp} \approx 0.2, \quad \left(\frac{\sigma^C}{\sigma^P}\right)_{\pi^- p} \approx 1. \tag{3.8}$$

Such a difference between the nucleon-nucleon and meson-nucleon interactions will be of importance to us in what follows. For the time being we emphasize that peripheral interactions play a noticeable (essential) role in all processes and at accelerator energies they are satisfactorily described by the simplest variant of the OMA (actually in the pole approximation). To the contrary, at higher energies the pole approximation meets with considerable difficulties even in the estimate of the value of the total cross section. Let us discuss this in greater detail.

At high energies, s_1, s_2, $s \gg M^2$, the expression for the total cross section, as already mentioned, is obtained from (3.6) with R = 1. We can write

$$\frac{d^2\sigma_{12}}{s_1\, ds_1 s_2\, ds_2} = \frac{3}{8\pi^2 s^2} \int \frac{dk^2}{(k^2+\mu^2)^2}\, \sigma_1(s_1, k^2)\, \sigma_2(s_2, k^2). \tag{3.6a}$$

In the pole approximation the cross sections σ_i are equal to the cross sections for the interaction of real particles, and consequently at high energies they can be assumed constant. It then turns out that the integral of (3.6), taken over the region bounded by the conservation laws, gives a cross section which increases with energy, $s_{12} \sim s$.[62] This result contradicts the initial premise that σ approaches a constant value as $s \to \infty$, and contradicts in general the unitarity condition. The region of values of k^2 which make a contribution is in this case also very large and increases with increasing energy s. Already at $E_L = 10^{11}$ eV the cross section calculated in this manner[62] turns out to be $\sigma \approx 1000$ mb, which of course is absurd. The characteristic values of k^2 reach in this case $10^3\mu^2$.

The absurdity of these results indicates that the pole approximation is not valid in the region of large k^2 which grow without limit. A way out is to make the integrand $\sigma_i(s_i, k^2)$ limit the region of integration in s_i and k^2*. This served as the basis for the third method of the theory of peripheral collisions, the so-called one-meson approximation[48]*. On one hand, it can be assumed that $\sigma_i(s_i, k^2)$ in each of the two knots decreases with increasing k^2 all the more rapidly, the larger s_i. In this case a nonvanishing contribution to the cross section should be made by a process in which both vertices represent central interactions and do not break up into a larger number of knots. Processes in which there are more than two knots can contribute here, but this contribution is small and does not increase with increasing energy. This variant of the OMA will be arbitrarily called the two-center model.

On the other hand, it can be assumed that for a given k^2 the cross sections in the vertices $\sigma_i(s_i, k^2)$ decrease rapidly with increasing s_i. In the limiting case we can assume that $\sigma_i(s_i, k^2)$ differs from zero only in a region of very small s_i that are sufficient for the formation of two particles only. The process is then realized for high energies because each knot of the diagram of Fig. 12a is subdivided into a large number of knots connected by meson lines. We thus arrive at the multicenter or completely peripheral (multiperipheral) model.

3. The Two-center Model

Many authors[43,46] have attempted to confine themselves at high energies to an account of the contribution made from the region of values of k^2 smaller than a certain limited value δ^2 = const, assuming that, independently of the value of s_i, the pole approximation can certainly be used for arbitrary energy when $\delta^2 \lesssim \mu^2$. This assumption that the contribution of small k^2 is independent of s_i is equivalent to some degree to the assumption that, at least for small k^2,

$$\sigma_i(s_i, k^2) = \sigma_0(s_i)\, \varphi(k^2), \qquad \sigma_0(s_i) \equiv \sigma_i(s_i, -\mu^2). \tag{3.8'}$$

However, no matter how we choose δ^2, this approach also leads to contradictions. An important aspect in this case is the factorization of the dependence on the two variables contained in σ_i. Namely, assuming that $\sigma_0(s_i)$ is constant as $s_i \to \infty$ and substituting $\sigma_i = \sigma_0\varphi(k^2)$, we find that σ_{12} is proportional to the logarithm of the energy[46,43]. Although this result does not contradict the unitarity conditions[6], it does offer evidence that the scheme is logically incomplete.†

*One might think that there is another way—forego the use of the approximate value of the propagator

$$D(k^2) = (k^2+\mu^2)^{-1}.$$

However, from the Lehmann representation

$$D(k^2) = (k^2+\mu^2)^{-1} + \int \varrho(\varkappa^2)\, (k^2+\varkappa^2)^{-1}\, d\varkappa^2,$$

where $\rho(\kappa^2) > 0$, it follows that in this case the total cross section σ_{12} would increase even more.

*Thus, the method which we call the one-meson approximation differs from the so-called one-particle exchange (OPE) approximation [43,44], which in accordance with our terminology coincides with the pole approximation.

†In a complete scheme the cross sections should have the same energy dependence on the right and on the left of (3.6). Such a requirement can be satisfied if we assume that σ_0 decreases logarithmically with energy, $\sigma_0 \sim 1/\ln s$. This possibility was discussed extensively in the literature for some time [46,22] but was subsequently refuted both because of disagreement with experiment (apparently there was no observed decrease in the cross section) and because of the inapplicability of the multiplicative relation

In addition, the already mentioned difficulties of different nature arise here. Namely, from a comparison of the theoretical calculations with experimental data in the region $E_L \lesssim 10$ BeV it follows that $\delta^2 \sim (50-60)\mu^2$[64,65]. However, if we use the same quantity even at 10^{11} eV, the total cross section is already many times larger than the observed one[62].

Thus, we cannot confine ourselves within the framework of the two-center model to the simplest multiplicative form of $\sigma(s, k^2)$. In the general case, if we write

$$\sigma_i(s,\ k^2) = \sigma_i(s) F_i(s,\ k^2), \tag{3.9}$$

then F_i depends essentially on s. The function $F_i(s, k^2)$, which is sometimes called the pion form factor[54], is positive. Obviously, $F_i(s, -\mu^2) = 1$ if $\sigma_i(s)$ is the cross section for the interaction of real particles. The properties of the function F_i were investigated separately in [48,63]. It was ascertained that the class of possible functions F_i is greatly limited by four conditions: natural requirement of positiveness, analytic properties in k^2 (in the region $k^2 > 0$), the condition $F_i(s, -\mu^2) = 1$, and the condition of asymptotic constancy of all cross sections. For example, the function F_i cannot be a ratio of two polynomials in k^2, etc. All these conditions are not sufficient for a unique determination of F_i. By way of an example satisfying all requirements we can consider some expression, with $k^2 > 0$ and $s \gg M^2$, which goes over into the function

$$F_i(s,\ k^2) \approx \mu^2 \gamma \ln \frac{s}{2M^2}\, e^{-\gamma k^2 \ln \frac{s}{2M^2}}. \tag{3.9a}$$

We see that the k^2 region contributing to the integral (3.6) decreases here with increasing energy in such a way that the effective values of k^2 are of the order of

$$k^2_{\text{eff}} \sim \frac{1}{\gamma \ln \frac{s}{2M^2}}. \tag{3.9b}$$

Such a logarithmic decrease in the effective k^2 is quite likely, in spite of the fact that the function F_i itself is not single valued. Indeed, this behavior of F_i is simply the consequence of the fact that the integral (3.6) with $F = \text{const}$ is logarithmically dependent on the energy. Consequently, in order for this dependence to disappear when σ_i is constant, we must decrease logarithmically the region of integration with respect to k^2.

Further, the effective region is determined by the parameter γ. Experience in the application of the method at accelerator energies, where $\ln(s/2M^2) \sim 1$ and $k^2_{\text{eff}} \sim M^2$[55] indicates that this parameter has an order of magnitude $\gamma \sim 1/M^2$.

We note that an analogous behavior is displayed not only by the invariant quantity k^2, but also by the modulus $|\mathbf{k}|$, and the components $k_{\parallel}$ and $k_{\perp}$ of the three-dimensional momentum, calculated in the c.m.s. of the process. In particular,

$$k^2_{\perp\,\text{eff}} \sim \frac{1}{\gamma \ln \frac{s}{2M^2}}.$$

This denotes that in the one-meson interactions the effective impact parameter $r_{\text{eff}} \sim k^{-1}_{\perp\,\text{eff}}$ increases with increasing energy logarithmically

$$r_{\text{eff}} \sim \sqrt{\gamma \ln \frac{s}{2M^2}}.$$

Any inelastic process causes some elastic process, as follows at least from the optical theorem. Let us clarify the properties that should be possessed by particle elastic scattering due to an inelastic process of a one-meson character. Using the optical theorem (2.4) we can rewrite (3.6) in the form

$$A_{12}(s, 0) = \frac{2}{\pi s} \int \frac{A_1(s_1,\ k^2,\ 0)\, A_2(s_2,\ k^2,\ 0)}{(k^2+\mu^2)^2}\, ds_1\, ds_2\, dk^2, \tag{3.10}$$

where $A_{12}(s, 0)$ is the imaginary part of the amplitude of the mutual forward scattering of two real particles 1 and 2; $A_1(s_1, k^2, 0)$ and $A_2(s_2, k^2, 0)$ are the imaginary parts of the amplitudes of the forward scattering of a virtual pion by real particles 1 and 2.

The diagram of elastic scattering resulting from a one-meson inelastic process (Fig. 12) can be obtained by squaring the inelastic-process diagram. It is shown in Fig. 14. Calculating the imaginary part of the amplitude of this process by Feynman's rules, we can readily arrive at an expression for $A(s,t)$ which goes over into (3.10) when $t = -(k_1 - k_2)^2 = 0$.

From the fact that, in accordance with (3.9a), all the components of the vectors k_1 and k_2 in the c.m.s. decrease with increasing energy, it follows that t should also decrease at least as rapidly, for example like

$$-t_{\text{eff}} \sim \frac{1}{\gamma \ln \frac{s}{2M^2}}.$$

We recall that this is precisely the behavior of elastic scattering in the MMP.

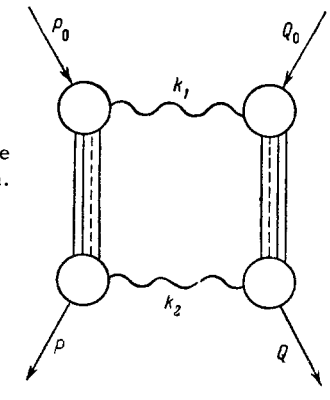

FIG. 14. Elastic scattering due to one-meson inelastic interaction.

$$\sigma(s,\ k^2) = \sigma_0(s)\, \varphi(k^2).$$

The latter follows, as shown in [63] from the general properties of the scattering amplitude in the so-called Dyson-Jost-Lehmann[64] representation.

Let us consider within the framework of the two-center model the mutual connection between the total interaction cross sections of different particles [65]. It is caused by the properties of the form factors $F_i(s, k^2)$. It seems quite natural to assume that F_i depends only on the properties of the pion which transfers the interaction, and does not depend on the properties of the real particle with which it interacts. Then

$$\sigma_i(s, k^2) \equiv \sigma_{i\pi}(s, k^2) \approx \sigma_{i\pi} F(s, k^2), \qquad (3.11)$$

where $F(s, k^2)$ does not depend on the type of the real particle denoted by the index i (this can be the symbol for a nucleon, pion, etc.). In the cases of nucleon-nucleon collisions (the cross section is σ_{NN}) and a nucleon-pion collision (cross section $\sigma_{\pi N}$) we obtain from (3.6), respectively,

$$\sigma_{NN} = \sigma_{N\pi}^2 J_\pi, \qquad (3.12a)$$

$$\sigma_{\pi N} = \sigma_{\pi N}\sigma_{\pi\pi} J_\pi, \qquad (3.12b)$$

where J_π denotes a universal quantity which depends only on the properties of the pion, particularly its mass:

$$J_\pi = \frac{3}{8\pi^2 s^3}\int \frac{s_1\, ds_1 \cdot s_2\, ds_2\, dk^2}{(k^2+\mu^2)^2} F(s_1, k^2) F(s_2, k^2). \qquad (3.13)$$

It follows from (3.12b) that

$$J_\pi = \frac{1}{\sigma_{\pi\pi}}. \qquad (3.13a)$$

Consequently, (3.12a) yields

$$\sigma_{NN}\sigma_{\pi\pi} = \sigma_{\pi N}^2. \qquad (3.14)$$

Analogously, for the interaction of any other particles we obtain the relations already obtained in the MMP [see (2.18)].

We emphasize that in this case all these conclusions are the results of an investigation of the inelastic process. We shall see later that similar results are obtained also in the multiperipheral model. At the same time, they coincide with the analogous deductions of the MMP. Even the parameters γ turn out to be the same (in order of magnitude). All this suggests that a deep connection exists between the OMA and the MMP. This connection was considered in more general form in [66] (we shall discuss this question in greater detail in Chapter V). All these results give grounds for assuming that the known asymptotic behavior of the elastic-process cross section, prescribed by the MMP when account is taken of the extreme right "vacuum" pole, is due precisely to the fact that the inelastic processes which generate such an elastic process are of the one-pion type. If we assume this point of view, then it becomes possible, in order to verify and refine the MMP, to make use of the abundant information on inelastic processes at energies $E_L \gtrsim 10^{11}$ eV. Then, by verifying the validity of describing the processes with the aid of the OMA, we by the same token verify the correctness of the MMP in this region.

We recall that investigation of elastic scattering in this energy region is practically impossible at present. Therefore there is no direct way as yet of verifying the MMP in this region.

We note also that these conclusions concerning the connection between the two methods were advanced recently [65,66] and are not universally accepted. Nonetheless, we shall henceforth use these conclusions in some cases (in comparisons with experimental data).

Let us now list the main assumptions and the main attributes of two-center interactions.

1. The diagram of the inelastic process must break up at least into two parts (and perhaps even more parts), connected by a single pion line. The diagram of the elastic process breaks up in this case into parts which are connected by two pion lines.

2. The interference between the two beams of generated particles can be neglected.

3. The cross sections are calculated in accordance with the Feynman rules, and it is necessary to take into account in the quantities $\sigma_i(s_i, k^2)$ the non-multiplicative dependence on s_i and k^2, which gives the necessary decrease of s_i with increasing k^2. General theoretical considerations show that it is possible to take this dependence into account, for example, by a factor of the type $\exp[-k^2 \ln(s/2M^2)]$ (comparison with experiment shows that in such a case $\gamma \sim M^{-2}$).

It follows therefore that the square of the 4-momentum transferred from one of these jets to the other should decrease with increasing energy, apparently in logarithmic fashion:

$$k_{\text{eff}}^2 \sim \frac{M^2}{\ln(s/2M^2)};$$

The elastic scattering which results from such an inelastic process should have "Regge" properties.

In this connection, when comparing the experimental data with the theoretical ones, the quantity k^2 assumes a fundamental significance.

So far we have dealt principally with the integral characteristics of the process: the total cross section, its asymptotic behavior, and the mean square of the momentum transfer. In inelastic collisions, the most important are questions of multiplicity, angular distribution of the secondary particles, etc.

The one-meson approximation encompasses a rather broad circle of processes, which can differ greatly from one another in these attributes. To describe a process in detail it is necessary to be more specific.

Experience shows that it is hardly possible to propose a single scheme to describe the entire variety of encountered processes (see Chapter IV). We therefore consider the possible processes separately. They differ in the specific form of the vertices of the diagrams, which remain the only undetermined element.

1. Assume that neither of the two vertices can be broken up into further parts connected by a single

meson line. In other words, let the interaction at the knots (the interaction between the virtual and the real particle) have a peripheral character. We shall arbitrarily call it central.* A typical process which involves the production of many particles in one collision, and which is essentially caused by the many-meson interactions, is the hydrodynamic process. It is therefore natural to assume that here, too, the "central" collision at the vertex follows the hydrodynamic scheme (of course this is not at all obligatory according to the Landau hydrodynamic theory). This assumption signifies, however, that in the asymptotic region the peripheral interactions do not account for all the possible processes, and along with these there should be a finite and constant contribution from other, central processes. Indeed, in (3.6a), as $s \to \infty$ the effective s_1 and s_2 also increase without limit. In order for the cross section of the one-meson process on the left side to be constant as $s \to \infty$, it is necessary that the cross sections under the integral sign also not decrease as s_1 and $s_2 \to \infty$. However, in our variant of the OMA we have under the integral sign in the right the cross sections of central collisions (of the pion and nucleon). Consequently, they themselves should make a contribution which does not vanish asymptotically.

Thus, in this variant the peripheral and central (hydrodynamic) collisions are not contradictory but supplement each other. The model is peripherally hydrodynamic. In the general case we obtain complicated formulas. We confine ourselves to two limiting possibilities:

a) Let the excitation of the nucleons by symmetrical

$$s_1 \approx s_2 = s_0 \equiv \mathfrak{M}^2.$$

According to (3.5b) and (3.9b)

$$s_0^2 \approx k^2 s \sim M^2 \frac{s}{\ln (s/2M^2)}.$$

In the common c.m.s. the Lorentz factor $\bar{\gamma}$ of the excited nucleons is (E_c and $M\gamma_c$ are the energies of each of the colliding nucleons in the c.m.s.)

$$\bar{\gamma} = \frac{E_c}{\mathfrak{M}} = \frac{1}{2}\sqrt{\frac{s}{s_0}} \approx \sqrt{\frac{\gamma_c}{2}}\left(\ln \frac{s}{2M^2}\right)^{1/4}. \qquad (3.14')$$

At high energies this quantity is large and increases with energy. The number of secondary particles, if determined at each knot by the hydrodynamic Landau theory (or by the statistical Fermi theory), is

$$n = 2\cdot 2\left(\frac{s_0}{2M^2}\right)^{1/4} \approx 4\left(\frac{s}{4M^2 \ln (s/2M^2)}\right)^{1/8}. \qquad (3.15)$$

Thus, the number of secondary particles increases in this process with the energy somewhat more slowly than in the case of central collisions; the angular distribution in the common c.m.s. is essentially anisotropic (this is ensured by the large values of $\bar{\gamma}$). Specifically, for $E_L \sim 10^{13}$ eV ($\gamma_c \approx 70$) we obtain $\bar{\gamma} \approx 10$ and $n \approx 10$. The distribution over the variable $\lambda = -\log \tan \theta$, where θ is the angle of emission of the particles (see Chap. IV) will have for such a jet the form of two strongly separated groups, with approximately three charged particles (altogether $\frac{3}{2} \times 3 \sim 5$ particles) in each group. Such a scheme, consequently, can correspond only to "lean" jets with n appreciably smaller than in central collisions. The angular distribution (for no other reason than that for secondary particles $p_\perp$ does not depend on n, see Chap. IV) is very anisotropic because n is small.

b) Let the excitation be essentially asymmetrical. In the limiting case, when one nucleon is not excited at all and in the other the multiplicity is given by the Landau hydrodynamics (in this case the second term in (3.5b) assumes a role), we obtain

$$s_1 = M^2, \quad s_2 = \sqrt{\frac{k^2}{M^2}}\, s,$$

$$n = 2\left(\frac{s_2}{2M^2}\right)^{1/4} = 2\left(\frac{s}{2M^2 \ln (s/2M^2)}\right)^{1/4}.$$

The angular distribution can again be characterized by one quantity $\bar{\gamma}$ of the excited nucleon. The formula

$$\bar{\gamma} = \sqrt{\frac{s}{4s_2}}$$

is not sufficiently accurate here; using the conservation laws, we obtain the following more accurate formula:

$$\bar{\gamma} = \frac{1}{2}\left(\sqrt{\frac{s}{s_2}} + \sqrt{\frac{s_2}{s}}\right).$$

The multiplicity and the angular distribution in such interactions do not differ very strongly from those obtained for noncentral collisions. For example, for $E_L \sim 10^{13}$ eV we obtain $n \approx 14$ and $\bar{\gamma} \sim 1.2$. It is not excluded that such interactions describe asymmetrical jets with essentially different inelasticity coefficients ($K_{lab} \neq K_{mir}$, see Chap. IV).

2. Let now the number of knots, which can no longer be separated into smaller knots connected by a single meson line, be larger than two but still small, say three or four. The diagrams of such processes are shown in Figs. 15 and 16. The cross section of such a process can be obtained from (3.6) if $\sigma_1(s_1, k^2)$ or $\sigma_2(s_2, k^2)$ is expressed again with the aid of (3.6). Accordingly, for example if we express in this manner only one of the vertices, we obtain the diagram of Fig. 15 and the corresponding formula[62] (with $s_1 - m^2$, $s_2 - m^2$, $s_{\pi\pi} \gg \mu^2$)

$$\sigma = \frac{1}{(2\pi)^8 s}\int \frac{d^4k_1\, d^4k_2}{(k_1^2+\mu^2)^2 (k_2^2+\mu^2)^2}(s_1 - m^2)(s_2 - m^2)\, s_{\pi\pi} \times \sigma_1(s_1, k_1^2)\, \sigma_2(s_2, k_2^2)\, \sigma_{\pi\pi}(s_{\pi\pi}, k_1^2, k_2^2). \qquad (3.16)$$

In order for such a mechanism to make a nonvanishing

*This type of process can be visualized as follows: owing to the pion exchange, two (and only two) excited nucleons or excited clusters are produced, and then emit secondary particles. This process was considered many times in the literature[35,39].

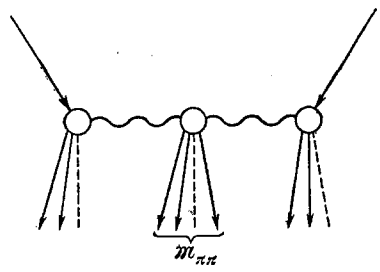

FIG. 15. One-meson inelastic interaction with formation of one additional knot.

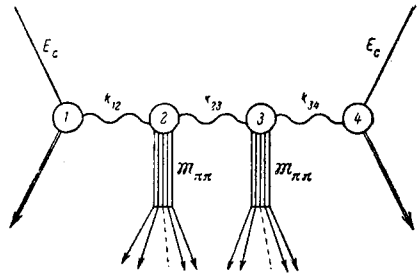

FIG. 16. One-meson interaction with formation of two additional knots.

contribution at high energies, it is necessary that at least one of the cross sections contained in the integrand not be small when the corresponding s_i increases without limit. As in the preceding case, it is therefore necessary to suggest that there exists a nonperipheral central process which gives a nonvanishing contribution at high energies. However, unlike the preceding case, such a process can now be the interaction between two virtual pions. The degree of excitation of the nucleons themselves can remain low in this case if the energy of the entire process is high (for example, this may be excitation to the isobar states $T = 3/2$, $J = 3/2$). In this case, as before (except that now we are considering a strongly excited $\pi\pi$ cluster), we must turn to the hydrodynamic theory.

An interpretation of the experiment in accordance with the scheme of Fig. 15 [67] or Fig. 16 [68] was proposed by the experimenters (in the outer knots, corresponding to the collision between a virtual pion and a nucleon, it was assumed by the experimenters either that no new pions are produced at all, or that their number does not exceed one or two). As shown by comparison with experiment, in such an interpretation the multiplicity is connected with $s_{\pi\pi}$ by the relation [67-69]

$$n \sim \frac{\sqrt{s_{\pi\pi}}}{0.5M^2}.$$

It corresponds to the multiplicity in a hydrodynamic process with a Heisenberg equation of state [70].

A concrete example of such a process for a collision of nucleons with energy $E_L \sim 3 \times 10^{11}$ eV in accordance with the experimental data obtained in [67] was considered theoretically in [62].

The calculation of the diagram of Fig. 15 has led to the following results. The effective values of the squares of the transferred momenta k_1^2 and k_2^2 are of the order of $(20-25)\mu^2$. The distribution over the "masses" of the $\pi\pi$ knot has a sharp maximum near

$$\mathfrak{M}_{\pi\pi} \equiv \sqrt{s_{\pi\pi}} \approx (3-4)M.$$

The excitation of the nucleons, that is, the "masses" of the isobars in knots 1 and 2, is of the order $\mathfrak{M}_{\pi\pi} \sim 1.5\,M$.

To estimate the number of pions produced in the $\pi\pi$ knot, the multiplicity law corresponding to the hydrodynamic theory with the Heisenberg equation of state was used. Then

$$n_\pi = \frac{\mathfrak{M}_{\pi\pi}}{0.5M} \approx 6, \quad n_{\pi^\pm} = \frac{2}{3} n_\pi \approx 4.$$

The angular distribution of the secondary particles in the rest system of the $\pi\pi$ isobar is in this case isotropic. The total number of charged particles in the process (if we take into account the fact that the decay of each of the nucleon isobars results predominantly in charged particles) is found therefore to be $n_s \sim 7-8$. The inelasticity coefficients of the nucleons lie in the interval $0.05 \lesssim K \lesssim 0.25$. The Lorentz factor of the $\pi\pi$ isobar in the c.m.s. of the entire process is $\bar{\gamma} \approx 1.1$ and is consequently small.

All these results are in good agreement with part of the experimental data obtained in [67]. Namely, the diagram under consideration can describe satisfactorily symmetrical showers with small inelasticity coefficients. Another part of the showers has different characteristics. We shall dwell on this in greater detail in Chapter IV.

The process shown in Fig. 16 is important at higher energies, namely $E_L \sim 10^{12}-10^{13}$ eV. It will also be discussed in Chapter IV.

4. The Multiperipheral Model

Expression (3.6) can be used to describe a process with any number of intermediate "knots." For this it is sufficient, using an iteration procedure, to substitute successively in the right half of (3.6) the cross sections $\sigma_i(s_i, k^2)$ in the one-meson form. The limiting case of such a process, the multiperipheral model, has been discussed in the literature. It was first considered by Amati, Fubini, Stanghellini, and Tonin (AFST) [71] (it was already mentioned in [46]). Let us dwell on this model in greater detail. It is assumed here that the smallest possible number of particles—two pions—is formed in each knot of the diagram of Fig. 17 and the process in this knot proceeds via formation of one resonant particle, for example a real meson, or in general a "meson isobar," which then breaks up into two pions, while the number of the knots increases with the energy. The interferences between the different knots are neglected. Such neglect is common to any OMA

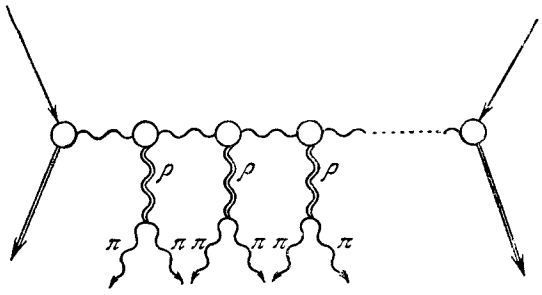

FIG. 17. Feynman diagram of the AFST model (multiperipheral model) of a completely peripheral interaction.

case. In the given model this neglect is equivalent to assuming that in the rest system of any meson isobar the other isobars move relative to it with relativistic velocities. We emphasize that the latter condition is thus also included in the model (although this was not stipulated in the original papers), and here it becomes quite stringent.

The cross section for the interaction in the knot $\sigma^{(R)}(s_i)$ plays a fundamental role in the model. The assumption that only weakly excited two-pion isobars are produced in the knots is equivalent to assuming that the cross section σ^R of interaction of all the virtual pions in the knot has a resonant character and is large only at low energies, $s_i \sim s_0 = 0.5\,M^2$ (that is, in the region where the pions can be produced via a ρ meson, η meson, etc.). In order for the contribution from large s_i not to enter, it is assumed that $\sigma^{(R)}$ does not decrease with increasing s_i more slowly than s_i^{-2}. This assumption is principal in character. It is precisely because of this assumption that the more complicated knots of the diagrams are excluded from consideration. For the same reason, there is no place for the hydrodynamic theory in the framework of the model. To some degree the hydrodynamic theory even contradicts the model, since the main assumption of the model is equivalent to stating that the many-meson exchanges make no contribution whatever to inelastic processes. This is exactly why the model can be called "completely peripheral." We note that such a model is closely connected with the approximate method of the investigation of double dispersion relations, called the strip approximation [66].

The model was investigated in [71-74,50]. It was found that the cross section $\sigma_{\mathfrak{N}}(s)$ of each individual process with $\mathfrak{N}$ vertices, as a function of s, becomes different from zero at a threshold value $s = s_{min} = \mathfrak{N}^2 s_0$, increases, reaches a maximum, and then decreases in power-law fashion. When $s \gg s_{min}$ we have

$$\sigma_{\mathfrak{N}} = a_0 \frac{\left(\beta \ln \frac{s}{s_0}\right)^{\mathfrak{N}-1}}{s^2 (\mathfrak{N}-1)!}, \qquad (3.17)$$

where a_0 and β are some constants. Thus, each individual process (with given $\mathfrak{N}$) makes roughly speaking a contribution only to a definite region of the values of s, after which it gives way to the next process.

The value of $\sigma_{\mathfrak{N}}$ as a function of $\mathfrak{N}$ for a given s is described, in accordance with (3.17), by a Poisson distribution and has a sharp maximum at

$$\mathfrak{N} = \mathfrak{N}_0(s) \approx \beta \ln \frac{s}{s_0}$$

with half-width

$$\Delta\mathfrak{N} \sim \sqrt{\beta \ln \frac{s}{s_0}}$$

(All these estimates, of course, are valid only if $\mathfrak{N} \gg 1$).

The total cross section is equal to the sum of the cross sections

$$\sigma_{tot} = \sum_{\mathfrak{N}} \sigma_{\mathfrak{N}} = \frac{a_0}{s^2} \sum_{\mathfrak{N}} \frac{\left(\beta \ln \frac{s}{s_0}\right)^{\mathfrak{N}-1}}{(\mathfrak{N}-1)!} = \frac{a_0}{s_0^2}\left(\frac{s}{s_0}\right)^{\beta-2}$$
$$= \text{const}\left(\frac{s}{s_0}\right)^{\alpha-1} \qquad (3.18)$$

(where $\alpha = \beta - 1$), and according to the optical theorem the amplitude of scattering through zero angle is equal to the sum of the amplitudes

$$A_{tot}(s, 0) = \sum_{\mathfrak{N}} A_{\mathfrak{N}}(s, 0) = \frac{1}{16\pi} \frac{a_0}{s_0}\left(\frac{s}{s_0}\right)^{\alpha}. \qquad (3.19)$$

The quantities α and β in this model are connected with the quantity $\sigma^{(R)}(s_i)$ and with s_0. This connection has the form [72]

$$\alpha(\alpha+1) = \frac{1}{16\pi^3} \int \sigma^{(R)}(s_i)\, ds_i. \qquad (3.20)$$

It must be noted that the quantity α (and consequently the quantity s_0 which is basic to it) is of fundamental significance for the entire model and determines the main characteristics of the process.

Indeed, when $\alpha < 1$ the total cross section $\sigma_{tot} \sim A/s$ will decrease with energy in a power-law fashion. In this case the model cannot claim to describe the process and consequently becomes meaningless. When $\alpha > 1$ the cross section will increase with energy in power-law fashion, in contradiction to the unitarity condition.

Let us ascertain first what results are obtained with the AFST model when taken literally. According to AFST, it is necessary to confine the integration in (3.20) to the region near $s_i \sim s_0 \sim 0.5\,M^2 \approx 25\,\mu^2$, for it is precisely here that the resonances ρ, η, etc., are located. In this case, according to [72] we get $\alpha \approx 0.3$. This value is appreciably smaller than unity and consequently already offers evidence that the model is not "realistic."*

*The authors state, to be sure, that they can "stretch" their estimates and make α close to unity. But to this end it is necessary to increase the integral (4.20) by almost one order of magnitude (see below). This is difficult to do if the region of integration with respect to s_i is not increased.

Let us consider other characteristics of the act in this model at high energies. The relations given above are valid in the asymptotic region, that is, when $s_{min} = \mathfrak{N}_0^2 s_0 \ll s$ or, since

$$\mathfrak{N}_0 \approx \beta \ln \frac{s}{s_0},$$

when

$$\left(\beta \ln \frac{s}{s_0}\right)^2 \ll \frac{s}{s_0}^*.$$

The number of knots $\mathfrak{N}_0$ is equal to

$$\mathfrak{N}_0(s) = (1+\alpha) \ln \frac{s}{s_0} \approx 1.3 \ln \frac{s}{0.5 M^2}. \qquad (3.21)$$

It follows therefore that the multiplicity in this model increases slowly (logarithmically) with the energy (see also [50]).

The angular distribution in the AFST model is essentially anisotropic. With respect to the coordinate $\lambda = -\log \tan \theta$ it is characterized by a very large width σ_λ, which increases with energy like ln s (in the hydrodynamic model $\sigma_\lambda \sim \sqrt{\ln s}$).

All these results can be explained by considering a simplified variant of the model. Let us assume that "pion isobars" of definite mass $\mathfrak{M}_0 = s_0$ are produced at the knots, and also that all the momentum transfers k_i^2 are identical and equal to k_a^2.

Let us consider two neighboring knots. In the rest system of one of the isobars, the others move with relativistic velocity. Even for the neighboring isobars the relative velocity u should correspond to a large Lorentz factor $\bar{\gamma}_0$ (otherwise we cannot neglect the interference of the particles arising in the neighboring isobars, something which is essential for the method). This of course makes the Lorentz factors of the neighboring isobars $\bar{\gamma}_i$ and $\bar{\gamma}_{i+1}$, in the common c.m.s. of the process all the larger. From the formula for the addition of the Lorentz factors [see Chap. IV below, formula (4.20)] it follows that

$$(1-u^2)^{-\frac{1}{2}} \equiv \bar{\gamma}_0 = \bar{\gamma}_i \bar{\gamma}_{i+1} - \sqrt{\bar{\gamma}_i^2 - 1}\sqrt{\bar{\gamma}_{i+1}^2 - 1}$$

$$\approx \frac{1}{2}\left(\frac{\bar{\gamma}_{i+1}}{\bar{\gamma}_i} + \frac{\bar{\gamma}_i}{\bar{\gamma}_{i+1}}\right). \qquad (3.22)$$

The quantity γ_i decreases as i increases from 1 to $\mathfrak{N}/2$ and then again increases for $\mathfrak{N}/2 < i < \mathfrak{N}$. Therefore $\bar{\gamma}_i > \bar{\gamma}_{i+1}$ for $i < \mathfrak{N}/2$. From the expression for γ_0 it follows that the ratio

$$\frac{\bar{\gamma}_i}{\bar{\gamma}_{i+1}} = a = \bar{\gamma}_0 + \sqrt{\bar{\gamma}_0^2 - 1} > 1$$

is constant, that is, it does not depend on the number i and on the energy s. It follows therefore that when $1 < i < \mathfrak{N}/2$ we can write

$$\gamma_i = a\gamma_{i+1} = a^i \bar{\gamma}_a.$$

The law of energy conservation for an $\mathfrak{N}$-th order process gives

$$E_c = \sqrt{s} = 2\sum_{i=1}^{\mathfrak{N}/2} \sqrt{s_0}\bar{\gamma}_i \approx 2\sqrt{s_0}\bar{\gamma}_0 a^{\frac{\mathfrak{N}}{2}-1}, \qquad (3.23)$$

$$s = 4 s_0 \bar{\gamma}_0^2 a^{\mathfrak{N}-2}. \qquad (3.24)$$

From this we get for the process which makes the largest contribution for a given s*

$$\mathfrak{N}_0(s) = \frac{1}{\ln a} \ln \frac{s a^2}{s_0 \cdot 4\bar{\gamma}_0^2} \approx \frac{1}{\ln a} \ln \frac{s}{s_0}. \qquad (3.25)$$

Thus the multiplicity actually increases logarithmically with the energy.

In the angular distribution of $dn/d\eta$ each knot will make a contribution with respect to η in the region $\eta_i \approx \ln \bar{\gamma}_i = i \ln a\bar{\gamma}_0$. When these contributions are added, they lead to a "table-like" dependence on η. The maximum value of η_{max}, which determines the width of the distribution, will be

$$\eta_{max} = \frac{1}{2} \ln \bar{\gamma}_{\mathfrak{N}_0} = \mathfrak{N}_0 \ln a \approx \frac{1}{2} \ln \frac{s}{s_0}, \qquad (3.26)$$

and in λ coordinates the half-width is

$$\sigma_\lambda = \frac{1}{2}\Delta\lambda = \frac{1}{2.3}\eta_{max} = \frac{1}{2} \log \frac{s}{s_0}.$$

For the energy interval 10^{11}—10^{13} eV the numbers $\mathfrak{N}_0(s)$ [in accord with (3.25)] are given in the table (for $s_0 = M^2/2$). The table lists also the corresponding expected values of the half-width σ_λ. The effective value of k^2 does not depend here on the energy and its order of magnitude is $k^2 \lesssim s_0$. Thus, in the literally-taken AFST model we have $k^2_{eff} \sim 0.5 M^2$. A comparison of these deductions with the experimental data will

E_L, eV	10^{11}	10^{12}	10^{14}
$s/0.5\ M^2$	400	4000	$4\cdot10^5$
$\mathfrak{N}_0 \sim$	6	8	13
$n = 2\mathfrak{N}_0 \sim$	12	16	26
$\sigma_\lambda \sim$	1.3	1.8	2.8

*If $\beta = 2$ we get the condition $s/s_0 \gg 70$. When $\beta = 1.3$ we should have $s \gg 40 s_0$.

*On the other hand, for $\mathfrak{N}_0(s)$ we have $\mathfrak{N}_0(s) = \beta \ln(s/s_0)$. Comparing these expressions, we can estimate the quantities $a = \exp \beta^{-1}$ and $\gamma_0 = (a + 1/a)/2$. When $\beta = 1.3$ we obtain $a = 2.2$ and $\bar{\gamma}_0 = 1.33$. However, if the cross section is asymptotically constant, then $\beta = 2$. Consequently $\bar{\gamma}_0 = 1.15$ (this corresponds to a velocity $v_0 = 0.5$). This fact urges some caution, since the assumption that there is no interference (which is essential for the model) can be justified only for large $\bar{\gamma}_0$; we note that within the framework of the model $\bar{\gamma}_0$ does not depend on s_0 and is determined only by the value of the coefficient β.

be discussed in Chapter IV. We note beforehand, however, that for the majority of the experimental data on the angular distribution we get $\sigma_\lambda \sim 0.5-1$, in sharp disagreement with these predictions.

Let us attempt to improve this model by bringing it closer to reality.

We ascertain first under what conditions we can eliminate the principal defect—bring α close to unity. To this end it is necessary to extend the integration over larger values of s_i, which is equivalent to taking into account the higher resonances in the $\pi\pi$ interaction. Indications of the possible existence of such resonances (for example, in the reaction $\pi\pi \to \rho\rho \to 4\pi$) can be found in the latest papers [75]. In addition, we can expect in principle for the $\pi\pi$ interaction that a resonance will appear at energies on the order of $s_i \sim (2M)^2$. (This resonance appears if a nucleon-antinucleon pair is produced in the intermediate state [76].) Then the integral in (3.20) will cover a wide area. It is sensible to assume $\sigma^{(R)}$ in this region to be equal to the geometrical cross section, $\sigma^{(R)} \sim 1/\mu^2$. The upper limit of integration is determined from the condition $\alpha = 1$, $s_{i.max} \sim \mu^2 \times 2 \times 16\pi^3 \approx 20\,M^2$. We note that in the case of a nucleon-nucleon collision these considerations do not pertain to the extreme vertices, in which the πN isobars can be produced. The character of these isobars does not influence the exponent α, so it is sensible to leave them the same as before in the framework of the model.

This variant of the model no longer has these attractive features referred to above. Namely, we can no longer assume that the character of the inelastic interactions at high energies is determined completely by the processes at low energies, since energies $s_i \sim 20\,M^2$ cannot be regarded as low. However, this variant is much closer to reality. The number of secondary particles is no longer determined here completely by the number of knots. The question of the character of the decay of the clusters—the states produced in the knots—into secondary particles becomes important. It becomes necessary to apply to this process the statistical and hydrodynamic theories. The model thus acquires the principal features of the "fire ball" model. The quantities $s_0 \sim 20\,M^2$ also approach the experimentally observed values for the fire ball scheme, $\mathfrak{M}_{fb} = \sqrt{s_0} \sim (3-5)\,M$.

The asymptotic region in which the simple relations of the type

$$\mathfrak{N}_0 \approx 2 \ln \frac{s}{s_0}$$

are valid, moves higher in this case [see the footnote preceding Eq. (3.21)], up to $s \gg 70\, s_{0.max} \sim 500\,M^2$, that is, to energies of the order of $E_L \gg 10^{12}$ eV. On the other hand, in the region $E_L \sim 10^{11}-10^{12}$ eV we can only say that the number of $\pi\pi$ knots is small (on the order of one or two).

Thus, if we wish to come in the AFST model closer to the actual properties of the process we find it necessary to greatly increase the size of each pion isobar (to approximately $\mathfrak{M}_0 \sim 3-5$ BeV), and to decrease their numbers.

We note that we have thus arrived at an estimate of the characteristic size of one cluster, given in [77], and that the possibility of increasing the number of clusters with increasing energy corresponds in a certain sense to the Hasegawa hypothesis [78].

The amplitude of the elastic scattering due to a multiperipheral inelastic process, as already explained, has properties predicted by the MMP and satisfies the Mandelstam representation.

In this model we can explain the physical meaning of the swelling of the radius of the interaction and relate the parameter s_0 of the multiperipheral model with the parameter

$$\gamma = \frac{\partial l_0(t)}{\partial t}\Big|_{t=0},$$

which determines the "velocity" of motion of the pole and the increase of the radius in the MMP. The collision parameter of two neighboring knots r_i can be defined as

$$r_i^2 \sim r_0^2 \sim \frac{1}{k_\perp^2} \sim \frac{1}{k_{eff}^2}.$$

Inasmuch as the directions of the transverse components $k_{i\perp}$ corresponding to different virtual pions are independent in the model, the total interaction radius for $\mathfrak{N}$ knots will be

$$R = \sqrt{\sum_i r_i^2} \approx \sqrt{\mathfrak{N} r_0^2} \approx \sqrt{\frac{\mathfrak{N}}{k_{eff}^2}}.$$

But

$$\mathfrak{N} \sim \beta \ln \frac{s}{s_0}.$$

Consequently we get a logarithmic increase in the radius

$$R \approx \sqrt{\frac{\beta}{k_{eff}^2} \ln \frac{s}{s_0}}.$$

Thus, the increase in the radius, the shrinkage of the diffraction cone, and other effects predicted by the MMP are simply related with the fact that the number of knots $\mathfrak{N}$ increases with increasing energy. Comparing the obtained expression for R with the expression that follows from the MMP,

$$k_\perp \approx \sqrt{\gamma \ln \frac{s}{s_0}},\ \gamma = l'(0),$$

we find

$$\gamma \approx \frac{\beta}{k_{eff}^2} \approx \frac{\beta}{s_0}.$$

In the literally taken AFST model, where $\beta \approx 1$ and $s_0 \sim 0.5\,M^2$, the parameter γ is sufficiently large to be observable experimentally. On the other hand, in the model with the "burdened" knots (where $\beta \approx 2$

and $s_0 \sim 10\,M^2$), the parameter $\gamma \sim 0.2\,M^{-2}$ is appreciably smaller than the value $\gamma \sim M^{-2}$ corresponding to the observed shrinkage of the cone in pp scattering. The shrinkage of the diffraction cone is in this case very small. Under modern experimental conditions it can hardly be noted.

5. Supplementary Remarks

So far we have considered inelastic interactions that result from the exchange of one pion. Naturally, the question arises of what role can be played by analogous processes due to the exchange of a quantum of different nature, for example an η meson, K mesons, etc.

The relative contribution of these processes can be estimated only by making two assumptions (which, to be sure, are quite natural): (a) the cross sections of the interaction between all the strongly interacting particles are of the same order of magnitude; (b) the pole terms predominate in the propagation functions of the particles in the region of small k^2:

$$D_j(k^2) = \frac{1}{k^2 + m_j^2}, \qquad (3.27)$$

where m_j is the mass of the exchanged quantum.

Let us consider by way of an example the inelastic process due to exchange of a kaon. The total cross section is written in analogy with (3.6); the contribution for asymptotically large energies will, as in the case of (3.6), be made by the region of small k^2. Therefore the cross section $\sigma^{(K)}$ of the process with a one-kaon exchange will be proportional to $|D_K(0)|^2$, whereas in the one-pion exchange (considered above) $\sigma^{(\pi)} \sim |D_\pi(0)|^2$. Their ratio will be of the order of

$$\frac{\sigma^{(K)}}{\sigma^{(\pi)}} \sim \left|\frac{D_K(0)}{D_\pi(0)}\right|^2 \sim \frac{m_\pi^4}{m_K^4} \sim 10^{-2}. \qquad (3.28)$$

Analogous arguments can also be applied to any stable or resonant particle which the incoming particles can exchange. The ratios of all the cross sections to the cross section due to the pion exchange will be small. The pion is singled out because it is the lightest of all the strongly-interacting particles.

All the foregoing pertains to the main group of interactions, in which $k^2 \sim s_1 s_2/s$. There exists, however, a different group of peripheral processes, which makes a small contribution to the total cross section (at asymptotically large energies), but is nevertheless of interest. In this group the principal process is diffraction generation of particles, which we shall consider in Chapter V.

IV. EXPERIMENTAL DATA FOR $E_L \gtrsim 10^{11}$ eV. COMPARISON WITH THEORY

Data on the interactions at $E_L > 10^{11}$ eV are obtained from cosmic-ray experiments. These experiments are difficult, but, as in the past, they yield significant results at lower energies. A distinction must be made here between two energy regions. When $E_L \sim 10^{11}$—10^{13} eV, owing to the extensive use of the emulsion methods (recently—emulsions interlined with lead) and of ionization calorimeters, particularly calorimeters combined with a cloud chamber in a magnetic field, it has been possible to accumulate rather detailed information on the interaction mechanism, over and above the information previously obtained from studies of extensive air showers (and now confirmed with the aid of the indicated new procedures). On the other hand, in the energy region 10^{13}—10^{16} eV, extensive air showers remain as before practically the only source of knowledge. New results were obtained here, too.

1. Summary of Earlier Results

The main results, which were known already a few years ago, can be summarized in the following fashion [79,80].

1. The cross section for collision between a nucleon (and apparently also a pion) with the nucleus of an air atom or with a heavier element remains constant to high degree—from approximately 2×10^9 to at least 10^{13} eV—and equal (accurate to $\pm 20\%$) to the so-called geometrical cross section σ_{0A} of the nucleus (there is one exception—the unreliable and unconfirmed indication that $\sigma_A \sim (2-3)\sigma_{0A}$ for $\sim 10^{14}$ eV in the case of lead). Data on extensive air showers enable us to assume that this is true with the same accuracy, $\sim 20\%$, up to $E_L \sim 10^{15}$ eV and even higher.

2. Pions are generated almost exclusively ($\sim 80\%$ of the particles).

3. The average multiplicity $\bar{n}$ increases very slowly with the energy. It is customary to assume that up to $E_L \sim 10^{15}$ eV we have $\bar{n} \sim E_L^{1/4}$. However, a larger spread in the values of n in individual events is typical. In nucleon-nucleon collisions at $E_L \sim 10^{12}$ eV we have $\bar{n} \sim 15$—20.

4. In a very large number of events, the nucleon retains an appreciable part, $1 - K$, of its energy after the collision: the average "inelasticity coefficient" K is of the order of 0.2—0.3 for nucleon-nucleon collisions, and 0.4—05 for nucleon-air collisions. These values are approximately the same for all energies at least up to 10^{14} eV. A characteristic feature is the tremendous scatter in the values of K, with both $K \sim 0.01$ and $K \sim 1$ encountered.

5. The particles generated in the collision are scattered in a very characteristic manner: they form in the c.m.s. two sharply collimated cones, which are not necessarily of the same size.

On going over to the laboratory system (L-system), the "front" cone (the cone of particles moving in the mean in the direction of the primary particle) shrinks even more, while the "rear" cone "turns inside out" in the opposite direction and turns into a relatively broad fan or cone of particles, also directed along the motion of the primary particles, enveloping the narrow "front cone."

6. The transverse momentum $p_\perp$ of the produced particles is practically independent of the energy. When $10^{11} < E_L < 10^{15}$ eV the average $\bar{p}_\perp$ for pions lies near 0.4 BeV/c, or $(2.5-4)\mu c$. For nucleons it is 2–3 times larger. The most probable value of $p_\perp$ is close to $2\ \mu c$. We see therefore that very large values of $p_\perp$ are also encountered.

Thus, for high energies in the L system, the particles move forward in a narrow jet, which shrinks with increasing E_L (in inverse proportion to E_L), and this is the term used to denote the entire phenomenon.

This general information have been firmly established during the last years. Thus, in [22] there is an analysis of data on the cross section of collisions between nucleons and nuclei of atoms. The authors reach the conclusion that up to $E_L \sim 10^{15}$ eV the cross section for the collision between the nucleon and the air nucleus, as well as the law $\sigma_A \sim A^{2/3}$, hold within $\pm 10-20\%$. However, very important new features were disclosed on top of this, principally on the basis of a study of the angular distribution of the emitted particles. Many important new indications, which call for further study, have been obtained by investigating extensive air showers in the region $E_L \sim 10^{14}-10^{16}$ eV (see Sec. 3h, below).

2. Methods of Experiment Analysis

Perhaps the most difficult experimental problem in the study of the elementary act in emulsions is the determination of the energy E_L of the primary particles which produces multiple generation. If $E_L \lesssim 10^{12}$ eV, then the secondary charged particles (pions) frequently have an energy still low enough to be determined by combining the data on ionization, distance between grains (blobs), etc. Using the firmly established fact that $\bar{p}_\perp$ is approximately constant, the momenta $|\mathbf{p}|$ of the secondary particles are sometimes estimated from their angle of emission θ in the L-system, assuming that $|\mathbf{p}| \approx \bar{p}_\perp/\theta \approx M/2\theta$. (Such a determination, of course, can be sufficiently reliable only for average values.) If E_L is large, however, the best that can be done is to estimate the lower limit of E_L.

Long ago (and this method is still used) the energy determination started to be based on the so-called half-angle $\theta_{1/2}$. Namely, if we assume the following: (1) that the nucleon-nucleon collision could be separated, and (2) that the products are scattered symmetrically forward and backward in the c.m.s. of these two particles, then we can easily find that the Lorentz factor γ_c for the motion of the c.m.s. relative to the L-system is

$$\gamma_c = \frac{1}{\operatorname{tg}\theta_{1/2}} \approx \frac{1}{\theta_{1/2}}, \qquad (4.1)^*$$

where

$$\gamma_c = \frac{E_c}{M} = \sqrt{\frac{\gamma+1}{2}}, \qquad (4.2)$$

$$\gamma = \frac{E_L}{M} = 2\gamma_c^2 - 1, \qquad (4.3)$$

M is the mass of the nucleon, E_c is the energy of the nucleon in the c.m.s., and $\theta_{1/2}$ is the laboratory system angle (relative to the direction of the primary particle) separating one-half of the secondary particles ("front" cone) from the second ("rear" cone in the c.m.s.).

Indeed, the transformation to angles ϑ of the same particles in the c.m.s. is by means of the following formula, which results from the law of velocity addition,

$$\operatorname{tg}\theta = \frac{\sin\vartheta}{\gamma_c\left(\cos\vartheta + \frac{\beta_c}{\beta}\right)}, \qquad \gamma_c = (1-\beta_c)^{-\frac{1}{2}}, \qquad (4.4)$$

where β is the velocity (in fractions of c) of the particle in the c.m.s, and β_c is the velocity of the c.m.s. itself in the L-system. Since both β and β_c are close to unity and θ is small, we have

$$\operatorname{tg}\theta \approx \frac{1}{\gamma_c}\operatorname{tg}\frac{\vartheta}{2}. \qquad (4.5)$$

In the case of front-rear symmetry in the c.m.s., half the particles lie at $\vartheta < \pi/2$ or, according to (4.5), at $\theta > 1/\gamma_c$. Consequently, by determining this half-value angle, we obtain γ_c from (4.1), and then also E_L from (4.2) (the error due to assuming $\beta_c/\beta = 1$ is apparently small [81].

However, the assumption that the scattering in the c.m.s. is symmetrical in each individual act (and not in the mean) can generally speaking not be justified. Indeed, it was shown directly [67] that when $E_L \approx 3 \times 10^{11}$ eV at least half of the jets are sharply asymmetrical (see below). It is obvious, furthermore, that the half-value angle method is certainly unreliable at very low multiplicity, and the number of such acts is not small.

By using this method we can introduce an error of a factor of several times in the estimate of E_L (according to [67], for symmetrical showers the error is $\sim 30\%$, for asymmetrical ones it can reach a factor of 5).

Recently two new methods, based on similar ideas, have been employed. The first, the ionization calorimeter method, was proposed in [82] and developed and employed in [83], and later used in combination with a cloud chamber [67]. Alternating layers of heavy material (iron or lead) and ionization chambers are placed under the chamber in which the interaction is investigated. The total thickness of the material is sufficient to absorb all the ionizing particles and the electron-photon cascades which they produce. Since the overwhelming part of the energy of the primary particles, after all the cascades of interaction, multiplication, and decays, is consumed in final analysis in ionization produced by the relativistic particles, we can, by

*tg = tan.

measuring the ionization in the many layers, determine this energy with an error of several times 10% (apparently ~30%). This method has already been used and yielded interesting results in the region $E_L \sim 3 \times 10^{11}-10^{13}$ eV[67,82,83,102,105].

In the second method, thick pellicle stacks are used, interlined with layers of heavy metal and operating essentially on the principle of the ionization calorimeter. By tracing the ionization in a cascade which first increases and then decreases over the entire thickness of the emulsion, it is possible here, too, to determine the energy of the cascade and consequently of the primary particle which produced it. This latter method has made it possible to proceed to a systematic study of all the interaction events in which only a few particles are produced at very high energy of the primary particle ("lean jets"). Such cases were frequently missed by the emulsion heretofore. Now it is possible to notice even the production of a single π^0 meson, since it gives rise to a powerful electron-photon cascade which can be readily observed and studied.

However, even if E_L is not accurately determined, it is possible to extract interesting results by studying the angular distribution in a special manner, with special coordinates.

Direct observations give the angles of emission of individual particles θ in the laboratory system. Instead of investigating the distribution with respect to θ, it is advantageous to consider the distribution with respect to the coordinate

$$\lambda = -\lg \operatorname{tg} \theta. \qquad (4.6)^*$$

Since θ is a small quantity, we have $\lambda > 0$. According to (4.5)

$$\lambda = \lg \gamma_c - \lg \operatorname{tg} \frac{\vartheta}{2}.$$

Therefore, by observing in the laboratory system the distribution of the particles with respect to θ and by plotting it as a distribution $n(\lambda)$ with respect to λ, we immediately obtain the actual distribution with respect to log tan $\vartheta/2$, that is, the distribution in the c.m.s., but shifted along the axis by log γ_c. Consequently, for example, we can see directly whether symmetry exists in the distribution with respect to the angles ϑ.

Sometimes even the primary experimental material is plotted in terms of λ. Thus, the lower part of Fig. 23 below, and also Fig. 26, show values for individual relativistic ionizing particles in one jet. Each vertical bar denotes λ for one individual particle. It is clearly seen that the particles form two groups, and their common center of gravity moves in the L system with a velocity corresponding to γ_c, the logarithm of which lies somewhere in the vicinity of the dashed line.

Along with λ it is convenient to use also a variable η, which pertains directly to the angles in the c.m.s. (this was the variable which appeared first in the Landau hydrodynamic theory[84], and therefore it is sometimes called, like λ, the Landau variable; see also [85]):

$$\eta = -\ln \operatorname{tg} \frac{\vartheta}{2} \approx -2.3 \lg \operatorname{tg} \frac{\vartheta}{2}, \quad \operatorname{tg} \frac{\vartheta}{2} = e^{-\eta}. \qquad (4.7)$$

According to (4.5)—(4.6) we have

$$\lambda = \lg \gamma_c + \frac{\eta}{2.3}, \qquad \eta = 2.3(\lambda - \lg \gamma_c). \qquad (4.7a)$$

Thus, the transition from the distribution in the L system (coordinate λ) to the distribution in the c.m.s. (coordinate η) is by shifting the entire pattern by an amount log γ_c along the abscissa (and by changing the scale by a factor ~2.3, owing to the transition to natural logarithms, which is by far not obligatory).

If the distribution in the c.m.s. is of the form

$$dn(\vartheta) = \frac{1}{2} n(\vartheta) \sin \vartheta \, d\vartheta,$$

then

$$dn(\eta) = n(\vartheta(\eta)) \frac{d\eta}{(e^{\eta}+e^{-\eta})^2} = n_1(\lambda) \frac{2.3 d\lambda}{(10^{\lambda - \lg \gamma_c} + 10^{-(\lambda - \lg \gamma_c)})^2} \qquad (4.8)$$

[$n_1(\lambda) \equiv n(\vartheta(\lambda))$]. Thus, if the distribution is isotropic in the c.m.s., $n(\vartheta) = n_0 = \text{const}$, then it has in the λ scale a symmetrical bell-shaped form with maximum at $\lambda = \log \gamma_c$, decreasing exponentially on the skirts. Obviously, if the distribution in λ is not isotropic but has a front-back symmetry, that is, $n(\vartheta) = n(\pi - \vartheta)$, and consequently

$$n_1(\lambda) = n_1(2 \lg \gamma_c - \lambda)$$

or

$$n_1(\lambda - \lg \gamma_c) = n_1(-(\lambda - \lg \gamma_c)),$$

then symmetry is also conserved in the λ scale. The center of symmetry λ_0 will again yield log γ_c directly.

In practice this means that by plotting in the λ scale the distribution with respect to the angles θ, observed for a given jet in the laboratory system, we can obtain directly γ_c, and consequently E_L from (4.2), provided a symmetrical curve was initially obtained.

The λ scale has the property that the narrower the front and rear cones (the more anisotropic the jet), the broader the distribution with respect to λ. For a jet which is isotropic in the c.m.s. we find, by approximating the curve in the λ scale to a Gaussian curve, that the standard (half-width) of the distribution is equal to

$$\sigma_{\lambda, \text{isotrop.}} \approx 0.39. \qquad (4.9)$$

Integral construction in the λ scale is very useful. If we form the c.m.s. quantity

$$F_c(\vartheta) = \int_0^{\vartheta} \frac{1}{2} n(\vartheta) \sin \vartheta \, d\vartheta \Big/ \int_0^{\pi} \frac{1}{2} n(\vartheta) \sin \vartheta \, d\vartheta \qquad (4.10)$$

(it gives the fraction of the particles emitted at an angle smaller than ϑ relative to the direction of the primary), then in the case of isotropy in the c.m.s.

*lg = log.

$[n(\vartheta) = n_0 = \text{const}]$ we have $F_c(\vartheta) = \sin^2(\vartheta/2)$ and

$$\lg \frac{F_c(\vartheta)}{1-F_c(\vartheta)} = \lg \operatorname{tg}^2 \frac{\vartheta}{2} = 2 \lg \gamma_c - 2\lambda. \qquad (4.11)$$

To each ϑ in the c.m.s. there corresponds a definite θ in the L system. Therefore in place of $F_c(\vartheta)$ it is possible to substitute in (4.11) the integral distribution in the L system. By plotting from the experimental data the function $\log[F(\theta)/(1-F(\theta))]$, as proposed by Duller and Walker[86], we ascertain immediately whether the distribution in the c.m.s. is isotropic (in this case a straight line should be obtained with a slope equal to 2), or at any rate, if the line is symmetrical, then we immediately obtain $\log \gamma_c$ from the intercept on the abscissa axis.

A shortcoming of this method is first that in nucleon-nucleon collisions in the region $E_L \lesssim 10^{13}$ eV, where the most intense research has been carried out so far, the total number of generated charged particles n_s is still not very large ($n_s \lesssim 20$), and is frequently even quite small ($n_s < 10$). Therefore the plotting of the distribution curves is not an easy matter. Further, it is sufficient for one of the particles to carry away a very large fraction of the energy in order to produce a considerable error, if this particle is charged and can be seen in the emulsion. Such a particle will turn out to be far on the edge, there will be no true symmetry, and the determination of γ_c will be impossible. However, if some group of particles has symmetry by itself, then its center gives the Lorentz factor γ of this group (or of the cluster of matter from which the particles arise) as a whole, relative to the laboratory system.

The method of the λ coordinates turned out to be quite effective for the analysis of the experiments.

In addition to the difficulty in the determination of E_L, experimenters are faced with the serious problem of separating the nucleon-nucleon collisions from the observed jets. It is customary to assume that the high-energy pions are too little represented in the cosmic-ray flux for the primary particle to be a pion.* Only when the jet is generated in the emulsion by a charged particle which was produced in a different jet in the same emulsion can this particle be regarded as a pion in the overwhelming majority of cases. On the other hand, the emulsion consists predominantly of heavy nuclei. If there are very many black tracks in the jet, characteristic of slow protons, then it is clear that a collision with the central part of the nucleus took place. On the other hand, if the number of such tracks N_h is small, then it is customary to assume that a collision with a peripheral nucleon took place, and we deal with a nucleon-nucleon collision. This is usually confirmed by the fact that in collisions with the center of the nucleus the number of produced particles is much larger than in collisions with a single nucleon—even when $E_L \sim 10^{13}$ eV their number is on the order of 100. The choice of a definite criterion is the result of weighing many subtle details. The Krakow school[68] is of the opinion that if $N_h \leq 5$ and the number of relativistic tracks is $n_s \leq 20$, then a nucleon-nucleon collision has occurred. This criterion is not universally accepted. Thus, the criterion $N_h \leq 2$ is also used[88], and even $N_h = 0$. There is also the danger here that by the same token we discard nucleon-nucleon collisions with large multiplicity n_s, that is, we select artificially only that part of the nucleon-nucleon collisions, for which the inelasticity coefficient is anomalously small.

In experiments using a cloud chamber in a magnetic field and an ionization calorimeter[67], the collision with the nucleon occurs in an LiH plate. All the nuclei are light here, and we can assume that almost all the collisions are nucleon-nucleon.

An important characteristic of the interaction is the already mentioned inelasticity coefficient. In each interaction of two nucleons there are two such quantities.

The inelasticity coefficient K_{lab} of the incoming nucleon, frequently denoted simply K, and a "mirror" inelasticity coefficient K_{mir}, have been in use for a long time[60,67]. K_{lab} gives the fraction of the energy of the primary particle going into the production of new particles,

$$K_{lab} = \frac{E_{Li} - E_{Lf}}{E_{Li}} = \frac{\Sigma' \varepsilon_j}{E_{Li}}, \qquad (4.12)$$

where E_{Li} is the energy of the primary nucleon in the laboratory system of coordinates; E_{Lf} is the energy of the same nucleon after the interaction; $\Sigma' \epsilon_j$ is the sum of the energies of the secondary particles after subtracting the energy of the nucleon itself. The quantity K_{mir} is determined analogously, but in a system in which the primary "incident" nucleon is at rest, and the laboratory nucleon—the target—moves with energy E_L in a system which is called the "mirror" system relative to the laboratory system (or the anti-laboratory system).

If the collision is symmetrical in the c.m.s., then, of course, $K_{lab} = K_{mir}$. However, symmetry does not obtain, as shown in [67], in each individual collision. Therefore certainly only equality of the average values should occur, $\bar{K}_{lab} = \bar{K}_{mir}$, and in general equality of the distributions over K_{lab} and K_{mir}.

It is possible to define analogous quantities for both nucleons in the c.m.s., where their initial energies $E_{ci}^{(1)}$ and $E_{ci}^{(2)}$ are equal, and the final energies $E_{cf}^{(1)}$ and $E_{cf}^{(2)}$ are generally speaking different:

$$K_1^c = \frac{E_{ci}^{(1)} - E_{cf}^{(2)}}{E_{ci}^{(1)}}, \quad K_2^c = \frac{E_{ci}^{(2)} - E_{cf}^{(2)}}{E_{ci}^{(2)}}. \qquad (4.12a)$$

In the general case these quantities differ from K_{lab} and K_{mir}. However, if the initial energy E_L is sufficiently large, and consequently, the Lorentz factor

*It was shown recently, however, that this generally accepted premise may be very inaccurate [87].

of the transition from the c.m.s. to the L system is large, $\gamma_c \gg 1$, and the inelasticity coefficients are not very small, namely if $K_{lab}\gamma_c \gg 1$ and $K_{mir}\gamma_c \gg 1$, then K_1^c coincides with K_{lab} and K_2^c coincides with K_{mir}, accurate to quantities of the order of $(\gamma_c K_{lab,mir})^{-1}$. We note that in practice K varies between 0.1 and 1 (it cannot exceed unity by definition). In this connection, inaccurate measurement of K ("order of magnitude" measurement) is meaningless.

Yet, for an experimental determination of K it is necessary to know not only the energy of the primary particles, but also its energy after the collision, or else the energies of all the newly produced particles. If we know only the angular distribution (for example, in cloud-chamber observations without a magnetic field), then K_{lab} and K_{mir} can be determined only on the basis of additional assumptions. Usually use is made not only of the assumptions made above (the transverse momentum is the same for all particles and is equal to the average $\bar{p}_\perp \approx 2.5\,\mu$, and the particles are emitted in the c.m.s. symmetrically forward and backward), but also the hypothesis of charge symmetry of the emitted pions. Namely, it is assumed that the number of neutral mesons (which are not seen in the photoemulsion and which are detected only if electromagnetic cascades produced by the decaying π^0 mesons can be traced) is equal to half the number of charged mesons. Then, owing to the assumed front back symmetry, $K_{lab} = K_{mir}$, E_L is determined from (4.1), with

$$\Sigma\varepsilon_i' = \frac{3}{2}\sum_{i=1}^{n_s}\frac{p_{\perp i}}{\theta_i} \approx \frac{3}{2}\bar{p}_\perp \sum_{i=1}^{n_s}\frac{1}{\theta_i}, \tag{4.13}$$

where θ_i is the angle of emission of the particle in the L system, As a result we obtain

$$K \equiv K_{lab} = \frac{\frac{3}{2}\bar{p}_\perp \sum_{i=1}^{n_s}\frac{1}{\theta_i}}{2M\gamma_c^2}. \tag{4.14}$$

Under special assumptions concerning the scattering symmetry and the energy per particle, we can obtain also other simpler formulas [see (4.24) below].

It is possible to measure K_{lab} more accurately by measuring independently both the energy of the primary particle (for example, by calorimetric means), and the energy of the secondary charged particles (for example, in a magnetic field in a cloud chamber). It is then possible to use formula (4.12) directly, taking into account the contribution of the neutral particles by using the factor $^3/_2$.

There is no need to assume here that the scattering is symmetrical in the c.m.s.; to the contrary, it is possible to check whether the symmetry actually exists.

The value of the "mirror" coefficient K_{mir} can also be determined from experimental data in the laboratory system. To this end we note that K_{mir} is connected with the so-called "target mass" m_t, which was introduced and investigated in detail in [60]. It is equal to*

$$m_t = \sum_{i=1}^{n}(\varepsilon_{iL} - p_{iL}\cos\theta_i), \tag{4.15}$$

where ϵ_{iL}, p_{iL}, and θ_i are the laboratory-system energies, momenta, and recoil angles of the newly formed particles, with the target experiencing recoil eliminated from the sum.

Transforming this equation to the system where the incoming nucleon is at rest, we can readily verify that

$$m_t = K_{mir}\,M. \tag{4.16}$$

We see that here, unlike in the preceding case, there is no need to know the energy of the primary particle in order to determine m_t and K_{mir}.

The smaller the secondary-particle energy in the laboratory system and the larger the angle, the larger their contribution to m_t. This circumstance is also very favorable, since the characteristics of such particles can be measured more accurately. Thus, K_{mir} can be determined more reliably than K_{lab}.

As seen in Chapter 3, an important role is played in the theory of two-center peripheral collisions by the width of the square of the 4-momentum k^2 transferred from one group of particles to the other. Namely, it is proved for this model that for the meson which carries the interaction k^2 is small and decreases with energy. In the analysis of the experiment this gives rise to the question whether the jet particles can be divided into two groups in such a way that the

*Indeed, if a collision occurs between a primary particle of energy E_L and momentum p_L and a resting particle with mass M, then from the conservation of the energy and the longitudinal-momentum $p_{||}$ we obtain

$$E_L + M = \sum_i \varepsilon_{iL} + E_t,$$

$$p_{L||} \equiv p_L = \sum_i p_{iL}\cos\theta_i + p_t\cos\theta_t,$$

where E_t, p_t and θ_t characterize the target after the collision. Recognizing that

$$p_L \approx E_L - \frac{M^2}{2E_L} \approx E_L,$$

we get from this

$$M = \sum_i (\varepsilon_{iL} - p_{iL}\cos\theta_{iL}) + E_t - p_t\cos\theta_t.$$

The value of m_t, defined by (4.15), is

$$m_t = M - (E_t - p_t\cos\theta_t).$$

It is smaller than the mass M and is interpreted in [60] as the mass of that "part" of the target, which interacts strongly with the incoming particle. For example, if $m_t \approx \mu$, then this is a certain indication that the collision occurred with a virtual target pion, that is, it has a peripheral character. On the other hand if $m_t \sim M$ we can assume that we are dealing with a central collision. There is no doubt, at any rate, that if m_t is much larger than M, for example $m_t \approx 3M$, then the collision has occurred with the center of the nucleus and not with a single nucleon.

square of the difference of their 4-momenta is small.

An attribute of low momentum transfer in a process may be non-monotonicity of the particle distribution relative to the parameter λ, and the presence of several, say two, maxima in this distribution. Then the jet breaks up in "natural" fashion into jets corresponding to these maxima. The values of k^2 transferred from jet to jet are minimal in just such a "natural" breakdown. To determine k^2 by formula (3.5b) in the case of two jets, it is necessary to know s_1, s_2, and $\cos\theta_{\mathfrak{M}}$ (where $\theta_{\mathfrak{M}}$ is the angle between the momentum of the primary particles and the momentum of one of the jets in the c.m.s.). In principle, of course, all these quantities can be determined by measuring the momenta of the secondary particles. Actually, however, the requirements this imposes on the measurement of $\theta_{\mathfrak{M}}$ are very stringent, since the term $1 - \cos\theta_{\mathfrak{M}}$ in the expression for k^2 is preceded by a very large coefficient. In practice the accuracy with which the angle $\theta_{\mathfrak{M}}$ can be determined at present for high energies is quite insufficient.

The requirements imposed by formula (3.5b) on the accuracy with which s_1 and s_2 are determined are much lower, since the first terms contain small coefficients of the type $1/s$ or $1/s^2$.

From theoretical considerations it follows that in the OMA (see Chapter III) k^2 is of the same order as the first two terms in (3.5b). Therefore to determine the order of magnitude of k^2 it is sufficient to retain the first two terms of (3.5b), that is, to be satisfied with the determination of the lower limit, k^2_{min}. Thus, if we obtain from experiment a value of k^2_{min} which is larger than theoretically predicted for k^2, this means that the OMA is not applicable to this process.

Let us consider several cases.

1. If one of the particle groups contains only a nucleon (in this case $s_1 = M^2$), then the first term of (3.5b) vanishes and

$$k^2_{\min} = \frac{s_2 M^2}{s^2}. \tag{4.17}$$

In this case, using the conservation laws, we can relate k^2 with the inelasticity coefficient K and obtain by the same token a simple and effective method of determining k^2. Denoting k^2 for this process by k^2_N, we obtain

$$k^2_N = M^2 \frac{K^2}{1-K}. \tag{4.17a}$$

2. If there are several particles in each jet and s_1, $s_2 \gg M^2$, then the second term of (3.5b) can be neglected compared with the first, and

$$k^2_{\min} = \frac{(s_1 - M^2)(s_2 - M^2)}{s} \approx \frac{s_1 s_2}{s}. \tag{4.18}$$

3. If the jets are symmetrical we can use (4.14). We note, however, that in this case k^2 can be related also with the "generalized target mass" m_t^* proposed in [89]:

$$k^2 = 4 m_t^{*2} \gamma_c^2. \tag{4.19}$$

The quantity m_t^* is defined in analogy with m_t:

$$m_t^* = \sum_{(I)} (\varepsilon_{Li} - p_{Li}\cos\theta_i). \tag{4.19a}$$

The summation, however, unlike in (4.15), extends here only over particles which belong to the narrow cone in the laboratory system (the "front" cone in the c.m.s.).

3. Fundamental Experimental Results of Recent Years and Their Significance to the Theory

a) Model of two "fire balls" for nucleon-nucleon collisions. In 1958, a detailed analysis of both types of plots, namely $n(\lambda)$ and $\log F/(1-F)$, made by the Krakow group of M. Miesowicz for several jets and emulsions (and also for jets obtained by others), interpreted as nucleon-nucleon collisions, has led the Polish physicists to the conclusion [68] that in many cases the $n(\lambda)$ curve has two maxima. This analysis was continued [90] with the same result. During the last four years enough material has been accumulated in this field to confirm and refine the foregoing conclusion (although still disputed by many experimenters).

If we select the jets in accordance with the criteria adopted by the Krakow group for the separation of nucleon-nucleon collisions of sufficiently high energy, namely if we stipulate the following: (1) not too many slow recoil protons, $N_h \leq 5$; (2) not enough relativistic charged particles to be able to suspect collisions with the center of the nucleus, $5 < n_s \leq 20$; (3) γ_c determined from the half-value angle exceeds 23 (if this is a true symmetrical collision of the nucleon-nucleon system, then the cases with $E_L > 10^{12}$ eV are separated by the same token), then it turns out that all the material accumulated in the world's laboratories amounts to about 200 cases. The nucleon-nucleon collisions amount here to 35% of all the jets with $\gamma_c > 23$ ($N_h \leq 5$ and $5 < n_s \leq 20$). Seventy per cent of these have a half-width $\sigma_\lambda > 0.6$ in the λ scale.*

Inasmuch as $n_s \leq 20$, it is clear that a statistical reduction of each individual jet is not reliable. Nonetheless, we can conclude (special methods were used to group the material) [91] that all the nucleon-nucleon collisions with $\sigma_\lambda > 0.6$ agree with the two-maximum distribution in λ. Figure 18 shows a summary histogram of 11 jets (a total of 138 charged particles) for $23 < \gamma_c < 90$ ($10^{12} < E_L < 1.5 \times 10^{13}$) from the first report of [68], showing a total half-width $\sigma_\lambda \approx 0.55$ (consequently, since $\sigma_\lambda > 0.39$, the distribution as a whole is not isotropic in the c.m.s., but is rather strongly collimated). The histogram can be divided into two practically identical curves with appreciably smaller σ_λ. It was shown subsequently that such a structure (of course, with very large fluctuations) agrees with

*These figures were obtained and kindly supplied by Professor J. Gierula (Krakow), to whom we are very grateful.

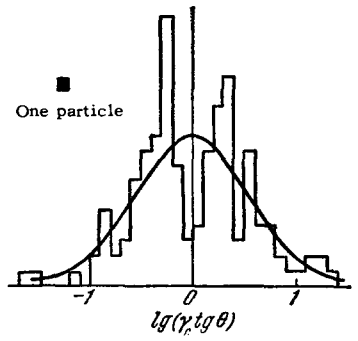

FIG. 18. Summary data showing a distribution with two maxima maxima [68].

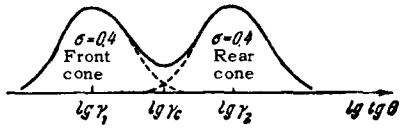

FIG. 19. Diagram showing the distribution in the case of two cones, displaying two maxima.

the data for many individual jets. This picture is shown schematically and in idealized fashion in Fig. 19. The interpretation given for this structure by the authors of [68] is based on further details of this structure. It turns out that the pertinent Duller-Walker curve for each individual jet has the character shown in Fig. 20 (we show here two jets from the Krakow laboratory and one from Chicago). On the other hand, if we consider separately the particles in the front (Fig. 21a) and in the rear cone (Fig. 21b), then both groups lie on a single straight line with a slope corresponding to the isotropy of the scattering of each subgroup in the c.m.s.

Starting from this, the authors propose the following scheme for the process. Actually the particles in each jet are generated in two centers, in two clusters of nuclear matter, in which the decay occurs independently. The particles are scattered isotropically in the c.m.s. of such a cluster, but since the centers move relative to each other, a front and rear cone are obtained in the c.m.s. of the entire jet. The velocity $\bar{v}_i$ of each cluster as a whole in the common c.m.s. is determined from the distance of one of the maxima from the center of symmetry of distribution (Fig. 19),

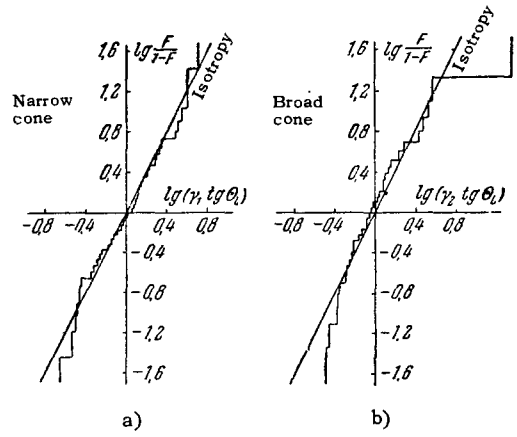

FIG. 21. Summary Duller-Walker plots shown for the front ("narrow") and rear ("broad") cones separately.

and is expressed usually by the corresponding Lorentz factor $\bar{\gamma}$ in the c.m.s.

As can be readily verified, the relativistic formula for addition of velocities

$$v_1 = \frac{v_2 \pm v_3}{1 \pm \frac{v_2 v_3}{c^2}}$$

corresponds to a formula for addition of Lorentz factors

$$\gamma_1 = \gamma_2\gamma_3 \pm \sqrt{\gamma_2^2 - 1}\sqrt{\gamma_3^2 - 1} \equiv \gamma_2\gamma_3\left(1 \pm \frac{v_2 v_3}{c^2}\right). \quad (4.20)$$

Using this formula to calculate the γ-factors $\bar{\gamma}_1$ and $\bar{\gamma}_2$ of the individual clusters in the c.m.s. of the entire jet, from their γ-factors γ_1 and γ_2 in the L system, we get

$$\bar{\gamma}_1 = \gamma_1\gamma_c - \sqrt{(\gamma_1^2 - 1)(\gamma_c^2 - 1)}, \quad \bar{\gamma}_2 = \gamma_2\gamma_c - \sqrt{(\gamma_2^2 - 1)(\gamma_c^2 - 1)},$$

from which, assuming $\gamma_i^2 \gg 1$ and, as is customary, that $\bar{\gamma}_1 = \bar{\gamma}_2 = \bar{\gamma}$, we can obtain the approximate formulas

$$\gamma_c^2 = \gamma_1\gamma_2, \quad \lg \gamma_c = \frac{1}{2}(\lg \gamma_1 + \lg \gamma_2),$$

$$\bar{\gamma}_1 = \bar{\gamma}_2 = \bar{\gamma} = \frac{1}{2}\frac{\gamma_1 + \gamma_2}{\sqrt{\gamma_1\gamma_2}}. \quad (4.21)$$

This parameter $\bar{\gamma}$ is small, while γ_c itself, as already noted, exceeds 23, so that $\bar{\gamma} \ll \gamma_c$. Additional experimental material has made it possible to construct the

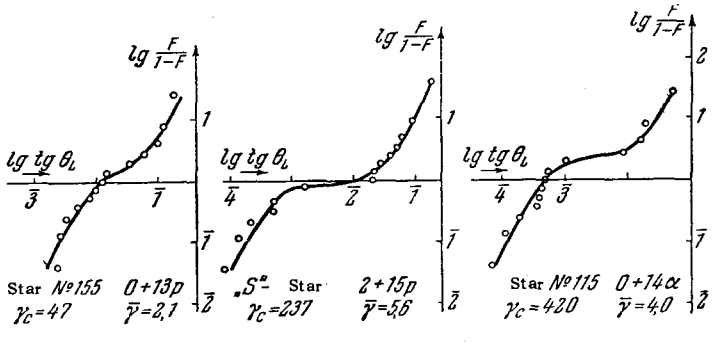

FIG. 20. Duller-Walker plot for individual jets, which show a two-maximum distribution.

following table, which still cannot be regarded as reliable [92].

E_L (eV)	10^{11}	10^{12}	10^{13}	10^{14}
$\bar{\gamma}$	1,2	1,5	2	4

The idea was expressed [93] that the decaying clusters are colliding excited nucleons, as had been assumed long ago in several papers [34,37]. Subsequently, however, the opinion accepted was that inasmuch as $\gamma \ll \gamma_c$ and K is small, these clusters, at least in the majority of cases (a special case is, for example, the "lean jets," see below) are separated from the primary nucleons, that they are emitted by the nucleons and explode like meteors or fire balls. Further, the experiment was interpreted at the very outset [68] in the sense that the produced pions have in the c.m.s. of the cluster approximately the same energy ϵ_π, which can be easily estimated by starting from the already noted constancy of the transverse momentum of the pions. The estimate yields

$$\varepsilon_\pi \approx 0.5\,\text{BeV} \approx \frac{1}{2} M. \tag{4.22}$$

In such a case, since there are $n_s/2$ charged pions in each cluster, and if we include the neutrals the number is $\frac{3}{2} \cdot \frac{1}{2} n_s$ particles, the mass of the two clusters is

$$2 \cdot \frac{3}{2} \cdot \frac{1}{2} n_s \cdot \frac{1}{2} M = \frac{3}{4} M n_s, \tag{4.23}$$

and their energy in the common c.m.s. is $\frac{3}{4} M n_s \bar{\gamma}$. If we assume that the energy 2E of the primary nucleons in the c.m.s. is correctly given by the position of the symmetry center of $\log \gamma_c$, that is, $2E \approx 2\gamma_c M$, then we can determine from this the inelasticity coefficient K — the fraction of the nucleon energy which goes over into newly formed particles:

$$K = \frac{3}{8} \frac{n_s \bar{\gamma}}{\gamma_c}. \tag{4.24}$$

Summarizing the results of these investigations and the properties of the above-described two-center or fire ball model, we must emphasize once more that owing to the smallness of n_s in the nucleon-nucleon collisions, only very few individual jets have a structure close to the ideal one shown in Fig. 19. There is undoubtedly an appreciable spread in the half-widths of all the jets σ_λ (as already mentioned, it exceeds 0.6 in 70% of the cases). It is by no means possible to state that the described mechanism actually occurs in all cases.* Moreover, there is a known case when spherically symmetrical scattering of all the particles in the c.m.s. is observed at very high energy $E_L \sim 10^{14}$ eV. [94] This clear-cut case certainly does not fit the two-fire-ball scheme.

Although the two-maximum character is sufficiently reliably established for the greater fraction of jets, the notion that the clusters that are scattered (and separated from the two primary nucleons) decay independently remains a plausible model possibility. At this point we encounter a difficulty which is particularly pronounced in the analysis of nucleon-nucleus collisions (see below).

It must be emphasized that the existence of two maxima in the λ scale is a subtle effect, which does not reduce at all to the presence of two narrow cones (front and rear) in the c.m.s. Thus, the usual hydrodynamic Landau theory also predicts for the central nucleon-nucleon collision two narrow oppositely directed cones, but with such an angular distribution $n(\vartheta)$, that in the η scale (meaning also in the λ scale) we get a single-maximum Gaussian curve [85], and the plot of $\log(F/(1-F))$ is a straight line with unity slope. Whether the hydrodynamic theory can be modified in such a way that in the λ scale, with $\lambda = \log \gamma_c$ (corresponding to $\vartheta = \pi/2$ in the c.m.s.) we get a maximum and not a minimum is an unsolved problem.

b) Comparison of the fire ball model with theory. We thus assume, subject to the stipulations made above, that a considerable part of the nucleon interactions at 10^{12}—10^{13} eV (by far not all of them) are described by the model of two fire balls. We shall attempt to compare the characteristics of such a process, obtained by experiment, with the proposed theory:

1) With the hydrodynamic theory of frontal nucleon collision.

2) With different variants of the OMA: (a) with the two-center model, which assumes that the nucleons are a part of the excited clusters; (b) with a one-meson scheme in which two virtual pions experience a central interaction (Fig. 15); (c) with a one-meson scheme in which two virtual pions experience a one-meson two-center interaction (Fig. 16); (d) with the multiperipheral model taken in its literal sense; (e) with the same model containing heavier clusters.

In this comparison we can make use of the experimental values of the inelasticity coefficients K and the squares of the momentum transfers k^2.

In the fire ball model, the K are small for both nucleons and of the same value, $K_{lab} \sim K_{mir} \sim 0.1$—$0.3$, show-

*In more than half of the cases, a nucleon-nucleon jet observed in emulsion has a rather disorderly appearance and it is impossible to construct not only a two-maximum but even a smooth single-maximum distribution with respect to λ. The widths σ_λ for the same values of E_L have a variety of values, from $\sigma_\lambda \approx 0.4$ (isotropy of the entire c.m.s. distribution) to $\sigma_\lambda \sim 1.2$ and more. This means that there exists some scatter in the initial conditions, perhaps (as indicated earlier [2]) determined by some parameter (for example—we are citing this exclusively by way of an example —the impact parameter). In the "fire ball" model we can assume that two clusters are always formed, but sometimes—owing to the smallness of $\bar{\gamma}_1$ and $\bar{\gamma}_2$—the two maxima almost overlap.

ing immediately the nonapplicability of the initial hydrodynamic theory of central "frontal" collisions of two nucleons. Indeed, this theory prescribes a distribution in the form [cf. (4.7a)]

$$dn=\frac{n}{\sigma_\eta\sqrt{2\pi}}e^{-\frac{\eta^2}{2\sigma_\eta^2(s)}}d\eta=\frac{n\cdot 2,3}{\sigma_\eta\sqrt{2\pi}}e^{-\frac{2,3^2(\lambda-\log\gamma_c)^2}{2\sigma_\eta^2}}d\lambda, \quad (4.25)$$

with

$$\sigma_\eta^2=0.56\ln\frac{s}{2M^2}+1.6.$$

Accordingly, the distribution with respect to λ has a single maximum (with half-width $\sigma_\lambda=\sigma_\eta/2.3$ approximately to 1.0 for $E_L=10^{12}$ eV and $s=2E_LM\approx 2000$). Each nucleon carries away after the collision an energy

$$\varepsilon_N\sim M\exp\sqrt{1{,}12\ln\frac{s}{2M^2}},$$

which is only M/μ times larger than the average meson energy, so that the inelasticity coefficient is very close to unity:

$$1-K\approx 2\exp\left(-\frac{1}{2}\ln\frac{s}{2M^2}+\sqrt{\ln\frac{s}{2M^2}}\right). \quad (4.26)$$

These two facts exclude the central hydrodynamic collision scheme for jets of this type, at least in the form that follows from Landau hydrodynamics.

Let us proceed to different variants of the OMA. The two-center model with identically excited nucleons (Sec. 2a) is immediately excluded, for in it the inelasticity coefficients are large and the multiplicity is small (when $E\sim 10^{13}$ eV we have $n\sim 10$).

To discuss other variants it is important to know the values of the momentum transfer in the fire ball model. We are talking of three values of the squared momentum-transfer: k_{12}^2, k_{23}^2, and k_{34}^2. In view of the symmetry of the process we can assume that $k_{12}^2=k_{34}^2$. To determine these quantities we use (4.17a) and (4.18).

If the extreme groups are simply nucleons, then according to (4.17a) we have for $K=0.3$

$$k_{12}^2=k_{34}^2\equiv k_N^2\approx 0{,}1M^2\approx 5\mu^2. \quad (4.27)$$

If the nucleons are excited to the state of isobars with masses $\mathfrak{M}=\sqrt{s_1}=1.3$ BeV, then we must start from the expression

$$(k_{12}^2)_{\min}=\frac{(s_1-M^2)(s_2-M^2)}{s}=0.7\frac{s_2}{s}M^2. \quad (4.27a)$$

The value of s_2 is obtained here as the difference between the square of the energy and the momentum of the entire system. If the total momentum of the two average clusters (the energy of each being $\bar\gamma\mathfrak{M}_{\pi\pi}$) is equal to zero, and the momentum of the second nucleon after collision is approximately equal to its energy $(1-K)E_C$, then we get

$$s_2=(2\mathfrak{M}_{\pi\pi}\bar\gamma+(1-K)E_c)^2-((1-K)E_c)^2$$
$$=4\mathfrak{M}_{\pi\pi}^2\bar\gamma^2+4\mathfrak{M}_{\pi\pi}\bar\gamma(1-K)E_c,\ \mathfrak{M}_{\pi\pi}=\frac{3}{8}n_sM. \quad (4.27b)$$

Substituting the experimental values, we obtain (for $E_L=10^{12}$ eV, $K=0.2$, $n_S=14$, $\mathfrak{M}_{\pi\pi}=5$ M, and $\bar\gamma=1.5$)

$$k_{12}^2\approx 0.28M^2$$

(when $E_L=10^{13}$ eV, $n_S=20$, $\mathfrak{M}_{\pi\pi}=7.5$, and $\bar\gamma=2$ we get $k_{12}^2\approx 0.14\ M^2$).

For the quantities k_{23}^2 we obtain much larger numbers. We can use here formula (3.5b), in which we must put $s_1=s_2=\mathfrak{M}_{\pi\pi}^2$ and s is taken to be the square of the sum of the 4-momenta of the colliding pions k_{12} and k_{34}, $\bar s\to s=-(k_{12}+k_{34})^2$. Since we have assumed that the total momentum of the two-pion clusters is equal to zero, we also have $k_{12}+k_{34}=0$. But the energy of each of these pions is equal to KE_C or, what is the same, to $\bar\gamma\mathfrak{M}_{\pi\pi}$. Thus, $\bar s=(2\bar\gamma\mathfrak{M}_{\pi\pi})^2$. As a result we obtain for $E_L\sim 10^{12}$—10^{13} eV, $\mathfrak{M}_{\pi\pi}\sim 5$ M, and $\bar\gamma\sim 1.5$—2,

$$k_{23}^2=\frac{\mathfrak{M}_{\pi\pi}^2}{4\bar\gamma^2}\sim(3-4)M^2\text{*}. \quad (4.28)$$

Let us compare these values of k_{12}^2 and k_{23}^2 with the results of variants (b)—(e) in the OMA.

The process shown in Fig. 15 corresponds to variant (b). It could lead to two "fire balls" if a cluster that decays with formation of two maxima in the Landau scale is produced following a central collision of the virtual pions. However, the only existing theory of central collisions is the hydrodynamic theory in all its variants, and it leads to a single-maximum distribution. It is possible, to be sure, that allowance for viscosity[96], allowance for the dependence of the velocity of sound on the temperature (such a possibility was indicated in a private conversation by G. A. Milekhin), or allowance for the resonant interaction between the particles in the final stage of their moving apart can lead to a two-maximum distribution. These possibilities, however, have not yet been sufficiently well investigated, and we must state here that the process of Fig. 15 is difficult to reconcile with the model of two fire balls.

Variant (c) of the OMA corresponds to the diagram of Fig. 16. In this case we naturally obtain small inelasticity coefficients for the nucleons, and two maxima in the λ-distribution. The value of k_{23}^2, as in general in the two-center model (see Chapter III) (with a c.m.s. energy $E_{\pi\pi}=2\bar\gamma\mathfrak{M}_{\pi\pi}$ of the two colliding pions) can be of the order of

$$k_{23}^2\approx\frac{2M^2}{\ln E_{\pi\pi}^2/2M^2}\approx 0{,}5M^2.$$

This is noticeably smaller than the experimental value $k_{23}^2=(3-4)\,M^2$.

We note that in variants (b) and (c) the diagrams of Figs. 15 and 16 should also give a constant contribution at higher energies. In order to check whether this is

*An analogous estimate was obtained for k_{23}^2 in [77,89].

so, it is necessary to ascertain whether the two-maximum structure is retained and whether the quantity k_{23}^2 varies at high energies.

Some information can be obtained here even now. Recognizing that $\mathfrak{M}_{\pi\pi} = \frac{1}{2}Mn/2$ and $n = 3n_s/2$, we can rewrite (4.28) in the form

$$k_{23}^2 = \frac{1}{4}M^2\left(\frac{3n_s}{8\bar{\gamma}}\right)^2. \qquad (4.28a)$$

If, as is customarily assumed, $n_s \sim E_L^{1/4}$ and $\bar{\gamma}$ is given correctly by the table that follows Eq. (4.21) and consequently, also varies approximately like $E_L^{1/4}$, then k_{23}^2 does not vary with the energy.* However, these data are not sufficiently accurate to be able to draw final conclusions.

Let us consider now the multiperipheral model [(d) and (e)].

The literally-taken AFST model (where we assume $s_{\pi\pi} \approx 0.5\,M^2$) cannot claim any agreement with experiment, as was already mentioned in Sec. 4 of Chap. III. First, the cross section at $E_L \sim 10^{12}$—10^{13} eV is obtained too small (see page 21); second, the angular distribution in this model has not two but many maxima and has too large a width in λ coordinates (see page 22). Third, in this model the values of k^2 should be small, on the order of $k^2 \lesssim s_0 = 0.5\,M^2$.

The model with the heavier clusters (variant e) comes closer to the experimental fire ball scheme. At $E_L = 10^{12}$ eV the main contribution is made in this model by the process with two intermediate $\pi\pi$ knots (that is, a diagram of the type of Fig. 16). The masses of the $\pi\pi$ knots, $\mathfrak{M}_{\pi\pi} \sim \sqrt{s_0} = (4-5)\,M_1$ correspond in this case to the observed masses of the fire balls. Within the framework of the model, as indicated above, k_{23}^2 may differ from k_{12}^2 and k_{31}^2, and can exceed them. Thus, this model agrees with the fire ball scheme if $E_L \approx 10^{12}$ eV. It must be emphasized that in accordance with this theory the number of fire balls should increase at higher energies and the angular distribution becomes multi-centered.

We note that variants (c) and (d) reduce for $E_L = 10^{12}$ eV to a consideration of the same diagram of Fig. 16. Therefore the decision as to which variant corresponds to reality can be made only at a higher energy.

c) Presence of two maxima in the nucleon-nucleus collision. It was shown as far back as in 1958 that a two-maximum structure is encountered also in the case of nucleon-nucleus collisions.[97,98] By now rather extensive material has been systematized[99] on nucleon-nucleus collisions (distinguished by the fact that $N_h > 8$, and in the mean it is much larger, $\bar{N}_h \gtrsim 15$ and $n_s > 40$). At energies $E_L > 10^{12}$ eV some 50 or more charged particles are produced here in one act. The $n(\lambda)$ distribution is therefore constructed with sufficient certainty. A scatter in the values of σ_λ is again observed for the entire curve. However, in those cases when the width is large, $\sigma_\lambda > 0.9$, two maxima are always observed clearly, with the same qualitative characteristics as in the nucleon-nucleon collision, approximate equality of the particles in the front and rear cones, isotropy of the scattering in the proper system of each cone, the same average energy for each of the particles in the proper system of the cluster, $\epsilon = M/2$, etc. (Actually, in the rear cone there are a few more particles and the cone is somewhat more collimated. But this can be attributed to distortion due to secondary interactions in the material surrounding the nucleus, since the particles of the rear cone leave the channel produced in the nucleus relatively slowly).

The general qualitative similarity between the nucleon—nucleon and nucleon—heavy nucleus collision patterns is so great that we are again induced to turn to the model of the two fire balls produced by the pions. Indeed, we can imagine that, as in the case of the nucleon-nucleon collision, the pion of the incident nucleon interacts with the group of pions of the target nucleus, and the nucleons themselves (their cores)—both the incident nucleon and the target nucleons—take no part in this process and retain a considerable part of their energy[100,101]. Favoring such a pattern are experiments which show that the nucleon retains a considerable fraction of its energy even following a collision with an iron nucleus[102]. Continuing in analogy with the nucleon-nucleon collision, we can state that in the OMA this pattern corresponds to the diagram of Fig. 22, where the nucleus is shown by a set of lines of individual nucleons. We recall that this picture of the interaction between the nucleon and the nucleus is preferable also from the point of view of the MMP (if we assume the correspondence between the OMA and the MMP discussed in Chap. III).

However, several questions arise in a more detailed examination of this mechanism. First, it is difficult to understand how a collision between several pions results in only two clusters which are furthermore of equal size and decay isotropically. Such a symmetry

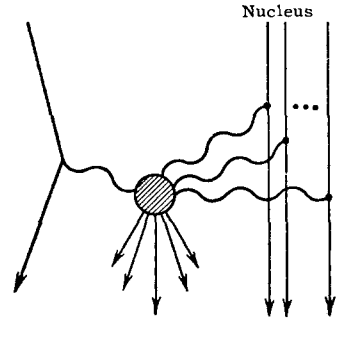

FIG. 22. Possible scheme for formation of a cluster in a one-meson interaction with a nucleus.

*A recent analysis of experiments has recently led Czech investigators [95] to the conclusion that the quantity k_{23}^2 (4.28a) can actually be constant.

could be ensured, naturally, by the hydrodynamic theory. However, as emphasized above, in those forms in which the theory is developed, it yields only one maximum in the angular distribution (in the λ coordinate).

To describe the two sharp maxima, each containing many particles, it would be necessary to modernize the hydrodynamic theory, as mentioned in the preceding section. This question has not yet been sufficiently thoroughly treated. To this end it is very important, first, to determine more accurately and more reliably the energy retained by the nucleon after interacting with the center of a sufficiently heavy nucleus. There is no doubt that the two-maximum structure in the nucleon-nucleus collision is one of the most interesting experimental facts, which so far has received not even a heuristic explanation.

d) "Lean jets" and excitation of one cluster at high energies. The second of the new facts are the properties of the "lean" jets. Improved procedures, which made their study possible (emulsions interleaved with lead), led to a detection at $E_L > 10^{12}$ eV of such jets with $n_s < 5$, in which there is one excited center, yielding 2—4 charged particles, and a second center yielding 1—2 particles[102]. They are so far apart in λ ($\bar{\gamma} \sim \gamma_c$) that they should be regarded more readily as the decay of excited nucleons rather than an explosion of "fire balls" emitted by the nucleons, or else as a decay of one "fire ball" and weak excitation of one of the nucleons (which gives not more than one additional particle). In this connection mention should be made of other similar cases, for example the known "Bristol jet"[104] (Fig. 23), where two clusters gave only three charged particles each, but they were so far apart in λ coordinates ($\bar{\gamma} \sim \gamma_c/2 \sim 40$) that they can be interpreted as the decay of excited nucleons.

From the theoretical point of view these processes can be interpreted in two ways. On one hand, they can be interpreted as the excitation of nucleons in the OMA [see (3.15) and the subsequent estimates]. Actually

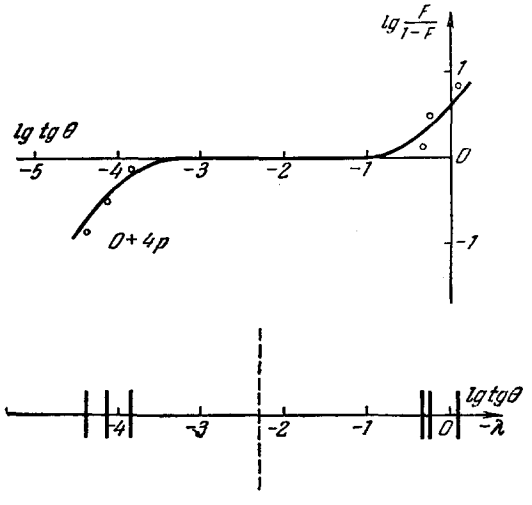

FIG. 23. "Bristol jet."

there should occur here showers of low multiplicity and with a very anisotropic angular distribution. On the other hand, diffraction inelastic processes (see Chapter V below) also lead to a similar picture.

The scarcity of experimental data (the investigation of such processes is only beginning) has not made it possible so far to draw any conclusions with respect to the preferred interpretation in this case.

As to cases of sharp asymmetry (one cluster) and considerable multiplicity, the authors of [103] compare them correctly with the one-center jets, which were previously observed at 3×10^{11} eV[67], and assume that this is the same phenomenon but at a higher energy.

e) Comprehensive study of interactions at $E_L \sim 3 \times 10^{11}$ eV. One of the most important latest results is the proof that front-back c.m.s. symmetry may not occur in individual nucleon-nucleon interactions. This proof was obtained[67] (the research was carried out on Pamir) through the use of a new procedure: a cloud chamber in a magnetic field, located above an ionization calorimeter. The first results were reported in 1959 (see [105]) and in more complete form at the end of 1960.

The average energy of the processed cases is $E_L \sim 3 \times 10^{11}$ eV (the energy was determined by the ionization calorimeter accurate to several dozen per cent). Knowing E_L, the entire picture could be transformed to the c.m.s. It was observed here that in approximately half the cases the number of particles emitted forward and backward was approximately equal (Fig. 24a), in one-quarter of the cases the particles moved predominantly forward, and in the other quarter backward (Figs. 24b and c). Knowing all the energies and assuming that the π^0 mesons can be accounted for by a factor $3/2$, it is possible to calculate the inelasticity coefficients K_{lab} and K_{mir} for each individual jet. The authors designate each case by a symbol in the K_{lab} and K_{mir} frames (Fig. 25) (the symbols ●, ▲, and ▼ denote the c.m.s. angular distributions shown in Figs. 24a—c respectively). There is an obvious correlation between the position of the symbol and the angular distribution, making it possible to interpret these events in the following fashion[106]. In the case of Fig. 24c, a collision occurred between the target nucleon and the pion from the meson cloud

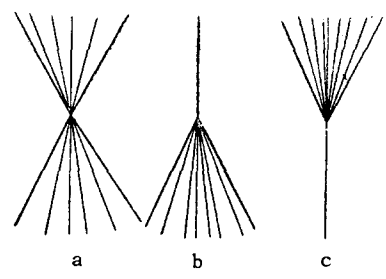

FIG. 24. Symmetrical and asymmetrical jets investigated in [67] (scheme).

of the incoming nucleon. The latter, giving up a pion, lost little energy ($K_{lab} \sim 0.2$—0.3), while the target nucleon experienced in the mirror system a catastrophic collision, $K_{mir} \sim 1$. This resulted in an excited cluster, which, decaying isotropically in its own rest system, produced in the c.m.s. (relative to which it moves) a backward-directed fan. The inverse case (Fig. 24b) corresponds to collision between the incoming nucleon with a pion from the nucleon cloud of the target ($K_{mir} \sim 0.2$—0.3 and $K_{lab} \sim 1$). These asymmetrical cases can thus be interpreted as single-meson processes, in which a virtual pion experiences a "central" interaction with one of the nucleons and greatly excites it (see Chap. III). Finally, among the symmetrical cases of Fig. 24a, when it turns out that $K_{mir} \sim K_{lab}$, we can distinguish, on the one hand, the catastrophic collisions with $K_{mir} \sim K_{lab} \sim 0.7$, which can be interpreted as "central" collisions of the nucleons, and on the other hand the cases $K_{mir} \sim K_{lab} \sim 0.2$—$0.3$, when it can be assumed that two pions from the clouds of the two impinging nucleons have collided. In addition, the last process can be regarded as a peripheral interaction between the virtual pion and the nucleon.

Such an interpretation enables us to estimate roughly the ratio σ^C/σ^P of the contributions of the central and peripheral collisions for πN and NN interactions. We represent the cross section of the NN interaction as the sum of central and peripheral cross sections $\sigma_{NN}^{tot} = \sigma_{NN}^{C} + \sigma_{NN}^{P}$. Using the Weizsäcker-Williams method, we can write $\sigma_{NN}^{P} = \sigma_{NN}^{P(1)} + \sigma_{NN}^{P(2)}$, where $\sigma_{NN}^{P(1)}$ is the cross section of the one-meson process, in which the target nucleon "gives up" its meson and its excitation is known to be little; the inelasticity coefficient in this case is small. $\sigma_{NN}^{P(2)}$ is the cross section of the analogous process when the meson is "given up" by the incoming nucleon. The last two cross sections are proportional to the total cross section σ_N^{tot} of the πN interaction, which can also be represented as the sum of the cross sections of the central and peripheral interactions, $\sigma_N^{tot} = \sigma_N^C + \sigma_N^P$. Then σ_{NN}^P will be proportional to the sum of the four cross sections

$$\sigma_{NN}^{P} \sim \sigma_{\pi N}^{C(1)} + \sigma_{\pi N}^{C(2)} + \sigma_{\pi N}^{P(1)} + \sigma_{\pi N}^{P(2)}.$$

However, in a peripheral interaction between a meson and a nucleon, the latter is also excited little. Thus, the two last terms describe identical processes: showers that are symmetrical in the c.m.s. and in which both inelasticity coefficients are small, with $K_{mir} \sim K_{lab}$. The cross sections $\sigma_N^{C(1)}$ and $\sigma_N^{C(2)}$ correspond to showers which are directed "forward" and "backward" in the c.m.s. The borderline value K_0 will be assumed for concreteness to be $K_0 = 0.35$. We then have the following:

1) The number of cases with $K_{mir} \sim K_{lab} > 0.35$ is proportional to the fraction of central NN interactions; according to Fig. 25, there are 15% such cases.

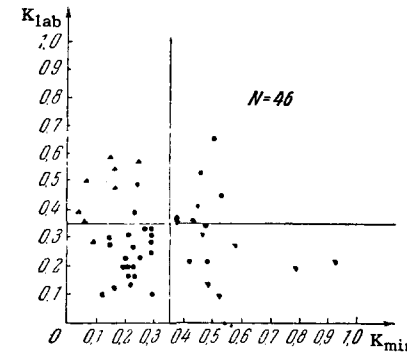

FIG. 25. K_{lab} and K_{mir} for individual showers: ● – symmetrical in the c.m.s.; ▲ – directed predominantly forward; ▼ – directed prodominantly backward.

2) The number of cases with $K_{mir} < 0.35$, $K_{lab} > 0.35$ or $K_{mir} > 0.35$, $K_{lab} < 0.35$ is proportional to the fraction of the central πN interactions, of which there are here 20 + 20 = 40%.

3) The number of cases with $K_{mir} \sim K_{lab} < 0.35$ is proportional to the fraction of the peripheral πN interactions; there are 45% such cases. Using these figures, we find that

$$\left(\frac{\sigma^C}{\sigma^P}\right)_{NN} = \frac{15}{85} \approx 0.2, \quad \left(\frac{\sigma^C}{\sigma^P}\right)_{\pi N} = \frac{40}{45} \approx 1. \qquad (4.29)$$

We note that analogous data for the ratios σ^C/σ^P were obtained from experiments at accelerator energies [61] [see (3.8)].

In addition, interpreting the groups of cases with $K_{mir} \sim K_{lab} \sim 0.35$ as a result of collision between virtual pions, we can extract from the experimental data the value of the "mass" of the pion cluster $\mathfrak{M}_{\pi\pi}$ and its c.m.s. Lorentz factor $\bar{\gamma}$. It turns out that the values of $\mathfrak{M}_{\pi\pi}$ center about a value $\overline{\mathfrak{M}}_{\pi\pi} \approx 4\,M$. The values of $\bar{\gamma}$ are different: for half of the collisions (namely, in the "symmetrical" cases) $\bar{\gamma} \approx 1.05$. In the "asymmetrical" cases $\bar{\gamma} \approx 1.3$.*

From the point of view of the OMA, this process is naturally considered on the basis of the diagram of Fig. 15.

This analysis was carried out in [62], and the theoretically obtained values $(\mathfrak{M}_{\pi\pi})_{eff} \approx 3M$ and $\bar{\gamma} \leq 1.1$ agree well with the experimental figures given above. Thus, the symmetrical cases agree qualitatively with the OMA. An increase in the statistics and an increase in the energy E_L will apparently permit in the near future to obtain more reliable data on the structure of the collision process. We note that although one decaying cluster is obtained here, analysis shows [62] that in a very large fraction of the cases the nucleon which has lost little energy turns out to be excited,

*It must be emphasized, however, that symmetrical and asymmetrical jets are not sharply distinguishable. The distribution of events with respect to $\bar{\gamma}$ is also smooth, and there is no sharp borderline between the regions of $\bar{\gamma}$.

with spin and isospin values $^3/_2$, that is, in the isobar state which usually appears in resonant scattering of pions by a nucleon in the pion energy region near 2μ. The conclusion that the nucleon which has lost little energy is usually in the isobar state ($^3/_2$, $^3/_2$) and then decays with emission of a single pion, is an assumption made also in several other investigations [100,107]. Such a decay can explain the existence of high-energy muons in extensive air showers (as a result of the decay $N^* \to N + \pi \to N + \mu + \nu + \tilde{\nu}$). The corresponding calculations were carried out [108], but comparison with experiment yielded no definite conclusions so far. The observed cases of decaying isobars in individual acts are more convincing [100,106].

f) Existence of the hydrodynamic process. The fact that the two-maximum jets predominate among the nucleon-nucleon collisions and the success of the model of peripheral interactions have cast doubts on the reality of the Heisenberg-Fermi-Landau hydrodynamic process. The opinion has been advanced that this process does not exist at all (the opinion was based essentially on the desire to explain the observed inelastic processes by means of a single scheme). The situation is not so simple, however. It is clear, first, that the central collisions initially considered in this theory should be rare events. In the majority of cases, inasmuch as the impact parameter of the two nucleons is not small and is of the order $1/\mu$, the picture should be different. It has been clear for quite some time that the hydrodynamic description should be applied to the decay of excited centers which are produced in peripheral collisions, that is, an appreciable part of the interactions must be considered using a mixed scheme, which can be called peripheral-hydrodynamic (which was indeed used in [62,106] and in other investigations). If we apply this scheme to each cluster ($\pi\pi$ fire ball) then, taking account of the experimental data, we arrive at the need for using the Heisenberg hydrodynamics in $\pi\pi$ interactions.

On the other hand, we can attempt to apply, as mentioned above, the hydrodynamic description to the decay of a heavier cluster and attempt to attribute the appearance of fire balls to the scattering asunder of the single hydrodynamic system produced upon collision between two virtual pions. However, attempts to modify the hydrodynamics by taking into account viscosity, etc., in such a way as to explain the appearance of two maxima with isotropic scattering and high multiplicity, have not yet been successful [96]. It is possible that this could still be attained by varying the equation of state. There is, however, one property inherent in the hydrodynamic process, which is quite typical, namely that the presence of a traveling wave should disclose a considerable number of cases (several times 10%) in which almost the entire energy of the primary particles is carried away by a single pion, and that in one-third of the cases this pion should be neutral [109]. From this point of view, considerable interest attaches to the observations of N. L. Grigorov and his co-workers [110], who used an ionization calorimeter to study nuclear-electron cascades generated in lead and iron by nucleons with $E_L \sim 10^{11}$–10^{12} eV. These experiments lead to the conclusion that in 5–10% of the investigated cases almost the entire primary energy is transferred to the electromagnetic cascade, that is, a π^0 meson of rather high energy is first produced. This clearly agrees with the hydrodynamic picture and can be interpreted only in very far-fetched manner as the decay of the nuclear isobar state ($^3/_2$, $^3/_2$) into which the primary nucleon goes over. Indeed, from experiments with a cloud chamber [67] (see Fig. 25) it is known that in nucleon-nucleon collisions the primary nucleon jumps forward, retaining a considerable fraction of its energy in less than half of the cases. In the case of nucleon-nucleus collisions, such cases should be even rarer. Further, in the rest system of the isobar the decay produces a pion with energy ~ 200 MeV and a momentum of the order of μ. The decay occurs in this system almost isotropically. In the L system the pion energy is

$$\varepsilon_{\pi L} = \gamma_B (2\mu + p v_B \cos\vartheta),$$

where γ_B is the Lorentz factor of the isobar relative to the L system, and ϑ is the angle of emission of the pion in the c.m.s. Obviously, $\gamma_B \leq \gamma_L = E_L/M$. Consequently, only in specially favorable cases, when $\cos\vartheta \approx 1$, can we hope that the pion energy in the L system will be

$$\varepsilon_{\pi L} \sim \gamma_L \cdot 3\mu = \frac{3\mu}{M} E_L.$$

Even in this case it cannot be close to E_L as is apparently obtained in experiment. One must expect that further experiments of this type will make more precise and more reliable the foregoing conclusions.

g) Multicenter jets. Hasegawa [78] advanced the hypothesis that with increasing energy (say, at 10^{14} eV) the distribution of the generated particles with respect to λ frequently displays not one (as in the case at 3×10^{11} eV, see Sec. 3c), and not two (as for 10^{12}–10^{13} eV), but four maxima, interpreted respectively as four independently decaying fireballs. Figure 26 shows examples of interactions so interpreted. The existence of such multicenter stars would be of great interest. It would correspond to the AFST theoretical scheme of the multiperipheral collision (modified to increase appreciably the mass of each cluster, see Chap. III). It is important that the observed values of the distribution widths σ_λ can be reconciled with the model of many centers only by foregoing the isotropy of the decay of each center in its own rest system and by assuming that the pions are emitted predominantly in a transverse direction. The experimental data are so far very skimpy and it is by far not clear whether such a grouping of the tracks goes beyond the limits of statistical fluctuations. We note that the cited experimental cases with this appearance are distinct in having a

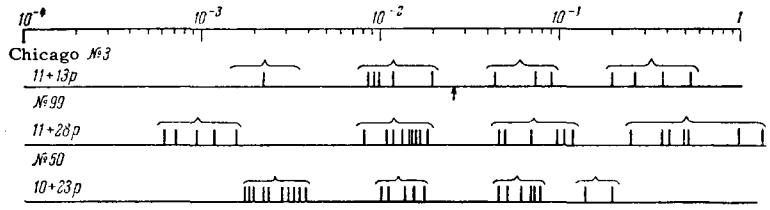

FIG. 26. Jets interpreted in [78] as having four centers.

relatively small number of particles (for such an energy).

h) The question of the change in the character of the elementary act at $E_L \gtrsim 5 \times 10^{14}$ eV. This question has been raised by investigations of extensive air showers of large size (the number of electrons of the observation level is $N \geq 10^5$, that is, the primary-particle energy is $E_L \gtrsim 5 \times 10^{14}$ eV). Things are far from clear here and further thorough research is greatly needed. The entire problem has been discussed in detail in a recent review by S. I. Nikol'skiĭ [111], and we confine ourselves here to a brief summary of the conclusions of this survey.

Experiments show apparently that many typical characteristics of extensive air showers change appreciably on going through the indicated energy region. Thus, the relative number of nuclear-active particles in the shower changes, the fluctuations in the distribution of the energy among the shower components decrease, the structure of the shower core changes, narrow showers with a small number of muons appear, and the fraction of the energy carried away by the nuclear-active component decreases. It should also be noted that the spectrum of the single photons in the the atmosphere changes at $E_L \sim 10^{12}$ eV.[112] This implies that the nucleon interaction which generates the photons changes at $E_L \sim 10^{14}$, etc.

All this may be due, as shown by an analysis [11], to a change in the elementary act of collision, such that: (a) the inelasticity coefficient of the colliding nucleons increases, and (b) additional electrons or photons appear, as well as muons with energy $E_L \sim 10^{12}$ eV and with transverse momenta $p_\perp < 10^{18}$ eV/c.

In this energy region, a change takes place also in the character of the primary spectrum. However, this change alone is insufficient to cause the entire aggregate of anomalies. To the contrary, an increase of 20—30% in the cross sections of the nucleons in interstellar matter could explain the change in the primary spectrum itself.

We note that the threshold $E_L \sim 5 \times 10^{14}$ eV corresponds quite accurately to the characteristic weak-interaction energy at which perturbation theory becomes inapplicable. However, the cross section of weak interactions is too small here to be able to ascribe any significance to this coincidence. [3]

Of all the possible causes for the increase in the fraction of the energy going over into the electron-photon component and the production of muons, we point to a mechanism [3,113,114] which explains the additional electromagnetic radiation as "black body radiation" of a cluster of nuclear matter, which occurs during the interaction process and decays into pions. Quantitatively, the role of this mechanism (which in itself undoubtedly exists) depends strongly on the rate of expansion and decay of the cluster or, what is the same, using hydrodynamic terminology, on the equation of state of the nuclear matter. At the present status of the theory, this question cannot be resolved unambiguously in quantitative terms.

4. Conclusion

The experimental data obtained recently offer evidence that the interactions between high-energy particles are varied and they cannot be fitted in the framework of one scheme.

The hydrodynamic theory of head-on collisions, which a few years ago was the only developed theory, is now certainly incapable of describing all (or even an appreciable part) of the interaction events. However, it is likewise impossible to state that it has no possible field of application. There are processes where it seems essential to use this theory.

Indeed, the decay of a meson cluster containing 10—20 mesons even in a nucleon-nucleon collision (and on the order of hundreds of particles in a nucleon-nucleus collision) naturally calls for the use of the hydrodynamic treatment. However, even here it may be adequate only after appreciable modifications. Namely, in the model of two fire balls the multiplicity and the angular distribution in the decay of each of the clusters are such that they correspond to hydrodynamics with an equation of state different from that assumed by Landau, and the square of the velocity of sound should be appreciably smaller than $\frac{1}{3}$. On the other hand, if two clusters result from a hydrodynamic decay of one larger cluster, then some other singularities should come into play, for example viscosity, etc.

The theory of peripheral interactions (OMA) contains some still undetermined parameters and therefore leads to several mechanisms and admits of many variants. Its limiting case, the multiperipheral AFST model, apparently has no region of application in the form in which it was developed in [71,72-74].

Different intermediate variants of the OMA, and primarily the model with "loaded" clusters (the pion

cluster breaks up not into two pions as in the AFST, but into approximately 10 pions) agree qualitatively with many experimental data. It can be assumed that an appreciable fraction of the nucleon collision processes at energies 10^{11}—10^{13} eV do not contradict this model.

The most general and most important property of the other variant of the OMA—the two-center model —can be seen in the fact that it predicts small values of the square of the momentum transfer (which decrease with energy) for inelastic collisions, and consequently also for elastic collisions.

In spite of the variety in the OMA variants, it seems to us that we can still not assume that this approximation can describe all the interaction acts. Further, cases are encountered in nucleon interactions when one energetically favored pion is produced (see Sec. 3f), cases which are difficult to understand in the framework of the OMA. One can therefore think that in addition to peripheral processes of the one meson nucleon-nucleon interaction, which occur in accordance with the OMA scheme, "central" collisions exist in 10 to 20% of the cases. This estimate is confirmed also by other independent considerations [see (3.8) and (4.29)].

Bearing in mind the correspondence between the OMA and the MMP, referred to above (Chap. III), we can reach the conclusion that in this energy region the method of moving poles in its canonical form can likewise not claim to describe all the nucleon-nucleon interaction processes.

V. CONNECTION BETWEEN THE METHOD OF MOVING POLES WITH THE DIAGRAM APPROACH AND THE ONE-MESON APPROXIMATION

1. Formulation of the Problem

The analysis of the MMP (Chap. II) on the one hand, and of the theory of peripheral collisions based on the one-meson approximation (Chap. III) on the other, raises, naturally, many questions.

First among them is the question of the connection between these two approaches, which lead in the main points to agreement between the results with respect to the elastic process, and also the question of what information can be obtained from the comparison. In particular, it is important to know whether this comparison can clarify the limits of applicability and the validity of each of the methods, and to attempt to understand why in some cases the MMP predicts correctly the experimental facts and in others it leads to errors.

The second question concerns the structure or the diagram interpretation of the vacuum reggeon. Oversimplifying somewhat, we can ask: what particles is the reggeon made of?

Finally, the third question consists in the following. In the MMP all the particles (both "compound," such as the resonant ρ and ω mesons, etc., and "elementary"—pion, nucleon, etc.) are regarded from a single point of view as "moving poles" in the plane of the complex orbital angular momentum. What new consequences follow from this when peripheral (single-quantum) inelastic processes are considered?

At first glance these questions seem to be far afield. Actually, however, they are related. This is seen in particular if we consider them from the point of view of diagram methods. This explains both the physical meaning of the postulates made in the MMP, and also the region of applicability of the MMP and the OMA.*

2. Diagram Interpretation of the MMP

Let us consider the diagram of elastic scattering through a zero angle, when $t = 0$, and let us consider the case of large s (when according to the MMP the main contribution is made to the amplitude by the vacuum reggeon). The amplitude is then pure imaginary.

Consequently it follows from the unitarity condition that this amplitude can be represented in the form of a product (more accurately, a sum of products) of the two amplitudes of the inelastic process. From the diagram point of view this means that the diagram of the elastic process can be cut in two by a line perpendicular to the s direction (Fig. 27), and the crossed lines "are on the mass shell," that is, they describe real and not virtual particles. (This is designated, as customary, by strokes through the lines.) Therefore each half of the thus obtained diagram represents a diagram of a real inelastic process.

It already follows from this that when $t = 0$ the vacuum reggeon propagating in the t channel (see Fig. 8) corresponds to the aggregate of the two rectangles joined by the vertical lines in Fig. 27. Therefore it cannot be described by a Feynman diagram

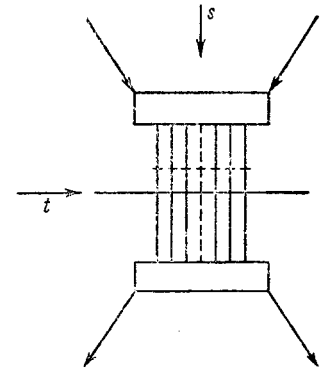

FIG. 27. Diagram of elastic scattering.

*We must note that some considerations advanced in this section are not yet fully accepted. In particular, the rapid development of the methods has not yet led to a single point of view even with respect to the MMP.

which contains only one virtual line. In other words, the vacuum reggeon consists of at least two quanta, one of which carries the interaction in the upper part of the diagram of Fig. 27, and the other in the lower. How many and which particles really take part here? By answering this question we not only determine the structure of the vacuum reggeon, but also explain the character of the inelastic process which results in elastic scattering of the Regge type.

We recall first that in the MMP we are considering not Feynman diagrams but the so-called dispersion diagrams, where the pion lines lie on the mass shell (that is, $k^2 = -\mu^2$ for these lines). Further, one of the fundamental premises of the MMP is the use of the two-particle unitarity condition in the interval $4\mu^2 < t < 16\mu^2$.

This means that the process shown by the Feynman diagram of Fig. 27 is represented in the MMP in the form of the "dispersion" diagram of Fig. 28. Such a limitation is also used directly to justify the absence of other singularities except the moving poles in the derivation of the relation between the cross sections (see the appendix). We can therefore say that the main contribution to the vacuum reggeon, a contribution without which the reggeon is meaningless, is made by a state of two pions. In this connection, a vacuum reggeon is sometimes called a bipion.

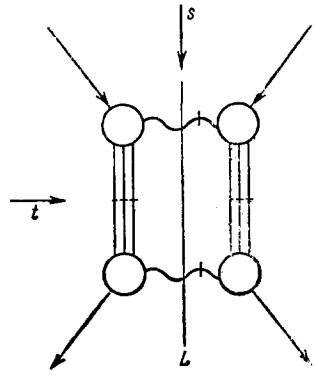

FIG. 28. Diagram corresponding to two-particle unitarity in the t channel.

If such dispersion diagrams, which take into account only the two-particle unitarity, are represented as an aggregate of Feynman diagrams, the latter will have the same property: the contribution of the process of Fig. 28 will be made only by those Feynman diagrams (Fig. 14) which admit, at least in one place, bisection by a line L which crosses not more than two pion lines. It follows in turn that the Feynman diagrams for the inelastic processes that serve as the basis for the considered elastic process are such that they admit (at least at one place) bisection by a line which crosses only one pion line (Fig. 12). But this is the main attribute of one-meson processes considered in the OMA; the same class of diagrams is thus considered in the OMA and in the MMP. This gives grounds for assuming that these methods are equivalent with respect to the character and extent of simplifying assumptions made[65,66].

The regions of applicability of both methods should also coincide in this case, and where the OMA is not applicable, the MMP can likewise not give good results.*

In light of the foregoing, it becomes understandable that many consequences obtained in the MMP (shrinkage of the diffraction cone, logarithmic decrease of the square of the momentum transfer, and the relation between the cross sections) can be obtained in the OMA in a manner which is to a considerable degree independent. This was already mentioned in Chap. III.

The question remains: what is the place occupied by many-meson or in general many-particle processes in the entire picture (as before, we shall call them arbitrarily "central")? Let us consider the Feynman diagram of an inelastic process, the bisection of which (perpendicularly to the t line) at any point crosses not less than $N \geq 2$ pion lines. The diagram of the corresponding elastic process will contain not less than 2N pion lines. If the aggregate of such diagrams makes a constant contribution to the cross section (that is, a contribution proportional to s to the imaginary part of the forward scattering amplitude), then the corresponding partial amplitude should have in the l-plane a singularity at $t = 0$ and $l = 1$. We note that such a many-meson amplitude cannot have a branch point at $t = 4\mu^2$. Its partial amplitude on the first and second sheets of the t plane should therefore be the same. However, the presence of a pole at the function $f(l, t)$ on two sheets simultaneously contradicts the analytic continuation of the unitarity condition in the l plane. The latter, however, is a unique consequence of the Mandelstam representation[10]. Thus, a constant contribution of many-meson processes is not compatible with the Mandelstam representation and can raise the question of the need for reconstructing the latter.

3. Mixed Model

In light of the foregoing, it becomes sensible to consider for the time being peripheral and central collisions separately and to use different formalisms for

*We can attempt to formulate the region of applicability of the asymptotic MMP (account of one vacuum pole) in the s and t variables. This will be the region where

$$\frac{s}{2M^2} \gg 1 \text{ and } t \lesssim \frac{M^2}{\ln s/2M^2}.$$

It must be borne in mind, however, that from the point of view of the OMA, the MMP may not be applicable even in this region of s and t, if for some reason the "central" collisions make a large contribution to the inelastic process in this region.

their description. In particular, to describe the contribution to the elastic amplitude from peripheral interactions we can use either the MMP or the OMA, while the contribution due to central collision is obtained by assuming the invariant amplitude of elastic scattering to be multiplicative: $A^C = sf(t)$, that is, we essentially apply the optical models [61].

Let us explain the physical meaning of the foregoing, considering the classical diffraction scattering by a black (or gray) disc from the diagram point of view.

The inelastic process responsible for diffraction in this case is merely absorption of the incident wave. This absorption causes heating of the body and subsequent radiation of softer (thermal) quanta. From the diagram point of view this process is essentially not a single quantum one. Indeed, it proceeds via an intermediate "compound" state, the existence of which is possible only if there are many quantum-transfer acts. Only from such processes can we expect that the distribution with respect to the quantity t, due to such processes, will not contract with increasing energy in the case of elastic scattering.

Peripheral one-quantum (in particular, one-meson) inelastic interactions have a different nature. The incident particle is not completely absorbed in this case and no "compound" state is formed. In this sense the peripheral process does not have a complete analog within the framework of the classical optical model. It is therefore clear that the elastic process which it produces does not have to have all the features of the classical diffraction scattering by a black disc.

This leads to a consequence which can be verified experimentally. Namely, if the inelastic processes in some interactions are well described by the OMA, and consequently the main contribution is made by peripheral collisions, then the elastic scattering should be well described by the MMP. On the other hand, if the inelastic processes fit poorly in the OMA framework (meaning that the contribution of the central interactions is appreciable), then the elastic process should be poorly described by the MMP. In other words, there should be a correlation between these properties.

By way of an example let us consider proton-proton and pion-proton interactions at accelerator energies. It was noted above (Chap. III) that pp collisions are well described by the OMA, while the contribution of central interactions was estimated to be 10—20%. At the same time, π^-p collisions are much more poorly described by the OMA. The contribution of central and peripheral interactions is of the same order here. In accordance with the considerations developed above, it should be expected that elastic pp scattering at the same energies will be well described by the MMP, while π^-p scattering will not fit fully in the MMP framework.

The experimental data apparently confirm this conclusion. It was already noted in Chap. II that in elastic pp interaction there appeared clearly a shrinkage of the diffraction cone, and this made it possible even to determine the parameters of the vacuum pole trajectory. It was also noted that in π^-p scattering the shrinkage of the diffraction cone was practically nil. [21] Attempts to describe simultaneously both the pp and π^-p elastic scattering within the framework of the MMP only have not been successful [33,21] even with a sufficiently large set of free parameters.

On the other hand, a mixed model was used in [61], wherein the amplitude of elastic scattering was written in the form

$$F(s, t)=\sigma^P F^P(s, t)+\sigma^C F^C(t). \qquad (5.1)$$

The first term represents here the contribution of the Regge scattering, identified with the peripheral scattering (index P), and therefore depends both on s and on t. The second term is the contribution of the central collision (index C), in which either the dependence on s is completely eliminated ("standing pole" in the MMP terminology) or the motion of the pole due to the many-meson interactions (and accordingly high thresholds with respect to unitarity) is so slow that the s-dependence can be neglected. These two terms enter with coefficients proportional to the corresponding total cross sections.

The expression for $F^P(s,t)$ must be taken in Regge form, with $l_0(t)$ borrowed, for example, from [20] or [21] (actually this quantity would have to be determined anew by applying to the experiment a formula of the type (5.1), but the error which this procedure introduces in the preliminary calculation is apparently insignificant). The expression for $F^C(t)$ can be taken from the optical model. In [61] a Gaussian distribution of the absorption was assumed. Thus,

$$F^P=e^{(l_0(t)-1)\ln\frac{s}{2M^2}+A_0 t}, \quad F^C=e^{\frac{R^2 t}{4}}. \qquad (5.1a)$$

Here A_0 for $t \lesssim M^2/2$ is a constant, $A_0 \approx 1.6/M^2$ [20,23], reflecting the additional dependence B(t) in (2.10). The quantity σ^C/σ^P was already discussed in Chapter III. It represents the relative contribution of the central collisions to the total pp and π^-p interaction cross sections. Experimental estimates were yielded by (3.8) and (4.29)

$$\left(\frac{\sigma^C}{\sigma^P}\right)_{\pi^- p} \sim 1, \quad \left(\frac{\sigma^C}{\sigma^P}\right)_{pp} \sim 0.2. \qquad (5.2)$$

With such an approach only the parameter R, the effective radius of the central collision, remains relatively arbitrary. Of course, it can be different for pp and πp collisions. However, even if we assume for simplicity that it has for both collisions a value $R \approx \frac{1}{2}\mu$, we can explain satisfactorily, within the limits of experimental error, the older experimental data on both pp and π^-p interactions [20,23,31]. More accurate measurements [21] necessitate either a two—three fold increase in the ratio $(\sigma^C/\sigma^P)_{\pi^- p}$ [which incidentally

comes closer to the estimate in [60] than does (5.2)], or the use of different values of R for pp and πp scattering.

The most important aspect of this approach is the breakup of the elastic amplitude into two different terms (peripheral and central), the relative roles of which are determined on the basis of the data on the inelastic interactions.

Let us discuss some consequences resulting from the addition of the non-Regge term in (5.1).

First, at high energies, when

$$\ln\frac{s}{2M^2} \gg \frac{1}{l_0(t)-1}\left(\frac{R^2t}{4}-A_0t+\ln\frac{\sigma^P}{\sigma^C}\right),$$

the second term becomes principal even for a small ratio σ^C/σ^P, since $t < 0$. Further shrinkage of the diffraction cone should then stop; the cross section for the elastic scattering will not decrease without limit, but will tend to a constant (to be sure, small) value. The average value of the square of the momentum transfer will also not decrease without limit, but will tend to a constant value ($|t|_{eff} \sim 2/R^2$). On the other hand, the effective interaction radius is determined by the peripheral, Regge term and therefore it will behave as predicted earlier, that is, it will increase with energy. According to estimates based on (5.1) and (5.2), all the foregoing properties should appear for pp scattering at $E_L \gtrsim 50$ BeV.

Second, at low energies and small values of $|t|$, the role of the first (Regge) term can be appreciable also in πp interactions. Therefore some shrinkage of the diffraction peak can occur also for πp scattering in the region of small s and t. In this region, however, the expression for F^P, which is contained in (5.1), may turn out to be incorrect for other reasons, merely because the contributions of other poles cannot be neglected when s is small.

Third, relations (2.18) and (3.14) between the cross sections for the interaction of different particles, due to the presence of the non-Regge term, should generally speaking not hold. They remain in force only for the cross sections of the peripheral interactions.

It must be noted that although qualitatively the foregoing properties of the collisions follow from the general considerations concerning the presence of many-meson interactions, which become superimposed on the Regge or one-meson interaction, the very breakup of the amplitude into two sharply distinct parts, expressed by (5.1), and also the quantitative estimates, are of course merely rough approximations and serve primarily only for illustration.

4. Inelastic Processes in the OMA and the MMP

Let us proceed now to the third question formulated at the beginning of the section, that of the relative role and difference in the character of interaction via particle exchange and general exchange of quanta of different nature. Thus, in the OMA (Chapter III) we have already talked of an interaction via exchange of K mesons and other particles. In the MMP, however, these interactions are due to the corresponding moving poles. It is not clear whether this fact that the poles move is taken into account in the OMA. On the other hand, there is a known class of inelastic interactions investigated in the MMP. We have in mind the inelastic diffraction processes, which until recently were considered independently of the one-quantum processes. [115-119] The experimentally observed diffraction generation of pions in nucleon collisions [120], called quasi-elastic nucleon scattering, was interpreted within the framework of the MMP as being due to reggeon exchange [121,122]. Yet a general analysis, which covers all the inelastic processes in a single scheme, is possible [123]. It is based on the application of the MMP to inelastic processes which proceed via exchange of any of the poles which represent a "stable" (pion, etc.) or "compound" (ρ meson, etc.) particle. The idea used here is that the inelastic processes represent mutual scattering of two initial particles with masses m_1 and m_2, accompanied by conversion of the particles into two "particles" with masses $\mathfrak{M}_1 = \sqrt{s_1}$ and $\mathfrak{M}_2 = \sqrt{s_2}$, which then decay in an independent process to form the final particles. Such a "scattering" act is shown by the diagram of Fig. 29. It was regarded as the cause of the main class of inelastic collisions in the OMA, where "scattering" was assumed to be realized via exchange of a meson (see Chapter III), and as the cause of diffraction generation in the MMP, where "scattering" is assumed to proceed via reggeon exchange [121,122]. Here, however, we shall regard Fig. 29 as a "Regge" diagram even for exchange of a "stable" particle. This means that the amplitude corresponding to such a diagram will be calculated not by following the Feynman rules, but the rule of correspondence between the imaginary part of the amplitude, say (2.11a) and (3) (see the appendix), and the diagram of Fig. 8 representing it. We see (this was already mentioned in Chapter II) that in place of the propagator

$$D(k^2) = (k^2+m^2)^{-1},$$

which corresponds in accordance with the Feynman

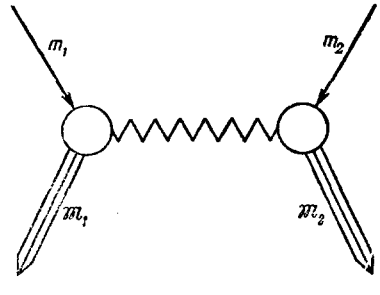

FIG. 29. Inelastic interaction due to reggeon exchange.

rules to an intermediate particle, we use here the function

$$-\frac{\pi\gamma}{2}\frac{1\pm e^{i\pi l}}{\sin\pi l}.$$

Further, the vertex part contains a Legendre polynomial $P_{l_i(t)}(z)$ of order $l_i(t)$. The technique of operating with Regge diagrams [124,28] has been developed only for the simplest cases, when the process can be represented by a diagram with one intermediate reggeon—a "particle" with definite parity, strangeness, isospin, and baryon number. The angular momentum of the reggeon—the "spin" J_i—is not included among these quantum numbers, since it changes when t is varied.

The Feynman and Regge diagrams coincide when $t = m^2$ (when the quantum transferring the interaction can be regarded as real). We note also that the Feynman and Regge diagrams would coincide everywhere if the pole of the corresponding quantum were to be standing, $l_i = \text{const} = J_i$.

The region $t = m^2 > 0$ is the unphysical region of the direct s channel (where s is the square of the energy and t is the square of the momentum transfer). In the physical region, as already noted, an appreciable contribution is made by the values $-t \ll m^2$. In this region the Regge one-particle diagram can be reduced to a one-particle Feynman diagram and, strictly speaking, a contribution must be made by the many-meson Feynman diagrams which ensure that $l_i(0)$ differs from J_i. However, the closer the employed region of negative values of t, $t < 0$, $|t| \ll m^2$, comes to the value $t = m_i^2$, that is, the smaller the difference $l_i(t) - J_i \approx m_i^2$ the smaller is this contribution (for pions, for example, this difference is of the order of $\mu^2/M^2 \sim 2\times10^{-2}$).

Using the rules for operating with Regge diagrams, we can write in following fashion the cross section for the inelastic processes due to exchange of the i-th quantum. For simplicity we confine ourselves to the case when only one of the primary particles is excited, $s_1 = m^2$ (the so-called single-jet processes)*. Then

$$\sigma_i=\int ds_2 dk^2 f^2\frac{s_2^2m^2}{\pi s^2}\left(\frac{\pi\gamma}{2}\right)^2\left(\frac{1\pm e^{i\pi l_i}}{\sin\pi l_i}\right)^2 P_{l_i(k^2)}(z)\sigma_i(s_2,k^2)$$
$$\times[(s_2-m^2+k^2)^2+4m^2k^2]^{1/2}. \qquad (5.3)$$

This expression differs from that obtained in the OMA [for example (3.7)]. However, the replacement of the propagator $(k^2-m^2)^{-1}$ by another function is of no significance and appears only when $k^2 + m_i^2 \gg M^2$, and this region makes a small contribution. The presence of the Legendre polynomial of order $l_i(k^2)$ in the cosine z of the angle in the crossing channel, on the other hand, plays an essential role. The value of z is given by (2.6c). In the most important case when $s_2 \gg m_i^2$ and $k^2 \ll m_i^2$, it simplifies considerably:

$$z \approx \sqrt{\frac{k^2}{m^2}}\frac{s}{s_2}. \qquad (5.4)$$

Of decisive significance in what follows is the fact that, as we have seen in Chapter III, the main contribution to the cross section for the inelastic one-quantum collision to the integral (5.3) is made by the region of values of k^2 for which

$$k^2 \sim \frac{m^2 s_2^2}{s^2}, \qquad (5.4a)$$

and s_2 are large. In such a case z is small, $z \sim 1$.* Accordingly, the function $P_{l_i}(z) \sim 1$ is also small (see also [125]). This factor is then insignificant and (5.3) coincides completely with the expression obtained in the OMA [for example, by integrating (3.7)].

The factor $P_{l_i}(z)$ appears only in the region where z is large and increases with increasing energy. We can put there

$$P_{l_i(k^2)}(z) \sim z^{l_i(k^2)}. \qquad (5.5)$$

It can be shown that in the same region there will appear effects connected with the motion of the poles corresponding to different elementary particles. We can state beforehand that in this region, too, the main contribution will be made by quantum exchange, for which $\mathrm{Re}\, l(k^2)$ is a maximum as $k^2 \to 0$, that is, exchange of a vacuum reggeon.

Integrating (5.3) over all the final states (for which it is necessary to integrate with respect to s_2 and k^2), we obtain the total cross section

$$\sigma=\frac{1}{s_2}\int dk^2 C_1\left(\frac{1\pm e^{i\pi l_i}}{\sin\pi l}\right)^2 P_{l_i}(z)\,s_2\,ds_2, \qquad (5.6)$$

where we put $C_1 = \pi f^2\sigma(s_2, k^2)$ and assume, since very small k^2 are effective when $\sigma(s_2, k^2) \approx \sigma_0$, that $C_1 = \text{const}$.

Expression (5.6), as expected, is analogous to the expression for the elastic cross section in the MMP [the integral of the square of the modulus of the amplitude (2.11a)]. The only difference is that there is an additional integration over the degree of excitation s_2.

In order to investigate the process in greater detail let us consider first the region of small s_2, where z is large. It is necessary to agree here on the manner in which z increases with increasing energy, with increasing s.

*It is shown in [123] that the deductions obtained for single-jet processes are valid also for two-jet processes.

*This exceedingly important circumstance constitutes the main difference between inelastic processes of this kind, which make the main contribution to the cross section, and the elastic processes (and also accordingly the quasielastic processes such as diffraction generation investigated in [121,122]) where z is always large when $s \to \infty$, $z \sim s/(t - 4m^2) \gg 1$. Thus, at large excitations (s_2 large) z is of the order of unity, while at small excitations and in the limit of elastic scattering ($\mathfrak{M}_i = m_i$) z is large.

In the region where z increases in proportion to s, as can be seen from (5.4), s_2 should be bounded. The contribution from this region to the integral (5.6), as can be verified, will decrease with the increasing energy in power-law fashion.

If z increases very weakly with increasing s, for example if we consider the region where $z \gtrsim (s/2m^2)^\nu$ with $\nu \ll 1$, then the substitution $P_l(z) = z^l$ will be valid only at very high energies, which are of no practical interest. It is therefore sensible to confine oneself to an investigation of the region $z \gtrsim (s/2M^2)^\nu$ with $\nu \sim 1-\nu \sim \frac{1}{2}$.

The contribution to the cross section (5.6) from the vacuum reggeon will in this case be equal to

$$\sigma^{(\text{vac})} = \frac{C_1}{\nu\gamma^2 \ln(s/2M^2)}. \qquad (5.5')$$

The contribution from other trajectories will decrease in power-law fashion with increasing energy. For example, the contribution made to this region from one-pion exchange (for which $l_\pi(0) = -\mu^2/M^2$) will be

$$\sigma^{(\pi)} = \left(\frac{s}{2M^2}\right)^{-2\nu} \frac{2}{\gamma^2\nu^2\pi^2} \frac{C_1}{\ln(s/2M^2)} \frac{M^4}{\mu^4}. \qquad (5.6')$$

We can thus conclude that at high energies the contribution of the vacuum reggeon, that is, of the inelastic diffraction processes, is predominant in interactions with small excitation (small multiplicity). However, even this contribution decreases logarithmically with increasing energy and cannot ensure a constant cross section. This is to be expected, since the cross section for elastic scattering itself (the consequence of which are the inelastic diffraction processes) decreases in the MMP logarithmically with increasing energy.

We note also that the inelastic diffraction process, which proceeds via exchange of one reggeon, makes a corresponding contribution, in accordance with the unitarity condition, to the amplitude of elastic scattering (which in this case contains exchange of two reggeons).

It is shown in [28,72] that in this case there appears in the function $f_l(t)$, in addition to a pole, also a branch point (cut) at $l = 1$. This contradicts the main premises of the MMP and has been recently the cause of lively discussions, as already mentioned before (see page 12).

Thus, the main contribution to the cross section of the peripheral interactions is made by the region $z \sim 1$, in which the predominant process is one-pion exchange and the OMA is valid.

The expression for $\sigma^{(\pi)}$ contains a large coefficient M^4/μ^4, not contained in the expression for $\sigma^{(\text{vac})}$, which describes an inelastic process that proceeds via a vacuum pole exchange.

This is connected with the fact that in the case of pion exchange we have in the region $k^2 \to 0$

$$\frac{1}{\sin \pi l} \sim \frac{M^2}{\mu^2} \gg 1,$$

and in the case of exchange of a vacuum reggeon this quantity is of the order of unity.

We can therefore conclude that at moderate energies (on the order of several dozen BeV), even in the region of small excitations, $z \gtrsim (s/2M^2)^\nu$, the contribution of the diffraction inelastic processes cannot predominate. Thus, we can expect that these processes will manifest themselves distinctly only when $(\mu^2/M^2)\, s/2M^2 \sim 1$, that is, for $E_L \sim 20$—30 BeV. In this region they were actually observed [120].

We now can formulate the main attributes of peripheral diffraction in elastic processes, which enable us to distinguish them against a background of other interactions.

a) The quantum numbers of the clusters—isospin, charge, strangeness—cannot differ from the corresponding quantum numbers of the colliding particles [121]. This follows directly from the fact that the corresponding quantum numbers of the vacuum reggeon are equal to zero. Consequently, the charge transfer, etc., is excluded from these processes. In particular, in the diffraction inelastic interaction between nucleons, isobars cannot be produced directly with isospin $\frac{3}{2}$, only with isospin $\frac{1}{2}$. It must however be noted that the same takes place for any diffraction generation, not only the one obtained by reggeon exchange. This property appears already in the phenomenological analysis of such processes [116,118].

The spin and parity of the clusters can differ from the spins and parities of the colliding particles. This is connected with the fact that $l(k^2 \to 0) \to 1$ for the vacuum reggeon and consequently it can cause momentum transfer.

b) The excitations s_1 and s_2, on which the multiplicity depends, are strongly limited by the condition $z \gtrsim (s/2M^2)^\nu$ [in conjunction with (5.4) and (5.4a)]. Their effective values are of the order of magnitude of $M^2(s/2M^2)^{1-\nu}$, that is, $(s/2M^2)^\nu$ times as small as in the case of one-pion exchange in the region $z \sim 1$ which is fundamental to it. In this connection, the diffraction mechanism of the inelastic processes (exchange of a vacuum reggeon) can be significant only for relatively lean jets.

c) Finally, as already noted above, when $z \sim 1$ the components of the momentum transfer are the same in order of magnitude: $k_\perp^2 \sim k_0^2 + k_\parallel^2$.

At small excitations, $z \gg 1$, these components are essentially different, namely $k_\perp^2 \gg k^2 - k_\parallel^2$. We recall that $k_\perp^2 = \frac{1}{4} s\theta_{\mathfrak{M}}^2$ (where $\theta_{\mathfrak{M}}$ —angle between the momentum of the primary particles and one of the jets) and $k_\parallel^2 - k_0^2 = s_1 s_2/s$. Both quantities can thus be measured experimentally. The inequality $k_\perp^2 \gg k_\parallel^2 - k_0^2$ can be used to clarify the mechanism of the process.

For an experimental observation of diffraction inelastic processes at accelerator energies, an original procedure for indirect study of the inelastic processes was developed [120] (described in detail in [22]). What

were essentially selected were "lean" jets, that is, cases in which one nucleon is not excited at all, and the other is excited to the resonance state. It turned out that only isobars with isospin $T = 1/2$ (and spins $J = 3/2$ and $5/2$) are produced in this case; isobars with spins $3/2$, $3/2$ are not formed. All this agrees with the attributes listed above and gives grounds to regard these processes as proceeding via vacuum reggeon exchange [121].

At higher energies, in cosmic rays, the experimental data are not sufficiently clear-cut to separate these relatively rare processes unambiguously. The principal role should be assumed here by one-pion exchange (for pp collisions) in conjunction with central interactions (for πp collisions).

Thus, on the whole, it is possible to answer the questions raised at the start of this section.

APPENDIX

1. As was already detailed in the footnotes of Chap. II, the amplitude A(s,t) for the elastic scattering of two scalar particles of mass m is best expanded in partial waves in the t-channel

$$A(s,\ t)=\sum_l (2l+1)\, f_l(t)\, P_l(z), \qquad z\equiv\cos\theta_t. \tag{1}$$

If, as assumed in Chapter II, this amplitude describes in the t channel an even state, $A = A_+$, then the terms with odd l should be missing. On the other hand if the state is odd, $A = A_-$, then there are no terms with even l. We can therefore write

$$A_\pm(s,\ t)=\frac{1}{2}\sum_l (2l+1)\,(1\pm e^{i\pi l})\, f_l^{(\pm)}(t)\, P_l(z). \tag{2}$$

This sum can be written in the form of a Watson-Sommerfeld integral

$$A_\pm(s,\ t)=\frac{1}{4i}\int_\Gamma f_\pm(l,\ t)\,(2l+1)\,\frac{1\pm e^{i\pi l}}{\sin\pi l}\,P_l(z)\,dl, \tag{3}$$

where the integral is taken over the contour Γ in the l plane (see Fig. 5). If the functions $f_\pm(l,t)$ are analytic in the right half plane (where they have only poles and decrease sufficiently rapidly as $|l|\to\infty$), then the contour can be deformed in such a way that the integral breaks up into two parts, the integral along the line C and the sum of the residues at the poles of the function $f_\pm(l,t)$ (see Fig. 6).

Elastic scattering unaccompanied by charge exchange in the s-channel corresponds to an even state in the t-channel. We shall therefore consider henceforth the function $f_+(l,t)$. Assume that it is expressed in the terms of the poles l_i and the residues r_i at these poles in the following fashion:

$$f_+(l,\ t)=\sum_i \frac{r_i}{l-l_i(t)}.$$

Then

$$A_+(s,\ t)=\frac{1}{4i}\int_{b-i\infty}^{b+i\infty} f_+(l,\ t)\,(2l+1)\,\frac{1+e^{i\pi l}}{\sin\pi l}\,P_l(z)\,dl$$

$$+\sum_j r_j(t)\,\frac{1+e^{i\pi l_j}}{\sin\pi l_j}\,P_{l_j}(z)\,(2l_j+1). \tag{4}$$

For $s \gg m^2$ and $|t| \to 0$ we have

$$|z|=\left|1+\frac{2s}{t-4m^2}\right|\gg 1.$$

The asymptotic expression for $P_l(z)$ is of the form [14]

$$P_l(z)=P_l(\cosh\eta)=\frac{\Gamma\left(l+\frac{1}{2}\right)}{\sqrt{\pi}\,\Gamma(l+1)}\,e^{l\eta}=\frac{\Gamma(2l+1)}{2^l\Gamma^2(l+1)}\,z^l \tag{5}$$

(we put $\cosh\eta \equiv z$). If the sum over i contains one higher-order term with a largest real part (that is, there are no two or more terms with identical real parts—there is no crossing of the poles, see above), then the remaining terms can be neglected.

We can also verify that the first term in (4), that is, the integral along the straight line C, where $\mathrm{Re}\, l = b = \mathrm{const}$, makes a contribution of the order of s^b, which vanishes as $s \to \infty$ compared with the contribution from the poles (inasmuch as $b < \mathrm{Re}\, l_i$). Thus, in the asymptotical region there remains only the contribution from the highest-order term—the extreme right pole. When $t \ll 4m^2$ we have

$$A_+(s,\ t)=\frac{i\pi}{2}\,r_0(t)\,(2l_0+1)\,\frac{\Gamma(2l_0+1)}{2^{l_0}\Gamma^2(l_0+1)}\,\frac{1+e^{i\pi l_0}}{\sin\pi l_0}\left(\frac{s}{2m^2}\right)^{l_0(t)}. \tag{6}$$

From the condition $\sigma \to \mathrm{const}$ as $s \to \infty$ it follows that $l_0(0) = 1$. Indeed, if $l_0 = 1$ for $t = 0$, then

$$A_+=i\,\frac{3\pi}{2}\,r_0\left(\frac{s}{2m^2}\right)^{l_0}.$$

We recall that $\Gamma(n) = n-1!$, $\Gamma(2) = \Gamma(1) = 1$, and

$$\sigma=\frac{16\pi}{s}\,\mathrm{Im}\,A_+(s,\ 0)=\frac{12\pi^2}{m^2}\,r_0(0)\left(\frac{s}{2m^2}\right)^{l_0(0)-1}=\frac{12\pi^2}{m^2}\,r_0(0).$$

We call attention to the following circumstances:

a) If two particles of mass m and μ are scattered in the s channel (for concreteness, $m > \mu$, so that in the t channel this is the process involving conversion of two particles of mass m into two particles of mass μ), then $z \approx 2s/4m^2$ for $t \ll 4m\mu$. Then the cross section is of the form

$$\sigma=12\pi^2 r_0(0)\,\frac{1}{m\mu}. \tag{6a}$$

b) If the state in the t-channel is odd, but $l_-(0) = 1$, then we have in (6) in place of the factor

$$\frac{1+e^{i\pi l_0}}{\sin\pi l_0}$$

the factor

$$\frac{1-e^{i\pi l_-}}{\sin\pi l_-}.$$

Then as $t \to 0$, first, this factor will tend to infinity,

and second, the real part of the amplitude will be much larger than the imaginary part. It follows therefore that states that are odd in the t-channel cannot ensure the correct asymptotic behavior of the scattering in the s-channel.

2. The unitarity condition for the partial amplitude is of the form

$$f_l(t)-f_l^*(t)=2i\frac{k}{\omega}f_l(t)f_l^*(t)=2i\sqrt{\frac{t-4m^2}{t}}f_l(t)f_l^*(t). \qquad (7)$$

Here $\omega=\sqrt{t}$ is the energy in the t-channel c.m.s. This relation is valid for* $4m^2 < t < 9m^2$, that is, in the interval where two particles can exist, but the inelastic processes cannot occur as yet and there cannot be even three intermediate particles.

When $t < 4m^2$ the quantity $f_l(t)$ is real (for real l and t).

This relation can be illustrated by the diagram of Fig. 28. The strokes denote that the particles are real, that is, $k^2=-m^2$ for these particles.

The analytic continuation of this condition to the complex l plane is of the form (Gribov[10])

$$f(l,t)-f^*(l^*,t)=2i\sqrt{\frac{t-4m^2}{t}}f(l,t)f^*(l^*,t). \qquad (8)$$

It follows from (8) that the function $f(l,t)$ tends to infinity (that is, has a pole) when

$$f^*(l^*,t)\to 2i\sqrt{\frac{t-4m^2}{t}}.$$

We investigate the behavior of $f(l,t)$ near the pole[16]. We represent $f(l,t)$ in the form

$$f(l,t)=\frac{r(t)}{l-l_0(t)} \quad \text{and} \quad f^*(l^*,t)=\frac{r^*(t)}{l-l_0^*(t)}. \qquad (9)$$

For $\sqrt{(t-4m^2)/t} \ll 1$ we can assume that $\operatorname{Im} r(t) \ll \operatorname{Re} r(t)$ and consequently $r^*(t)=r(t)$. Substituting (9) in (8) we get

$$r(t)=\operatorname{Im} l_0(t). \qquad (10)$$

It follows therefore that when $t > 4m^2$ the quantity $l_0(t)$ cannot be real (the pole cannot be on the real axis); in the opposite case the value of the residue $r(t)$ is equal to zero. In addition, it follows therefore that the sign of the imaginary part of $l_0(t)$ is connected with the sign of the residue [that is, the function $r(t)$]. It is shown in [16] that $r\sqrt{(t-4m^2)/t}$ is positive when $t > 4m^2$. This is connected with the fact that the total cross section in the s-channel is positive. Thus, $\operatorname{Im} l_0(t) > 0$ when $t > 4m^2$ (we note that the same condition, according to Regge, occurs also in the nonrelativistic case). When $t < 4m^2$, $r(t)$ and $l_0(t)$ are real. This determines the analytic properties of the function $l_0(t)$: it has a branch point when $t = 4m^2$, and t acquires a positive imaginary part when $t > 4m^2$. We note also that $l_0(t)$ should be bounded for all values of t on the upper (physical) sheet (in the opposite case $A(s,t) \sim s^{l_0(t)}$ would have an essential singularity on the physical sheet, in contradiction to the Mandelstam representation). Taking this into account, we can draw in the t plane a cut from the point $t = 4m^2$ to the right and represent $l_0(t)$ in the form of a Cauchy integral, after which we can assume that the integral over the semicircle of infinite radius vanishes

$$l_0(t)=1+\frac{t}{\pi}\int_{4m^2}^{\infty}\frac{\operatorname{Im} l_0(t')}{(t'-t)t'}dt'. \qquad (11)$$

We already took account here of the condition $l_0(0) = 1$ referred to above. Consequently,

$$\left.\frac{\partial l_0(t)}{\partial t}\right|_{t=0}=l_0'(0)=\gamma=\frac{1}{\pi}\int_{4m^2}^{\infty}\frac{\operatorname{Im} l_0(t')}{t'^2}dt'. \qquad (12)$$

It follows therefore that γ is positive and cannot vanish (otherwise we would have

$$\operatorname{Im} l_0(t)=0 \qquad (13)$$

and the residue would vanish). In other words, $l_0(t)$ cannot be a constant, that is, the pole cannot be "standing."

2. Let us consider now the relation between several processes. Let the amplitude $f_{11}(l,t)$ describe in the s-channel scattering of particles of mass μ (we designate these particles with the index 1), let $f_{12}(l,t)$ be the scattering of the particle of mass m by a particle of mass m (we designate it with the index 2), and let $f_{22}(l,t)$ be the scattering of particles of mass m (for concreteness let $m > \mu$). Then in the two-particle interval the unitarity relation takes the form

$$f_{11}(l,t)-f_{11}^*(l^*,t)=2i\sqrt{\frac{t-4\mu^2}{t}}f_{11}(l,t)f_{11}^*(l^*,t), \qquad (14a)$$

$$f_{12}(l,t)-f_{12}^*(l^*,t)=2i\sqrt{\frac{t-4\mu^2}{t}}f_{11}(l,t)f_{12}^*(l^*,t), \qquad (14b)$$

$$f_{22}(l,t)-f_{22}^*(l^*,t)=2i\sqrt{\frac{t-4\mu^2}{t}}f_{12}(l,t)f_{12}^*(l^*,t). \qquad (14c)$$

These relations follow directly from the diagrams of Fig. 30, in which the intermediate states are identical and consist only of two light particles (other real states in this interval are forbidden by the conservation laws).

Solving this system of equations, we obtain

$$f_{11}(l,t)=\frac{f_{11}^*(l^*,t)}{1-2i\sqrt{\frac{t-4\mu^2}{t}}f_{11}^*(l^*,t)}=\frac{r_{11}}{l-l_0(t)}, \qquad (15a)$$

$$f_{12}(l,t)=\frac{f_{12}^*(l^*,t)}{1-2i\sqrt{\frac{t-4\mu^2}{t}}f_{11}^*(l^*,t)}=\frac{r_{12}}{l-l_0(t)}, \qquad (15b)$$

$$f_{22}(l,t)=f_{22}^*(l^*,t)+2i\sqrt{\frac{t-4\mu^2}{t}}\frac{(f_{12}^*(l^*,t))^2}{1-2i\sqrt{\frac{t-4\mu^2}{t}}f_{11}^*(l^*,t)}$$

$$=f_{22}^*(l^*,t)+\frac{r_{22}}{l-l_0(t)}, \qquad (15c)$$

*If the particles are not scalar but pseudoscalar (say pions), then the transition from two to three particles is forbidden by G-parity. Then the next possible state includes not three particles but four, and the next threshold is equal to $16m^2$.

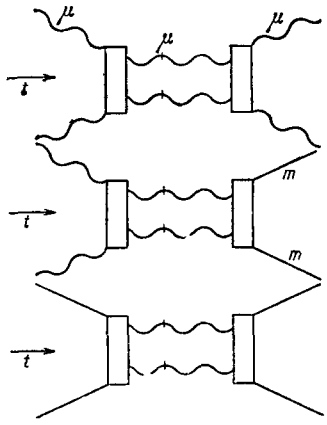

FIG. 30. Dispersion scattering diagrams. Straight lines–nucleons, wavy lines–pions.

where

$$r_{11}=\beta\sqrt{\frac{t}{t-4\mu^2}}\frac{1}{2i},\quad r_{12}=\beta f^*_{12},\quad r_{22}=\beta\,2i\sqrt{\frac{t-4\mu^2}{t}}(f^*_{12}(l^*,t))^2,$$

$$f^*_{11}(l^*,t)=\left[1-(l-l_0(t))\frac{1}{\beta}\right]\frac{1}{2i}\sqrt{\frac{t}{t-4\mu^2}}.$$

As $s\to\infty$ and for small t the elastic-scattering amplitude will be of the form

$$A_{11}=r_{11}(2l+1)z_{11}^{l_0(t)}\approx 3r_{11}\left(\frac{s}{2\mu^2}\right)^{l_0(t)},\qquad (16a)$$

$$A_{12}=r_{12}(2l+1)z_{12}^{l_0(t)}\approx 3r_{12}\left(\frac{s}{2m\mu}\right)^{l_0(t)},\qquad (16b)$$

$$A_{22}=r_{22}(2l+1)z_{22}^{l_0(t)}\approx 3r_{22}\left(\frac{s}{2m^2}\right)^{l_0(t)}.\qquad (16c)$$

It follows therefore that all the functions have a pole $l_0(t)$ in one and the same place, in the l-plane.

In other words, the pole trajectory $l_0(t)$ is universal and for large s it should determine the asymptotic behavior of the amplitudes of arbitrary strongly interacting particles. Further, it follows from (16a)–(16c) that the residues are related by $r_{11}r_{22}=r_{12}^2$. The total cross sections of the processes connected with the amplitudes A_{ij} of the optical theorem

$$\sigma_{ij}=\frac{s}{16\pi}A_{ij},$$

will therefore be connected by an analogous relation, which was already cited (2.18):

$$\sigma_{11}\cdot\sigma_{22}=\sigma_{12}^2.\qquad (17)$$

[1] I. L. Rozental' and D. S. Chernavskiĭ, UFN 52, 185 (1954).

[2] Z. Koba and S. Takagi, Fortschr. Phys. 7, 1 (1959).

[3] E. L. Feĭnberg, UFN 70, 333 (1960), Soviet Phys. Uspekhi 2, 147 (1960); Trudy, Ninth Conference on High-energy Physics, Kiev, 1959, VINITI, 1961, p. 690.

[4] V. B. Berestetskiĭ, UFN 76, 25 (1962), Soviet Phys. Uspekhi 5, 7 (1962).

[5] I. Ya. Pomeranchuk, JETP 34, 725 (1958), Soviet Phys. JETP 7, 499 (1958).

[6] M. Froissart, Phys. Rev. 123, 1053 (1961).

[7] See, e.g., P. Frank and R. von Mises, Die Differential-und Integralgleichungen der Mechanik und Physik, Vieweg, Brunswick, V. 2, ch. 23, Sec. 4.

[8] T. Regge, Nuovo cimento 14, 951 (1959); 18, 947 (1960).

[9] V. A. Fock, Izv. AN SSSR, ser. fiz. 14, 70 (1950).

[10] V. N. Gribov, JETP 41, 667 and 1962 (1961), Soviet Phys. JETP 14, 478 and 1395 (1962); Nucl. Phys. 22, 246 (1961).

[11] S. Mandelstam, 1962 Intern. Conf. of High Energy Phys., CERN, Geneva 1962, p. 513.

[12] G. Domokos, Dissertation, Joint Inst. Nuc. Phys. 1963.

[13] Logunov, Tavkhelidze, Todorov, and Khrustalev, Preprint, Joint Inst. Nuc. Res. D-1191 (1963); Nuovo cimento 29, 380 (1963); Logunov, Tavkhelidze, and Khurstalev, Preprint JINR R-1195 (1963); Phys. Let. 4, 325 (1963).

[14] I. S. Gradshteĭn and I. M. Ryzhik, Tablitsy integralov, summ, raydov i proizvedeniĭ, (Tables of Integrals, Sums, Series, and Products), Fizmatgiz, 1962, p. 1037.

[15] G. F. Chew and S. C. Frautschi, Phys. Rev. Letts. 7, 394 (1961).

[16] V. N. Gribov and I. Ya. Pomeranchuk, JETP 42, 1141 (1962), Soviet Phys. JETP 15, 788 (1962); Phys. Rev. Let. 8, 343 (1962).

[17] M. Gell-Mann, Phys. Rev. Letts. 8, 263 (1962).

[18] G. F. Chew and S. C. Frautschi, Phys. Rev. Letts. 8, 41 (1962).

[19] G. Lovelace, Nuovo cimento 25, 730 (1962); see also S. D. Drell, Proc. Aix-en-Provence Conference, 1961, vol. 11.

[20] Cocconi, Diddens, Lillethun, Manning, Taylor, Walker, and Wetherell, Phys. Rev. Letts. 7, 450 (1961); 9, 108, 111 (1962).

[21] Foley, Lindenbaum, Love, Ozaki, Russel, and Yuan, Phys. Rev. Letts. 10, 376 (1963).

[22] Birger, Mikhaĭlov, Rozental', and Sarycheva, UFN 79, 523 (1963), Soviet Phys. Uspekhi 6, 250 (1963).

[23] Diddens, Lillethun, Manning, Taylor, Walker, and Wetherell, 1962 Intern. Conf. on High-energy Physics, CERN, Geneva, 1962, p. 576.

[24] Bayukov, Birger, Leksin, and Suchkov, JETP 43, 339 (1962), Soviet Phys. JETP 16, 243 (1963).

[25] Frautschi, Gell-Mann, and Zachariasen, Phys. Rev. 126, 2204 (1962).

[26] Selove, Hagopian, Brody, Baker, and Leboy, Phys. Rev. Letts. 9, 272 (1962).

[27] G. F. Chew, Preprint (1962).

[28] G. Domokos, DAN SSSR 144, 1279 (1962), Soviet Phys. Doklady 7, 546 (1962).

[29] V. N. Gribov, JETP 41, 1962 (1962), Soviet Phys. JETP 14, 1395 (1963); see also Voprosy fiziki elemen-

tarnykh chastits (Problems in Elementary-particle Physics), AN ArmSSR, Erevan, p. 178.

[30] M. Gell-Mann and B. M. Udgaonkar, Phys. Rev. Let. 8, 346 (1962).

[31] Ting, Jones, and Perl, Phys. Rev. Let. 9, 468 (1962); Brandt, Cocconi, Morrison, Wroblewski, Fleury, Kayas, Muller, and Pelletier, Phys. Rev. Let. 10, 413 (1963).

[32] B. M. Udgaonkar, Phys. Rev. Let. 8, 142 (1962).

[33] Kanavets, Levintov, and Morozov, JETP 45, 679 (1963), Soviet Phys. JETP 18, 467 (1964).

[34] E. L. Feĭnberg and D. S. Chernavskiĭ, DAN SSSR 81, 795 (1951) and 91, 511, (1963).

[35] D. S. Chernavskii, Suppl. Nuovo cimento 8, 775 (1958).

[36] D. I. Blokhintsev, Proc. CERN Symposium 1956, v. 2, p. 155; Blokhintsev, Barashenkov, and Barbashev, UFN 68, 417 (1959), Soviet Phys. Uspekhi 2, 505 (1960).

[37] E. Friedländer, Acta Phys. Hung. 6, 237 (1956).

[38] G. T. Zatsepin, Suppl. Nuovo cimento 8, 746 (1958).

[39] S. Takagi, Progr. Theor. Phys. 7, 123 (1952).

[40] W. L. Kraushaar and L. J. Marks, Phys. Rev. 93, 326 (1954).

[41] Yu. A. Romanov and D. S. Chernavskiĭ, JETP 38, 1132 (1960), Soviet Phys. JETP 11, 819 (1960).

[42] G. Chew and F. Low, Phys. Rev. 113, 1640 (1959).

[43] F. Salzman and G. Salzman, Phys. Rev. Let. 5, 377 (1960); Phys. Rev. 120, 599 (1960); 121, 1541 (1961); 125, 1703 (1962).

[44] I. M. Dremin and D. S. Chernavskiĭ, JETP 38, 229 (1960), Soviet Phys. JETP 11, 167 (1960).

[45] S. D. Drell, Revs. Modern Phys. 33, 458 (1961).

[46] V. B. Berestetskiĭ and I. Ya. Pomeranchuk, JETP 39, 1078 (1960), Soviet Phys. JETP 12, 752 (1961).

[47] F. Bonsignori and F. Selleri, Nuovo cimento 15, 464 (1960).

[48] I. M. Dremin and D. S. Chernavskiĭ, JETP 43, 551 (1962), Soviet Phys. JETP 16, 394 (1963).

[49] E. Ferrari and F. Selleri, Phys. Rev. Letts. 7, 387 (1961); Nuovo cimento 21, 1028 (1961).

[50] Z. Koba and A. Krzywicki, Preprint 368/VII.

[51] Erwin, Mach, Walker, and West, Phys. Rev. Letts. 6, 628 (1961).

[52] Bogachev, Bunyatov, Gramenitskiĭ, Lyubimov, Merekov, Podgoretskiĭ, Sidorov, and Tuvdendorzh, JETP 37, 1225 (1959), Soviet Phys. JETP 10, 872 (1960).

[53] See [52].

[54] E. Ferrati and F. Selleri, Suppl. Nuovo cimento 26, 453 (1962).

[55] Gramenitskiĭ, Dremin, Maksimenko, and Chernavskiĭ, JETP 40, 1093 (1961), Soviet Phys. JETP 13, 771 (1961).

[56] Gramenitskiĭ, Dremin, and Chernavskiĭ, JETP 41, 856 (1961), Soviet Phys. JETP 14, 613 (1962).

[57] S. B. Treiman and C. N. Yang, Phys. Rev. Let. 8, 140 (1962).

[58] I. M. Gramenitskiĭ and M. I. Podgoretskiĭ, Preprint, Joint Inst. Nuc. Res. (1962).

[59] F. Selleri, Phys. Rev. Let. 6, 64 (1961); G. Da Prato, Nuovo cimento 22, 123 (1961).

[60] N. G. Birger and Yu. A. Smorodin, JETP 36, 1159 (1959) and 37, 1355 (1959), Soviet Phys. JETP 9, 823 (1959), and 10, 964 (1960).

[61] E. L. Feĭnberg and D. S. Chernavskiĭ, JETP 45, 1252 (1963), Soviet Phys. JETP 18, 861 (1964).

[62] I. M. Dremin and D. S. Chernavskiĭ, JETP 40, 1333 (1961), Soviet Phys. JETP 13, 938 (1961).

[63] I. M. Dremin, JETP 41, 821 (1961), Soviet Phys. JETP 14, 589 (1962).

[64] H. Lehman, Nuovo cimento 10, 579 (1958).

[65] Chernavsky, Dremin, Feinberg, and Roysen, Nucl. Phys. 44, 116 (1963).

[66] I. I. Roizen and D. S. Chernavskiĭ, JETP 44, 1907 (1963), Soviet Phys. JETP 17, 1283 (1963).

[67] N. A. Dobrotin and S. A. Slavatinskiĭ, Proc. Intern. Conf. on High-energy Physics, 1960, p. 819; Nucl. Phys. 35, 152 (1962). Guseva, Dobrotin, Zelevinskaya, Kotel'nikov, Lebedev, and Slavatinskiĭ, Izv. AN SSSR ser. fiz. 26, 549 (1962), Columbia Tech. Transl. p. 550.

[68] Ciok, Gierula, Holynski, Jurak, Miesowicz, Saniewiska, Stanisz, and Pernegr. Nuovo cimento 8, 166 (1958); 10, 741 (1958).

[69] D. S. Chernavsky, Postepy Fisyki 9, 653 (1958).

[70] G. A. Milekhin, Proc. of the Moscow Cosmic Ray Conf. (Moscow, 1959), vol. 1, p. 220.

[71] Amati, Fubini, Stanghellini, and Tonin, Nuovo cimento 22, 569 (1961).

[72] Amati, Stanghellini, and Fubini, Nuovo cimento 26, 896 (1962).

[73] Amati, Fubini, and Stanghellini, Phys. Let. 1, 29 (1962).

[74] Bertocchi, Fubini, and Tonin, Preprint 7974/TH 274; Nuovo cimento 25, 626 (1962).

[75] Belyakov, Wang, Veksler, Viryasov, Tu, Kladnitskaya, Kim, Kuznetsov, Mikhul, Nguyen, Penev, Sokolova and Solov'ev, 1962 CERN Int. Conf. on High-energy Phys. Geneva, p. 336.

[76] P. A. Usik and V. I. Rus'kin, JETP 39, 1718 (1960). Soviet Phys. JETP 12, 1200 (1961).

[77] E. G. Bubelev and G. T. Zatsepin, Trans. Intern. Conf. on Cosmic Rays, Moscow, 1959, v. I, p. 285.

[78] S. Hasegawa, Progr. Theor. Phys. 29, 128 (1963).

[79] C. F. Powell, Proc. IX Intern. Conf. on High Energy Physics, Kiev, 1959, vol. 11.

[80] D. H. Perkins, Proc. Intern. Conf. on Theor. Aspects of Very High Energy Interactions, CERN, 1961.

[81] S. Alper and E. M. Friedländer, Rev. phys. 7, 311 (1962).

[82] Grigorov, Murzin, and Rapaport, JETP 34, 506 (1958), Soviet Phys. JETP 7, 348 (1958).

[83] Grigorov, Kondrat'eva, Savel'eva, Sobinyakov, Podgurskaya, and Shestoperov, op. cit. [77], p. 122.

[84] L. D. Landau, Izv. AN SSSR ser. fiz. 17, 51 (1953); S. Z. Belen'kiĭ and L. D. Landau, UFN 56, 309 (1955).
[85] G. A. Milekhin, op. cit. [77], p. 212.
[86] N. M. Duller and W. D. Walker, Phys. Rev. Letts. 8, 166 (1958).
[87] N. L. Grigorov, JETP 45, 1919 (1963), Soviet Phys. JETP 18, 1318 (1964).
[88] P. K. Malhotra, Preprint (1962).
[89] Z. Koba, Proc. Intern. Conf. on Theor. Aspects of Very High Energy Interactions, CERN, 1961.
[90] G. Cocconi, Phys. Rev. 111, 1699 (1958); K. Niu, Nuovo cimento 10, 994 (1958).
[91] Gierula, Miesowicz, and Zielinski, Nuovo cimento 18, 102 (1960).
[92] J. Gierula, Proc. Intern. Conf. on Theor. Aspects of Very High Energy Interactions, CERN, 1961.
[93] E. M. Friedländer, Phys. Rev. Letts. 5, 212 (1960).
[94] Alekseeva, Gabuniya, Jen, Zhdanov, and Tret'yakova, JETP 43, 783 (1962), Soviet Phys. JETP 16, 554 (1963); Izv. AN SSSR ser. fiz. 26, 572 (1962), Columbia Tech. Transl. p. 571.
[95] V. Simak, Private Communication.
[96] A. A. Emel'yanov, JETP 36, 1550 (1959), Soviet Phys. JETP 9, 1100 (1959); M. Hamaguchi, Nuovo cimento 5, 1622 (1953) and 6, 1243 (1958); A. A. Emel'yanov and D. S. Chernavskiĭ, JETP 37, 1058 (1959), Soviet Phys. JETP 10, 753 (1960).
[97] Takibaev, Loktionov, San'ko, and Shakhova, op. cit. [77].
[98] Bartke, Ciok, Gierula, Holynski, Miesowicz, and Saniewska, Proc. of the Cosmic Ray Conf. (Moscow, 1959), vol. 1, p. 113.
[99] J. Gierula and M. Miesowicz, Preprint (1963).
[100] G. T. Zatsepin, Izv. AN SSSR ser. fiz. 26, 674 (1962), Columbia Tech. Transl. p. 673.
[101] G. Cocconi, 1962 Intern. Conf. on High-energy Phys., CERN, Geneva, 1962, p. 883.
[102] V. S. Murzin, Trudy, All-union Conference on Cosmic Rays, October 1963; Barkow, Chamany, Haskin, Jain, Lohrmann, Teucher, and Schein, Phys. Rev. 122, 617 (1960).
[103] J. Gierula and M. Miesowicz, Nuovo cimento 27, 149 (1963).
[104] Edwards, Losty, Perkins, Pinkau, Reynolds, Phil. Mag. 3, 237 (1958).
[105] Grigorov, Guseva, Dobrotin, Kotel'nikov, Murzin, Ryabikov, and Slavatinskiĭ, op. cit. [77], p. 143.
[106] S. A. Slavatinskiĭ and D. S. Chernavskiĭ, op. cit. [77], p. 161.
[107] G. Cocconi, Proc. 1962 Intern. Conf. on High-energy Physics, Geneva.
[108] Yu. D. Kotov and I. L. Rozental', JETP 43, 1411 (1962), Soviet Phys. JETP 16, 1001 (1963).
[109] N. M. Gerasimova and D. S. Chernavskiĭ, JETP 29, 372 (1955), Soviet Phys. JETP 2, 344 (1956).
[110] Brikker, Grigorov, Kondrat'eva, Podgurskaya, Savel'eva, Sobinyakov, and Shestoperov, Suppl. Nuovo cimento 8, 733 (1958); N. L. Grigorov and V. Ya. Shestoperov, JETP 37, 1147 (1959), Soviet Phys. JETP 10, 816 (1960). Zhdanov, Zamchalova, Tret'yakova, and Shcherbakova, JETP 34, 843 (1958), Soviet Phys. JETP 7, 582 (1958).
[111] S. I. Nikol'skiĭ, UFN 78, 365 (1962), Soviet Phys. Uspekhi 5, 849 (1963).
[112] Duthie, Fisher, Fowler, Kaddoura, Perkins, and Pinkau, Nuovo cimento 24, 122 (1962).
[113] E. L. Feĭnberg, Izv. AN SSSR ser. fiz. 26, 622, (1962), Columbia Tech. Transl. p. 619.
[114] Yu. S. Vernov and I. N. Sisakyan, ibid. 26, 642 (1962), transl. p. 641.
[115] I. Ya. Pomeranchuk and E. L. Feinberg, DAN SSSR 93, 439 (1953).
[116] E. L. Feinberg and I. Pomerancuk, Suppl. Nuovo cimento 3, 652 (1956).
[117] I. I. Ivanchik, JETP 35, 1050 (1959), Soviet Phys. JETP 8, 733 (1959).
[118] M. L. Good and W. D. Walker, Phys. Rev. 120, 1857 (1960).
[119] P. T. Mathews and A. Salam, Nuovo cimento 21, 126 (1961).
[120] Cocconi, Diddens, Lillethun, and Wetherell, Phys. Rev. Let. 6, 231 (1961).
[121] Gribov, Ioffe, Pomeranchuk, and Rudik, JETP 42, 1419 (1962), Soviet Phys. JETP 15, 984 (1962).
[122] K. A. Ter-Martirosyan, JETP 44, 341 (1963), Soviet Phys. JETP 17, 233 (1963).
[123] I. M. Dremin and D. S. Chernavskiĭ, JETP 45, 1943 (1963), Soviet Phys. JETP 18, 1334 (1964).
[124] Blankenbecler, Cook, and Goldberger, Phys. Rev. Let. 8, 463 (1962).
[125] S. C. Frautschi, Nuovo cimento 28, 409 (1963).
[126] S. Mandelstam, Preprint (1963).
[127] D. Amati and Cini, Preprint (1963).

Translated by J. G. Adashko